5-2012

# Synthesis and Structural Studies of Calcium and Magnesium Phosphinate and Phosphonate Compounds

Victoria Naa Kwale Bampoh
*Syracuse University*

ABSTRACT

The work presented herein describes synthetic methodologies leading to the design of a wide array of magnesium and calcium based phosphinate and phosphonates with possible applications as bone scaffolding materials or additives to bone cements. The challenge to the chemistry of the alkaline earth phosphonate target compounds includes poor solubility of compounds, and poorly understood details on the control of the metal's coordination environment. Hence, less is known on phosphonate based alkaline earth metal organic frameworks as compared to transition metal phosphonates. Factors governing the challenges in obtaining crystalline, well-defined magnesium and calcium solids lie in the large metal diameters, the absence of energetically available *d*-orbital to direct metal geometry, as well as the overall weakness of the metal-ligand bonds.

A significant part of this project was concerned with the development of suitable reaction conditions to obtain X-ray quality crystals of the reaction products to allow for structural elucidation of the novel compounds. Various methodologies to aid in crystal growth including hydrothermal methods and gel crystallization were employed.

We have used phosphinate and phosphonate ligands with different number of phosphorus oxygen atoms as well as diphosphonates with different linker lengths to determine their effects on the overall structural features. An interesting correlation is observed between the dimensionality of products and the increasing number of donor oxygen atoms in the ligands as we progress from phosphinic acid to the phosphorous acids. As an example, monophosphinate ligand only yielded one-dimensional

compounds, whereas the phosphonates crystallize as one and two-dimensional compounds, and the di- and triphosphonate based compounds display two or three-dimensional geometries.

This thesis provides a selection of calcium and magnesium compounds with one-dimensional geometry, as represented in a calcium phosphinate to novel two-dimensional sheets of magnesium and pillared calcium phosphonates. The preparation of these novel compounds has led to the establishment of synthetic protocols that allow for the direct preparation of compounds with defined structural features.

# Synthesis and Structural Studies of Calcium and Magnesium Phosphinate and Phosphonate Compounds

By

Victoria Naa Kwale Bampoh

Department of Chemistry, Syracuse University

MSc. in Chemistry, Syracuse University

DISSERTATION

Submitted in partial fulfillment of the requirements for the Doctor of Philosophy in Chemistry in the Graduate School of Syracuse University

May, 2012

ACKNOWLEDGEMENTS

This enormous research project would not have been possible without the grace of God and able leadership and support of two distinguished professors: Dr. Karin Ruhlandt and Dr. Jon Zubieta of the Chemistry Department of Syracuse University, who nurtured the seed for the bone project. I am especially grateful to them for allowing me to be part of this work.

Thank you Karin, my boss and advisor, for the lengths you have gone to ensure that I succeeded in this graduate program. You have been abundantly helpful. Your invaluable assistance, support and guidance are highly appreciated. You will forever remain very dear to me and my entire family.

I wish to express my gratitude to Professor Emeritus Marion Bickford, who gracefully accepted to chair my defense committee. To all members of the committee: Jon Zubieta, Mathew Maye, Donald Dittmer, James Spencer and Karin Ruhlandt, thank you for your time.

I owe my deepest gratitude to Nancy Cantor, Vice Chancellor, and Nancy Totah, Chair of Graduate Studies, who were both instrumental in my gaining admission into Syracuse University with scholarship to pursue this graduate program. It has been so beneficial in so many ways. Thanks to all the staff at the Chemistry Department of SU for your great support.

I also appreciate the valuable contributions from members of the Ruhlandt group, with whom I interacted daily over the years. My deepest appreciation goes to Doctors William Maudez, Abhilasha Verma and Ana Torvisco. I appreciate the roles you all played in my learning process. I am grateful to my undergraduate students Sarina and Seungmo for their contribution and input to this bone project. Peter, thanks for the deep thoughts we have often shared over lunch, I will miss that. My gratitude to Alan 'The Professor', Yuriko, Andrew, Valerie, Cathy and Adam for their valuable support.

I am indebted to my parents, late Rev. E.T. Quartey and Mrs. Bernice Quartey, who out of their scarcity found it imperative to invest in my education. Mama, thank you for being a good example and an encouragement to me all the time. To my brother James and family in Ohio and my sister Rejoice in Ghana, thank you all for the much needed moral support anytime it became necessary.

I am also deeply grateful to my husband and friend, Apostle Bismark Barima Bampoh for believing in me and sharing in my academic vision. Darling, your preparedness, eagerness and willingness to see me off for further studies in America, in spite of our prevailing peculiar family situation in Ghana, comes to me as a huge sacrifice and that sets you apart as a great leader in your own class. I am monumentally grateful.

Thank you my son Benard Nana Kwabena Bampoh for your maturity beyond your age, demonstrated in persistent patience and kindness, which allowed me to go for hours without much interruption in pursuit of this degree. Together with your late brothers Enoch and Caleb, you have encouraged and tremendously inspired me to work hard and I feel blessed to have you. To my dear daughters Cynthia and Rosemary, thanks for understanding and being there for me always.

My gratitude to all my friends: Tracy Duke and family, Janis Bernard, Dr. Sarah Darkwa, Julie Salvana, Sue Richardson, Silvio Baeiz, Dr. Kathryn Stam, Nila Gipson, Terry Virag, Mary Jane, Grace Bampoh (Nana), Linda Abbey, Dr. Ako A. Manasah, Isaac Ntansah-Boateng, Wenjie, Jenny, Peter, Michael and Agnes Asiedu, Grace and Maxwell Amoah, and William and Susie Agble. It is also a great honor for me to thank the Genants, Eugene and Paul Bailey families, the Meads, Lodovicos, Marquis, LaBarge, Keach family, Dale Williams's family, as well as the Geremias, Iovines, Weimars, Benders, Snyders, Binnings, and all the wonderful saints at Living Word Church and Word Miracle Church Int., for their love.

Bishop Charles and Vivian Agyin-Asare of the Word Miracle Church Int., Ghana, Pastor Robert and Fannie Mazur, and Pastor Bryan and Catherine Rocine of the Church of the Living Word, as well as Bro. Phil Mastroleo, principal of Living Word Academy, Syracuse New York, all stand out for special mention.

Finally, I eulogize God for the opportunities, daily strength and insight granted to me each step of the way. I owe it all to Jesus my Lord and personal Savior.

TABLE OF CONTENTS

**CHAPTER 2: Metal Organic Frameworks (MOFs)**

**CHAPTER 3: Ligand systems**

**CHAPTER 4: Synthesis and structural studies on calcium phosphinate, phosphonate, phosphite and phosphate compounds**

**CHAPTER 6: The synthesis and characterization of magnesium diphosphonates**

**CHAPTER 7: Calcium Alkylene diphosphonates**

**CHAPTER 8: Synthesis and characterization of calcium amino trimethylenephosphonate**

List of Illustrative Materials: Tables

List of Illustrative Materials: Figures

List of Illustrative Materials: Schemes

ABBREVIATIONS

| | |
|---|---|
| Ae | alkaline earth metal |
| abdc | 2-amino-1,4-benzenedicarboxylate |
| AEPH | 2-aminoethylphosphonic acid |
| azpy | azopyridine |
| dbc | 1,4-benzenedicarboxylate |
| BOBDC | 2,5-dioxido-1,4-benzenedicarboxylate |
| btc | 1,3,5-benzenetricarboxylate |
| bpt | biphenyl-3, 4',5-tricarboxylate |
| bpy | 4,4'-bipyridine |
| Dabco | 1,4-diazabicyclo[2.2.2]octane |
| DEO | US Department of Energy |
| DMF | N, N′- dimethylformamide |
| dpndi | N,N'-di(4-pyridyl)-1,4,5,8-naphthalenetetracarboxydiimide |
| $F_4$bdc | 2,3,5,6-tetrafluorobenzene-1,4-dicarboxylate |
| HA | hydroxyapatite |
| $H_6$ATMPA | amino trimethylenephosphonic acid |
| $H_2$bdp | 1,4-benzenedi(4-pyrazolyl) |
| $H_4$BDP | biphenyldiphosphonic acid |
| $H_3$btc | biphenyl-3,4,5-tricarboxylate |
| Hcam | (+)-camphoric acid |
| $H_4$dhtp | 2,5-dihydroxyterephthalic acid |
| $H_4$EDPA | ethylenediphosphonic acid |

| | |
|---|---|
| $H_8$EDTMPA | ethylenediaminetetramethylenephosphonic acid |
| $H_4$PDPA | propylenediphosphonic acid |
| HPPA | phenylphosphinic |
| $H_2$PPA | phenylphosphonic acid |
| $H_4$PPPA | 4-(4'-phosphonophenoxy) phenyl phosphonic acid |
| mein | 2-methylimidazolate |
| MOF | metal organic framework |
| ndc | 1,4-naphtalenedicarboxylate |
| PCL | poly($\varepsilon$-caprolactone) |
| PE | Polyethylene |
| PETE | polyethylene tetrafluoroethylene |
| PLA | polylactic acid |
| PLGA | poly(lactic-co-glycolic acid) |
| PGA | polyglycolic acid |
| PMMA | Poly(methyl methacrylate) |
| PPF | poly(propylene-*co*-fumarate) |
| pdc | pyridine dicarboxylate |
| pz | pyrazine |
| tbdc | triphenylene-2,6,10-tricarboxylate |
| ttca | 2,3,5,6-tetramethyl-1-4-benzenedicarboxylate |

# CHAPTER 1

# Background

## 1.1 Introduction

The study of bone substitute materials is of great research interest to improve on the materials and methods that are applied to treat fractured bone and bone related diseases. Extensive research led to the discovery of therapeutic potential of the diphosphonate drugs,[1-3] which have since been developed for clinical applications due to their ability to inhibit bone resorption.[2] As these drugs have adverse side effects,[4] there is a need to search for alternative and biocompatible materials to treat bone disorders.

Various materials have been developed as bone implant however, research has proved that the success of an implant is determined by the biomaterial-tissue interface where an interfacial bond is established between the implant and the bone.[5] Hence the use of bioactive and biocompatible materials such as bone cements (calcium phosphate), bioceramics (clay) and Bioglass® (consisting of $SiO_2$, $Na_2O$, CaO and $P_2O_5$ in specific proportions) have been developed for bone treatment. These materials however lack mechanical strength, and for this reason, efforts to improve on bone cements have led to the development of composite and hybrid biomaterials.[6] Another means to overcome the weakness in bone cements is the use of scaffold materials. These scaffolding materials must be three dimensional and allow for bone in-growth.

The objective of this project is to explore the use of phosphonate based ligands in the synthesis of three-dimensional frameworks that may be developed into scaffolds appropriate for bone substitution. The material is preferably bioactive and biocompatible,

suggesting it's use as additives to existing bone cements in order to improve their biometric properties.

The first three chapters of this thesis will focus on (a) a general introduction of bone and its properties, (b) metal-organic frameworks and (c) potential ligand systems used for this purpose. The remaining five chapters discuss the results of the studies.

This chapter starts with a description of the bone cell structure and function, followed by an overview of existing methods and materials, and how these impact bone therapy. The chapters conclude with the properties of currently used scaffold materials.

## 1.2 Bone Cell Structure and Function

Bone is a rigid, light-weight but strong and hard connective tissue found in vertebrates.[7] The human skeletal system is a network of bone and cartilage. The bone cells are living tissues that are mainly needed for support, motion, production of blood cells (hemopoesis), storage of minerals, and protection of sensitive organs such as the brain, heart and lungs in the body.[7-9] There are three types of bone cells; osteoblasts which synthesize the bone matrix and ensure bone mineralization, osteoclasts which are responsible for matrix resorption or breakdown in addition to osteocytes, which are inactive osteoblasts or mature bone cells.

Osteocytes are embedded in a matrix material (extra cellular material) which contains organic and inorganic materials.[8] The bone's flexibility therefore stems from the organic part which is a fibrous protein called collagen that makes up 35% of the bone mass. The rest of the bone is inorganic in nature and is made up of mineral salts which

afford the bone its compression strength, hardness, and durability.[9] The principal mineral is amorphous calcium phosphate (PCA) as "nanophosphate rods",[10] along with 4-6% of a mixture of calcium carbonate, traces of magnesium phosphate, sodium oxide and sodium chloride. Hydroxyapatite ($Ca_5(PO_4)_3OH$) is therefore a model compound of the inorganic component of bone.[11] The matrix, mineral and water in the bone are in the percentages of 60, 30 and 10 respectively.[12]

Bone is resorbed as a result of digestion by enzymes produced by large bone cells called osteoclasts; so throughout life, bone resorption and bone formation continuously occur. All together, an estimate of one fifth of the skeleton in an adult is replaced each year. Unfortunately, beyond 30 years of age, the rate of resorption outpaces the rate of formation leading to a decline in bone density. This is especially problematic in cases of bone disease, where damaged bone cannot be quickly rebuilt. In these cases, it might be advantageous to aid the healing process by using bone templating materials. Our research is geared towards the development of light-weight, flexible, bioactive and biocompatible materials that can be used in this application. These materials may also be used as components in bone cement that will make it bioactive ensuring a close connection between an implant and the living bone.

Figure 1.1 provides a detailed figure of bone material, representing a general overview of bone tissue. A typical bone consists of a shaft known as diaphysis which begins with the proximal and ends in epiphysis. In the hollow of the diaphysis lie the marrow, blood vessels and leukocytes (white blood forming cells). The diaphysis is covered by the periosteum (Figure 1.1a), a tough fibrous tissue which contains blood vessels, lymph vessels and nerves.[9]

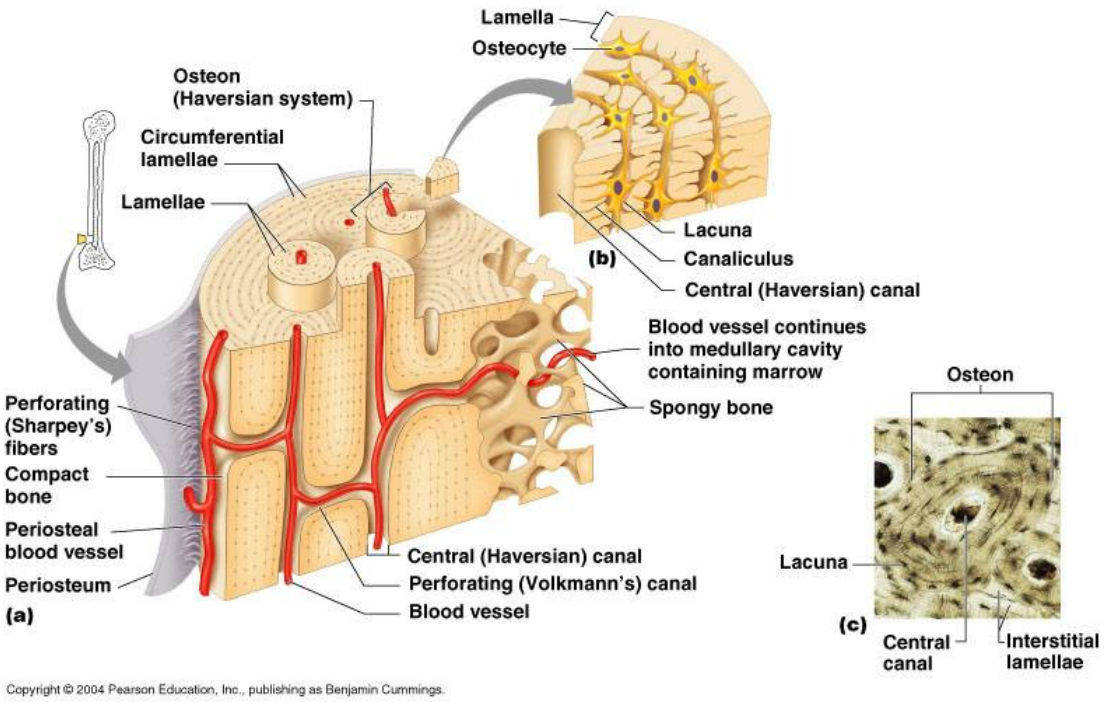


**Figure 1.1.** Detailed structure of human bone.[13]

Bone may be compact or spongy (Figure 1.1 a). The matrix in compact bone consists of closely packed structural units called the Haversian system (Figure 1.1c). The Harvesian system is made up of a central Haversian canal through which the blood vessels and lymphatic vessels run. The Volkmann's canal connects one Haversian canal to the other. The Haversian canal is bound by concentric, cylindrically shaped layers of calcified matrix known as lamellae. Imbedded in the spaces between the lamellae (lacunae), are the osteocytes. (Figure 1.1b) The lacunae are small cavities that contain periosteocytic fluid that contain calcium and phosphate ions. Small canals called canaliculi radiate from the lacunae to other canals.

In spongy bone however, there is no Harvesian system, instead, there is a web-like arrangement of marrow filled spaces that are separated by thin plates and bars of bone called trabeculae.[8] The human bone can therefore be described as a natural composite comprising of nano-apatite rods (<100 mm) arranged in lamellae and bound to collagen.[14,15]

## 1.3 Bone Fracture and Treatment

A fracture is a broken bone[16] and considered as a type of tissue failure (Figure 1.2). The bone becomes more prone to fracture as a result of bone cell loss. The propensity for fractures increase with age, and most occur between the ages of 50 to 59 years.[17] In addition, bone diseases such as osteoporosis lead to reduced bone mass.[18] Also, dislocation, effects of pathogens, falls and traffic accidents can exert an enormous pressure on the bone and bring it to fracture.

Osteoporosis is ranked the highest cause of bone fracture. It is estimated that an osteoporotic fracture occurs every three seconds in the world and 6.3 million fractures occur each year in the U.S.[17] Osteoporosis is the most common bone disease but other metabolic diseases such as diabetes and kidney diseases also reduce the quality and amount of bone mass.[7] In 2005, the cost of treating fractures that are related to osteoporosis in the US was estimated to be $17 billion, 72% of this cost is spent on hip fractures .[19]

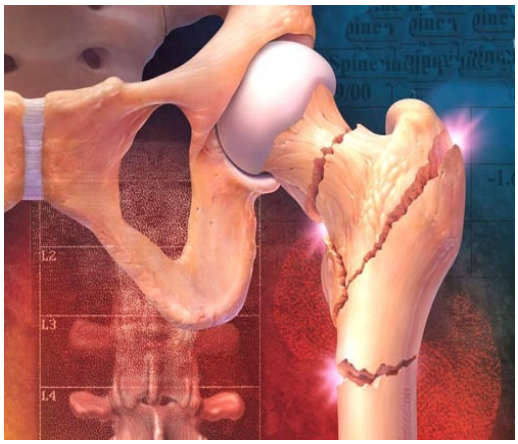

**Figure 1.2.** Fracture in a hip bone.[20]

A fractured bone may require bone replacement which is termed prosthesis.[6] Though there are several materials such as ceramics and coated metals for treating bone fractures by grafting or total replacement,[5] each procedure is associated with problems that must be dealt with. It has therefore become essential to find appropriate materials to treat bone fractures. This chapter describes various materials and procedures that are in practice for bone treatment.

## 1.4 Bisphosphonate Based Drugs

The development of diphosphonic acid based drugs for the treatment of bone loss began about three decades ago[21] when trace amounts of polyphosphonates were shown to be capable of inhibiting the crystallization of calcium salts. The collaborative work of several research groups led to the discovery of compounds containing P-N-P, P-C-P (bisphosphonates) and P-C-C-P (diphosphonates) motifs, that confirmed the potential of diphosphonates for the improvement of bone density, as the diphosphonates inhibit the dissolution of hydroxyapatite crystals.[22] By 1969, publications on diphosphonates based

drugs such as Clodronate® indicated their efficacy in resorbing osteoclasts, the cells that destroy bone. Editronate® became the first drug to be used in humans.[3] The selectivity of bisphosphonate drugs for their target organ made it efficient.[23] Further studies showed that the P-C-P backbone was a more effective inhibitor to bone resorption than the P-C-C-P and P-N-P based compounds. A few examples of bisphosphonate based drugs are shown in Table 1.1.

**Table 1.1.** Bisphosphonate based drugs.

| Name | Structure |
|---|---|
| Etidronic acid | 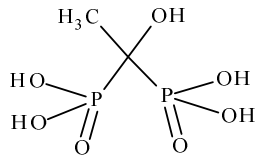 |
| Clodronic acid | 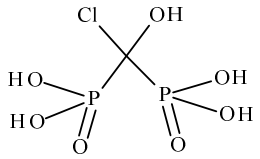 |
| Alendronic acid | 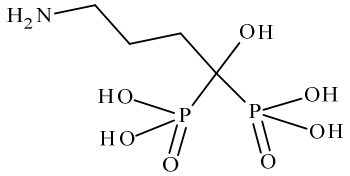 |
| Ibandronic acid | 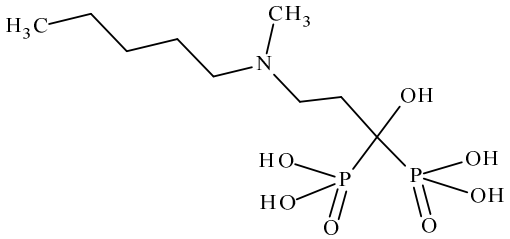 |
| Zoledronic acid | 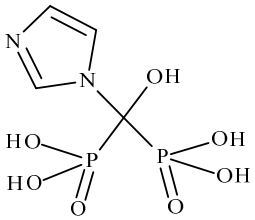 |

## 1.5 Hydroxyapatite

The word apatite is from the Greek word 'apate' meaning to deceive. Three main forms of calcium phosphate compounds include hydroxyapatite (HA)$Ca_5(PO_4)_3(OH)$, fluorapatite $Ca_5(PO_4)_3F$, and chlorapatite $Ca_5(PO_4)_3Cl$. The apatites have an appearance similar to gemstones (Figure 1.3), their main use is in the production of phosphorus containing fertilizers.

**a.** **b.** **c.**

**Figure 1.3.** Apatite based minerals: **a**. Hydroxyapatite,[24] **b**. fluorapatite[25]and **c**. chlorapatite.[26]

The apatites belong to the hexagonal crystal system with two formula units in each unit cell. Figure 1.4 describes the crystal structure of hydroxy, fluoro and chloro apatite.

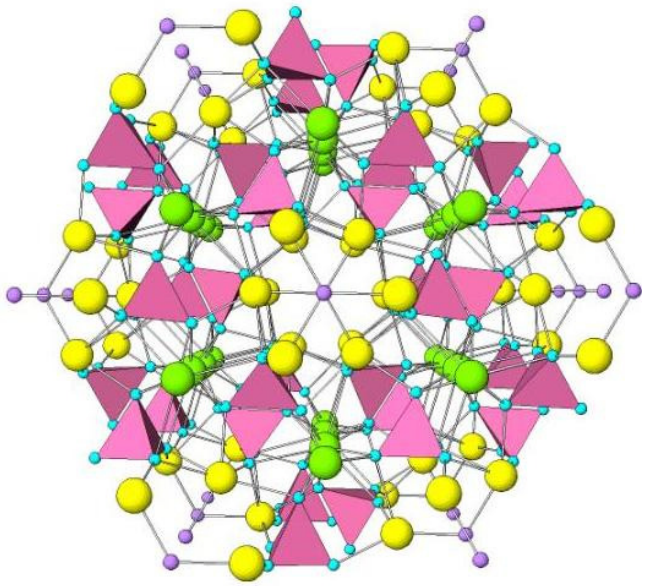

**Figure 1.4.** Crystal structure of Hydroxyapatite, purple sphere represent $OH^-$, pink tetrahedra are $PO_4^{3-}$ polyhedra, yellow sphere is Ca in $CaO_6OH$ and green is representing Ca in the $CaO_9$ polyhedra.

The main mineral component of bone (69 % vol.) and tooth enamel (98 % vol.) is hydroxyapatite (HA).[27] HA is a natural mineral that provides the rigidity needed for bone and teeth functionality. HA is composed of a nanoscale crystallites made up of a Ca/P ratio of 1.67, but also contains other ions such as $CO_3^{2-}$, $F^-$, $Na^+$, $Mg^{2+}$ and $Sr^{2+}$.[27] Being biocompatible and bioactive, synthetic HA has been developed for biomedical applications with the goal to attain materials to substitute natural bone.[19,28] The limitation to the use of HA in load bearing applications is due to its brittleness, lack of toughness and flexibility.[27] However, HA is used as coatings on implants, or fillers.

## 1.6 Bone Substitute Materials

A range of materials including calcium orthophosphates,[6,29,30] bioceramics,[5] glass[31] and polymers[6] are the major materials that are used to repair, replace, regenerate and accelerate the growth rate of bone cells. It is important that these materials form bonds with the surface of living tissue and have the mechanical strength and flexibility to mimic the functions of natural bone.[31] In each of these bone materials, efforts are made to achieve the unique properties that are comparable to HA but in a less dense form. Bioglass®, composed of $SiO_2$, $Na_2O$, CaO and $P_2O_5$ is one of such materials that was discovered to provide the interfacial bonding needed between an implant and the body soft tissue or bone depending on the amount of $SiO_2$ in the glass.[31] The following paragraph will describe each of these materials in more details.

### 1.6.1 Metal Implants

Stainless steel,[32] titanium[33] and transition metal based alloys (NiTi,[34] $Ti_6Al_4V$[35]) are the common metal used for bone replacement as they provide strength and the toughness needed in load bearing parts of the body such as the hip and knee. NiTi alloys are mainly employed as intervertebral infusion devices.[34] Other metals used afor implant applications include alloys containing Mg,[36] Zr, Hf, V, Nb, Ta, Re,[37] Ni, Fe, Cu, Ag[38] in the form of plates, rods and pins as depicted in Figure 1.5.

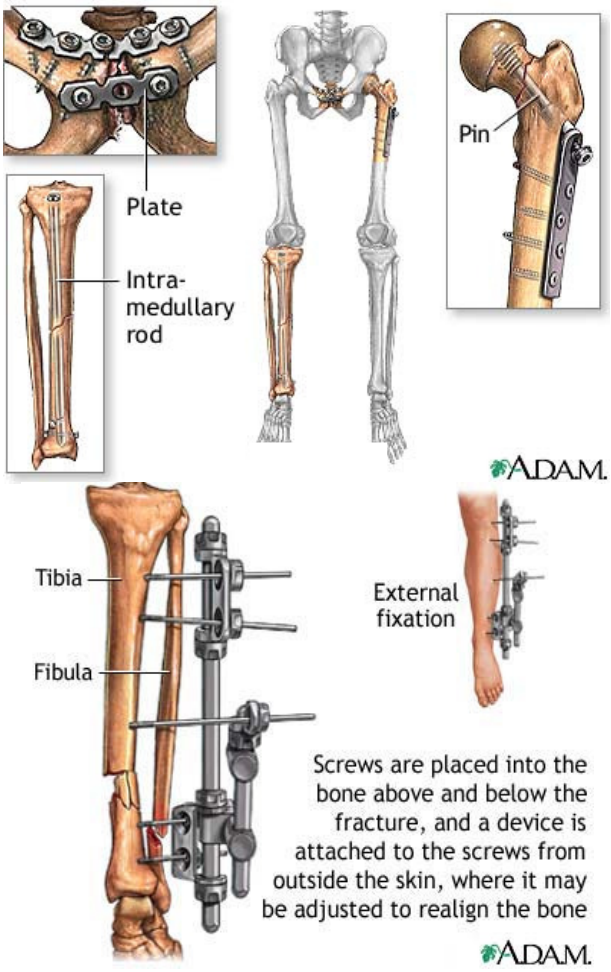


**Figure 1.5.** Bone fixation metal implants and devices.[39]

Placement of metal implants requires a surgical procedure and may include the use of plates, pins and screws.[40] Metals are not biomimetric but rather bioinert, but with time, they may corrode and release ions that react with human fluids to form undesirable precipitates and complexes in the body. In addition, the ions may hydrolyze to form oxides and hydroxides that can greatly trigger pH changes in the body.[41] To prevent the metals from dissolving,[42] they are either coated with biocompatible materials such as hydroxyapatite[43] or polyacrylic acid.[41]

### 1.6.2 Bioceramics

Bioceramics have been developed to facilitate the healing process of bone fractures and in dentistry as restorative materials. Based on their properties, bioceramics may be classified as bioinert (alumina), biodegradable (tricalcium phosphate) or bioactive (hydroxyapatite). Figure 1.6 shows a few examples of bioceramics; ceramic alumina is used for hip replacement.[44] The major problem with these inplants is the wearing over time,[45] and they also make noise. Recently, the US Food and Drug Administration approved the use a ceramic ball and metal socket for total hip replacement following a 2-year clinical trial.[46]

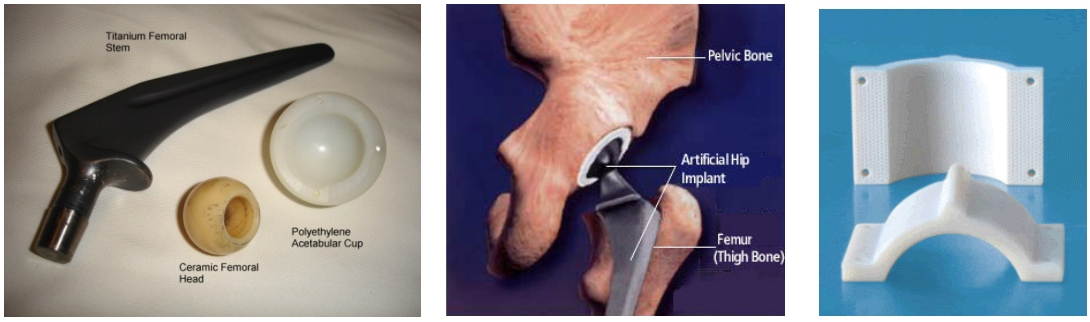


(**a**) (**b**) (**c**)

**Figure 1.6. a**. Examples of bioceramics used for bone treatment[20] **b**. showing hip joint with prosthesis in place,[47] **c**. hydroxyapatite artificial bone .[48]

Aluminum silicates with particle sizes less than 2 micrometers are termed clay. They have been in existence as an important molding material for decades due to their plasticity when wet and hard on drying.[49] Clay can be transformed into ceramics by moistening, casting into various shapes and firing, thereby producing many devices to improve the quality of life. Bioceramics were designed for repair and reconstruction of

various body parts with applications in the health care industry, in dentistry as restorative material and in orthopedics as implants.

Bioceramics used for the repair of musculo-skeletal systems, are categorized as bioinert, resorbable, bioactive, or porous based on the type of interaction or response of the implant in the living tissue. The major setback to the application of bioceramics as implants is their structural weakness.[5]

### 1.6.3 Bioglass

Bioglass is a bioactive glass composed of $Na_2O$, $SiO_2$, CaO and $P_2O_5$. It was first used in 1985 with the trade name MEP® as a device that replaces the bone of the middle ear to treat conductive hearing loss. Bioglass has other uses in head and neck surgery and tooth implants but due to limited mechanical strength and toughness, the material is combined with polymers or metals to enhance mechanical properties.[31]

### 1.6.4 Polymers

Several examples of polymers with biomedical applications exist, notable among them are biocompatible polymers including polyacrylates, poly(acrylonitrile-*co*-vinylchloride), polylysine, polyorthoester, poly($\varepsilon$-caprolactone) (PCL), polylactic acid (PLA), polyglycolic acid (PGA), poly(lactic-co-glycolic acid) (PLGA), polyethylene tetrafluoroethylene (PETE), polyanhydrides, polyurethanes, poly(propylene-*co*-fumarate) (PPF), polymethylmethacrylate (PMMA) and polyethylene (PE).[6,50] An important property of these polymers is viscoelasticity which makes it possible to form complex and porous structures with diverse applications, ranging from coating surfaces (for

example polyurethanes), drug delivery (polyanhydrides), orthopedic purposes (polyanhydrides, PMMA) and bone replacement (PPF, PE). With the exception of PLA, PGA and PGLA the polymers mentioned above are not degradable or bioactive, which is a major setback in their usage. In addition, the polymers lack mechanical strength hence they are usually combined with other materials or polymers.

### 1.6.5 Composite Biomaterials

Whereas each of the bone substitute materials described above has some desirable properties, none of them possesses them all, and this has challenged more research to identify a more suitable material that may better suit the function. As a result, composite materials are explored, aimed at combining the unique properties of well known materials to produce many biomaterials for biomedical applications. Table 1 lists the properties of some materials used as biomaterials.[6,51,52]

**Table 1.2** Properties and limitations to some biomaterials.

| Biomaterial | Examples | Properties | Limitation |
|---|---|---|---|
| Metal | Ti | Mechanical strength for load bearing bone implants | Bioinert, corrosion |
| Glass | Bioglass® | Bioactive | Limited mechanical strength |
| Bioceramic | Alumina | Biocompatible, bioactive | Limited mechanical strength |
| Calcium orthophosphate | Hydroxyapatite, β-tricalcium phosphate | Biocompatible, bioactive, non-toxic, degradable, osteointegrative | Brittle, poor fatigue resistant |
| Polymers | PMMA Polyanhydrides | Viscoelastic, form porous network and channels | Lacks rigidity, ductility, non degradable and bioinert. |

There are many composite materials developed with careful consideration of the mechanical strength, osteogenis, osteoconductivity, osteoinduciveness, biocompatibility, biodegradability, biosorbability, porosity and viscoelasticity that is needed for the

specific functions of the composite biomaterial.[6] Biocomposites and hybrid biomaterials include PMMA/HA, (PMMA = Polymethylmethacrylate),[53] HA/PE or HAPEX™ (PE = polyethylene) used as implants for the shafts in the middle ear,[6] as well as HA/collagen used as biodegradable drug delivery system.[54]

### 1.6.6 Scaffolds for Bone in growth

In tissue engineering, the growth of new cells is enhanced with a scaffold.[55,56] The scaffolds are usually modeled after the structure of the natural bone with pore sizes greater than 100µm to allow for bone cells in-growth.[56] Metal organic frameworks (MOFs) with open pores are currently being explored as scaffolds for bone repair and regeneration.[57] They are advantageous because the open pores allow for fluid transport,[58,59] new tissue vascularization and proliferation of cells.[60,61] We are particularly interested in finding three dimensional (3D) calcium and magnesium phosphonate based frameworks that are both bioactive and mechanically strong to form scaffolds for growing bone.

## 1.7 Conclusions

The bone is the supporting framework of the body that is needed for movement and other essential functions. Diseases and undue pressure on the bone can cause fractures leading to deformity and malfunction. Fortunately, the bone has a built-in mechanism to regenerate, so the goal will be on enhancing the healing process by introduction of a mechanically strong scaffold. Recent findings on the side effects of bisphosphonate drugs used widely to treat osteoporosis make it imperative to find an

alternative and more natural process to heal bone. This is why this project focused on the use of calcium and magnesium phosphonate compounds to prepare scaffolds to improve bone healing. One of the objectives of this work is therefore to prepare bioactive and biocompatible scaffold materials that have appropriate mechanical properties as a bone substitute.

## 1.8 References


(1) Russell, R. G. G. *Bone* **2007**, *40*, S21.
(2) Russell, R. G. G.; Rogers, M. J. *Bone* **1999**, *25*, 97.
(3) Russell, R. G. G. *Bone* **2011**, *49*, 2.
(4) Diel, I. J.; Bergner, R.; Grötz, K. A. *Journal of Supportive Oncology* **2007**, *5*, 475.
(5) Hench, L. L. *J. Am. Ceram. Soc.* **1991**, *74*, 1487.
(6) Dorozhkin, S. *J. Mater. Sci.* **2009**, *44*, 2343.
(7) Bone. *McGraw-Hill Encyclopedia of Science and Technology,* 10th ed; McGraw-Hill Companies, Inc.: New York, 2007; Vol. 3 p; 206.
(8) Thibodeau, G. A. *Anthony's textbook of Anatomy and Physiology,* Times Mirror/Musby College Publishing: St. Louis, 1990, p 20.
(9) Fan, E. *Body Structure and Function*; 7th ed.; Delmar Publishers Inc.: New York, 1989, p 34.
(10) Posner, A. S.; Betts, F. *Acc. Chem. Res.* **1975**, *8*, 273.
(11) Cukrowski, I. P., L.; Barnard, W.; Paul, S. O.; Van Rooyen, P. H.; Liles, D. C *Bone* **2007**, *41*, 668.
(12) Athanasiou K. A., Z., C.F.; Lanctot D. R. J.; Agrawal, C. M.; Wang, X *Tissue Eng.* **2000**, *6*.
(13) Department of Biological Sciences, Indian River State College, Facaulty WebPage, Anatomy and Physiology I, http://faculty.irsc.edu/FACULTY/TFischer/AP1/AP%201%20resources.htm (acessed May 11, 2011).
(14) Fratzl, P. H. G., S.; Paschalis, E. P.; Roschger, P *J. Mater. Chem.* **2004**, *14*, 2115.
(15) Miyamoto, Y.; Kamijo, R. *J. Oral Biosci.* **2010**, *52*, 1.
(16) In *Britannica Concise Encyclopedia*; Encyclopaedia Britannica: 2009.
(17) Johnell, O. K., J. A. *2006, Osteoporos Int.* **2006**, *17*, 1726.
(18) Siris, E. D., P. D. *Osteoporos Int.* **2008**, *19*, 449.
(19) Burge R.T.: Dawson-Hughes B, S. D., Wong J.B.; King, A. B.: Tosteson, A.N.A *J. Bone Min. Res.* **2007**, *22*, 465.
(20) U.S. National Library of Medicine, National Institute of Health, Hip Fracture, http//www.nlm.nih.gov/medlineplus (accessed Mar 20, 2011).
(21) Rogers, M. J.; Crockett, J. C.; Coxon, F. P.; Mönkkönen, J. *Bone* **2011**, *49*, 34.
(22) Robinson, J.; Cukrowski, I.; Marques, H. M. *J. Mol. Struct.* **2006**, *825*, 134.
(23) Cremers, S.; Papapoulos, S. *Bone* **2011**, *49*, 42.
(24) FMF Minerals Galary, The Folch Collection, http://www.mineral-forum.com/message-board/viewtopic.php?t=441 (accessed May, 2011).
(25) The Gemstone List, Fluorapatite, http://www.gemstoneslist.com/fluorapatite.html (accessed May 23, 2011).
(26) ScienceViews.com, Chlorapatite, http://www.scienceviews.com/photo/library/SIA1448.html (accessed May 23, 2011).
(27) Nawawi, N. A.; Alqap, A. S. F.; Sopyan, I. *Recent Pat. Mater. Sci.* **2011**, *4*, 63.
(28) Weiss, D. D. S., M. A.; Woodard, C.R, *Journal of Long-Term Effects of Medical Implants* **2003**, *13*.

(29) Rabiee, S. M.; Moztarzadeh, F.; Solati-Hashjin, M. *J. Mol. Struct.* **2010**, *969*, 172.
(30) Pilliar, R. M.; Filiaggi, M. J.; Wells, J. D.; Grynpas, M. D.; Kandel, R. A. *Biomaterials* **2001**, *22*, 963.
(31) Hench, L. *J. Mater. Sci.: Mater. Med.* **2006**, *17*, 967.
(32) Wang, G.; Xu, M.; Tian, X.; Gong, C. *Hanjie Xuebao* **2011**, *32*, 45.
(33) Kokubo, T.; Kim, H.-M.; Kawashita, M. *Biomaterials* **2003**, *24*, 2161.
(34) Bansiddhi, A. S., T.D; Stupp, S.I.; Dunand, D.C. *Acta* **2008**, *4*, 773.
(35) Bandyopdhyay, A. V. K. R., M.: Bose, S. *JOM* **2011**, *63*, 94.
(36) Cai, Y.; Zhang, S.; Zeng, X.; Sun, D. *J. Mater. Sci.: Mater. Med.* **2011**, *22*, 1633.
(37) Matsuno, H.; Yokoyama, A.; Watari, F.; Uo, M.; Kawasaki, T. *Biomaterials* **2001**, *22*, 1253.
(38) Uo, M.; Watari, F.; Yokoyama, A.; Matsuno, H.; Kawasaki, T. *Biomaterials* **2001**, *22*, 1787.
(39) Saint Thomas Health, Bone Fracture Repair - Series, http://www.sths.com/adm/?f=3&r=100077 (accessed Apr 2, 2011).
(40) Wirth, A. J.; Goldhahn, J.; Flaig, C.; Arbenz, P.; Müller, R.; van Lenthe, G. H. *Bone* **2011**, *49*, 473.
(41) De Giglio, E.; Cafagna, D.; Ricci, M. A.; Sabbatini, L.; Cometa, S.; Ferretti, C.; Mattioli-Belmonte, M. *Journal of Bioactive and Compatible Polymers* **2010**, *25*, 374.
(42) Willumeit, R.; Fischer, J.; Feyerabend, F.; Hort, N.; Bismayer, U.; Heidrich, S.; Mihailova, B. *Acta Biomaterialia* **2011**, *7*, 2704.
(43) Roy, M.; Balla, V. K.; Bose, S.; Bandyopadhyay, A. *Adv. Eng. Mater.* **2010**, *12*, B637.
(44) Sudo, A. U., A. Journal of bone and joint sugery **2006**, *88*.
(45) Taddei, P.; Affatato, S.; Fagnano, C.; Toni, A. *J. Mater. Sci.* **2006**, *41*, 399.
(46) Riley, K.; Administration, T. U. S. D. o. H. H. S. F. D., Ed.; US Fed News Service, Including US State News Washington, DC, June 15, 2011.
(47) http://hipreplacementsurgeryrecovery.org/what-to-expect-in-a-total-hip-replacement-surgery **April, 2011**.
(48) Made-in-China.com, Artificial Bone, http://www.made-in-china.com/showroom/windrainbow/product-detailCqVEDKTlhIcG/China-Artifical-Bone-Biomaterial-Hydroxyapatite-.html (accessed Mach 3, 2011).
(49) Velde, B., *Composition and mineralogy of clay minerals,* Ed.;Springer-Verlag New York, 1995, pp 8-42.
(50) Rezwan, K.; Chen, Q. Z.; Blaker, J. J.; Boccaccini, A. R. *Biomaterials* **2006**, *27*, 3413.
(51) Tadic, D.; Epple, M. *Biomaterials* **2004**, *25*, 987.
(52) Dorozhkin, S. *Materials* **2009**, *2*, 1975.
(53) Itokawa, H.; Hiraide, T.; Moriya, M.; Fujimoto, M.; Nagashima, G.; Suzuki, R.; Fujimoto, T. *Biomaterials* **2007**, *28*, 4922.
(54) Otsuka, M.; Hirano, R. *Colloids Surf., B* **2011**, *85*, 338.
(55) Chen, V. J.; Smith, L. A.; Ma, P. X. *Biomaterials* **2006**, *27*, 3973.
(56) Costa, H.; Mansur, A.; Barbosa-Stancioli, E.; Pereira, M.; Mansur, H. *J. Mater. Sci.* **2008**, *43*, 510.

(57) Salerno, A.; Zeppetelli, S.; Di Maio, E.; Iannace, S.; Netti, P. A. *Biotechnol. Bioeng.* **2011**, *108*, 963.
(58) Karageorgiou, V.; Kaplan, D. *Biomaterials* **2005**, *26*, 5474.
(59) Salerno, A.; Guarnieri, D.; Iannone, M.; Zeppetelli, S.; Di Maio, E.; Iannace, S.; Netti, P. A. *Acta Biomaterialia* **2009**, *5*, 1082.
(60) Silva, M. M. C. G.; Cyster, L. A.; Barry, J. J. A.; Yang, X. B.; Oreffo, R. O. C.; Grant, D. M.; Scotchford, C. A.; Howdle, S. M.; Shakesheff, K. M.; Rose, F. R. A. J. *Biomaterials* **2006**, *27*, 5909.
(61) Petrie Aronin, C. E.; Sadik, K. W.; Lay, A. L.; Rion, D. B.; Tholpady, S. S.; Ogle, R. C.; Botchwey, E. A. *J. Biomed. Mater. Res. Part A* **2009**, *89A*, 632.

# CHAPTER 2

# Metal Organic Frameworks

## 2.1 Introduction

Metal organic frameworks (MOFs) are a class of inorganic-organic hybrid materials based on coordination chemistry.[1] MOFs are also called coordination polymers and are defined as extended arrays composed of metal atoms or clusters that are linked by polyfuctional organic ligands.[2] MOFs are therefore solid state crystalline compounds with geometrically well defined structures, similar to zeolites.[3]

The wide application of MOFs, spans from gas storage,[4] gas separation,[5] catalysis, [1] to use in nonlinear optics, as fluorescence materials in sensors,[6] in molecular recognition in drug delivery[7] and chemical sensing[8,4,51,9,10] are described in details below. The wide variety of applications has led to the proliferation of MOF research over the last 20 years[11] as shown in Figure 2.1. The graph summarizes MOFs reported between 1978-2006.[12]

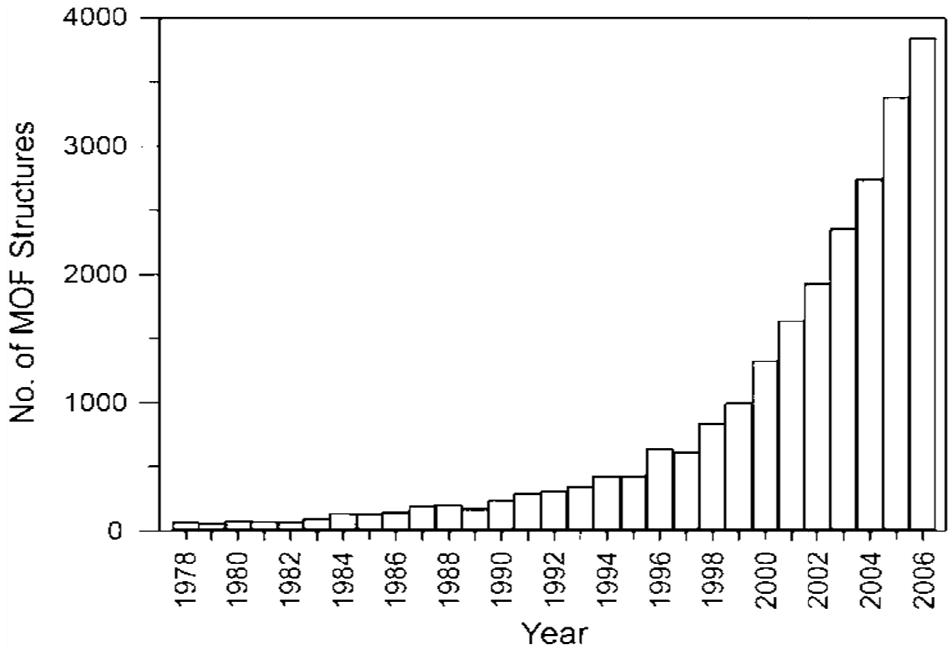


**Figure 2.1.** Number of metal–organic framework (MOF) structures reported in the Cambridge Structural Database (CSD) from 1978 through 2006. The bar graph illustrates the recent drastic increase in the number of reports.

The majority of these MOFs are based on transition metals, only few main group and even fewer s-block metal phosphonates exist.

We are interested in synthesizing metal organic frameworks based on the alkaline earth metals magnesium and calcium in combination with phosphonate ligands of various denticities, as these compounds have potential uses in bone therapy agents.

## 2.2 Metal Organic Frameworks Applications

The quest for a safe, efficient, and affordable storage system for hydrogen fuel has sparked extensive research leading to the synthesis of more than 200 porous MOFs. [13,14]

The advantages of porous MOFs as storage materials include large surface areas and the high volume of open pores.[15] MOFs designed for this purpose are designed to store large volumes of methane (natural gas), acetylene and hydrogen although the storage volumes achieved remain modest. [16] Recently, the synthesis of a MOF with methane storage capacity of 196 $cm^3/cm^3$ has been achieved, exceeding the United States Department of Energy (DEO) methane gas storage capacity of 180 $cm^3/cm^3$ target[17] that has long been the standard. A series of lanthanide based MOFs have also shown reasonable capacity for gas storage.[18,19]

Gas separation is another goal, including the removal of $CO_2$ as the major impurity in natural gas.[20,21] One of the most cost effective methods employed for the removal of atmospheric carbon dioxide by adsorption[22] is based on porous materials including zeolites, alumina and carbonaceous materials. Other gas mixtures such as $O_2/N_2$, $CO/CO_2$, and $CO_2/C_2H_4$ can also be separated by adsorption with MOFs. Recent research has shown that MOFs can also function as solid adsorbents for gas separation because of their characteristic high specific surface area and tunable pore size volume,[23,24] and achieved by employing linkers based on halogens, amine, amide or alkyl groups to affect the host-guest interactions.[9]

## 2.3 Metal Organic Framework Structure and Composition

Two examples of MOFs are shown in Figure 2.1, where the abbreviations bpdc, DMF, trz and BPT stand for biphenyldicarboxylate, N,N′-dimethylformamide, 1,2,4-triazolate and biphenyltriazolate respectively.

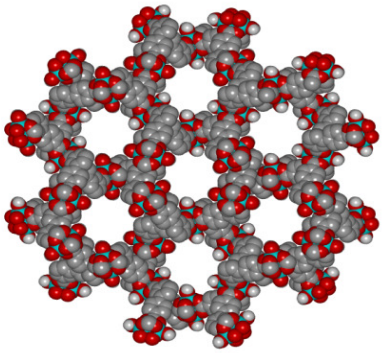

$[Cu(3,4'\text{-bpdc})(H_2O)\cdot 2DMF\cdot 4.5H_2O]_n$[25]

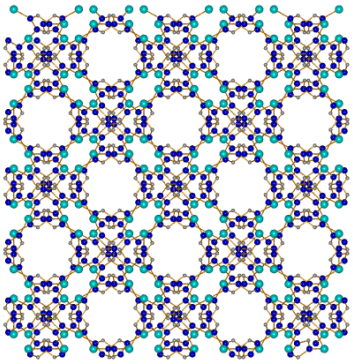

$[Cu_3(trz)_3(OH)_3(H_2O)_4]\cdot 4.5H_2O$ [26]

**Figure 2.2.** Some examples of Metal Organic Frameworks (MOFs).

MOFs with various dimensionality are constructed by the interaction of metal ions with ligands or from the assembly of secondary building units (SBUs) made of small, metal containing clusters in the presence of multidentate organic ligands.

The organic component of a MOF usually serves as a bridge between metal centers. Due to the special role of the organic groups in the building of MOFs, they are often described as spacers or linkers.[27]

Various organic linkers[21,22] have been employed in the synthesis of MOFs, and have been shown to play a major role in framework design. Carboxylate ligand systems are listed in Table 2.1;[28] phosphonate ligands that are employed in this work will be discussed in the next chapter.

**Table 2.1.** Common organic building units in MOFs.

| Organic ligands | |
|---|---|
| 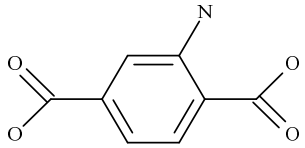 2-amino-1,4-benzenedicarboxylate[29-35] | 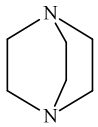 1,4-diazabicyclo[2.2.2]octane[36] |
| 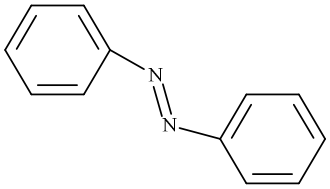 azopyridine[37] | 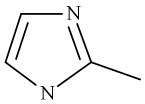 2-methylimidazolate[38,39] |
| 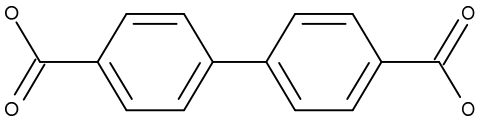 1,4-benzenedicarboxylate[40] | 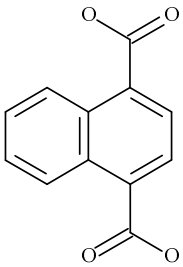 1,4-naphtalenedicarboxylate [41-42] |
| 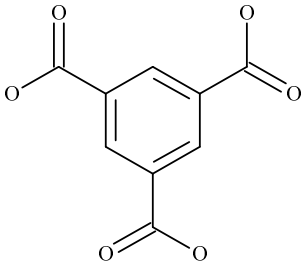 1,3,5-benzenetricarboxylate[43,44] | 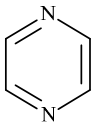 pyrazine[45-47] |

**Table 2.1** Common organic building units in MOFs (continued).

| Organic Ligands | |
|---|---|
| 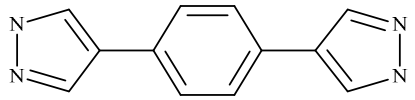 1,4-benzenedi(4'-pyrazolyl)[48] | 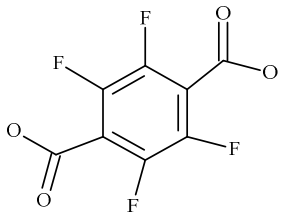 2,3,5,6-tetrafluorobenzene-1,4-dicarboxylate[49] |
| 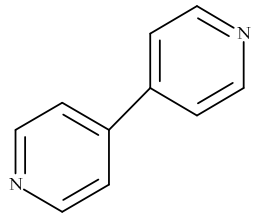 4,4'-bipyridine[28] | 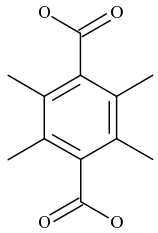 2,3,5,6-tetramethyl-1-4-benzenedicarboxylate[40,50,51] |
| 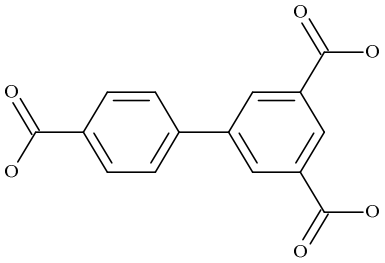 biphenyl-3,4,5-tricarboxylate[26] | 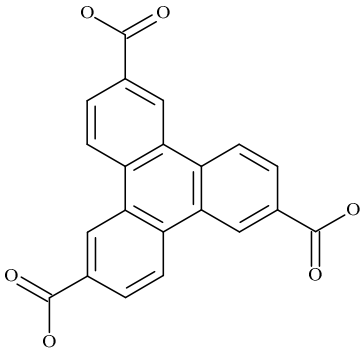 triphenylene-2,6,10-tricarboxylate[52] |

The inorganic subunits in MOFs traditionally comprise of transition metals and to a much lesser extent of main group elements, lanthanides or actinides. Among these, the majority of examples are monometallic, but there are a few heterometallic organic frameworks based on combinations of Cd/Ca, Cd/Sr[53] or Ln/Ba.[54]

Many MOFs have special characteristics such as uniform structured cavities, permanent pores with functionalities, extended network architectures and robust and high surface areas,[12] making them potential hosts for guest molecules.[55] Depending on the type of functional group in the layered framework, the channels may be either hydrophilic or hydrophobic,[12] with functional groups interacting with guest molecules.[56]

One of the greatest challenges in making MOFs is to predict and accurately design the structure of desired final products. The common route for their synthesis is by hydrothermal or solvothermal procedures where reaction conditions such as temperature, type of solvent, pH and concentration of solution are varied leading to diverse structural forms.[57] Limited predictability of structural features can be achieved through a careful selection of inorganic bridging ligands.

## 2.4 Metal Phosphonates

Phosphonate ligands have wide applications in industrial water treatment, oilfield drilling, mineral processing, corrosion control and metal sequestration by complexation. Metal phosphonates often occurring as MOFs displaying microporous structures that are applied in catalysis, sorption and ion exchange.[58] Extensive studies on phosphonate based MOFs gave rise to a large variety of compounds, mainly based on first row

transition metals.[59-64] Limited examples exist for Al, Ga and Pb,[65] and even fewer examples exist for lanthanide and s-block metals.

The study of metal phosphonates has been hindered by the formation of dense, insoluble compounds making it difficult to obtain crystals. In addition, the structures of the phosphonates are also are less predictable than that of the carboxylates.[66,67] The other reason why the field of metal phosphonates is challenging is that the synthesis is often independent of reagent ratios; hence the rational design for the synthesis of a specific targeted compound is challenging.[68]

Despite these setbacks, extensive studies have been conducted on mono-, di-, tri- and tetraphosphonates based on transition metals.[2,69-73] The use of heterofunctional ligands such as carboxyphosphonates[74-77] and sulfonophosphonates [78-80] has led to the preparation of many novel MOFs with interesting structural motifs and properties.[81] Majority of the studies have been conducted on diphosphonates. The vast majority of these are dense, few are microporous, an example being the three-dimensional $\{[Zn(DHBP)](DMF)_2)\}_n$, (DHBP = dihydroxy-2,5-benzenediphosphonate).[82] Other examples include aryl phosphonates based MOFs where the aryl groups in the ligand function as rigid spacers to achieve open structures.[83]

## 2.5 Alkaline Earth Metal Organic Frameworks

Compared to transition metal MOFs, limited examples of MOFs based on alkaline earth metals exist.[84] The s-block metals lack geometric directionality due to the spherical nature of the s-orbital. Furthermore, group II metals are very large requiring an extensive coordination sphere. In addition, the unavailability of energetically accessible d-orbitals

and hence lack of metal- ligand back bonding makes the alkaline earth- ligand bonds weaker and geometrically less well defined than that of the transition metals.[85] Among the group II metals, magnesium,[26,86-88] calcium,[27,84,89-92] strontium,[93-95] and barium[54,96-101] have been explored for MOF synthesis. The main method of synthesis is *via* hydro/solvothermal routes, but recently ionic liquids have also been used.[87] Most of the alkaline earth MOFs are based on carboxylic acids, which display interesting and varying coordination modes based on the number of carboxylic acid functional groups on the ligand as well as the coordination number around the metal center.[102-108]

Considering that the phosphonate MOF has been plagued with insolubility and that heavy alkaline earth metals are large, it is not surprising that very few alkaline earth metal phosphonates have been reported.[109]

## 2.6 Zeolites

The first well defined three-dimensional solid state materials were zeolites. Zeolites are microcrystalline aluminosilicate minerals ($M_{x/n}{}^{n+}[(AlO_2)_x(SiO_2)_y]^{x-}$) with uniform pore size of 0.3-1. 2 nm in diameter.[110,111] The pores may contain a cation, water or other small molecules. Based on their pore size and shape, zeolites can allow specific molecules to pass through their channels hence the zeolites are also termed molecular sieves. Zeolites are used as adsorbents in fields of medicine, agriculture and industry for water purification, as catalysts in nuclear processing and in the production of laundry detergents. In zeolites $[SiO_4]^{n-}$ and $[AlO_4]^{n-}$ units are the building blocks, to provide a network through oxygen bridging.[110]

## 2.7 Porous Metal Organic Frameworks

A porous material is a framework in which guest molecules can be removed or exchanged without loss of framework integrity. [112] The open framework structure depends on the rigidity and directionality of the building units in the framework. The voids in MOFs are usually filled by guest molecules. Examples of MOFs with different pore sizes exist; they are termed microporous (<2nm), mesoporous (2-50nm) [113] or macroporous ( >50nm).[114] Depending on the size of the pores, they might be accessible to small organic molecules while others are too small to incorporate any molecule. Examples include mesoporous MOFs, where the pores are used for drug delivery.[115]

Not all MOFs retain their structure upon removal of guest molecules. Though there are many examples of MOFs containing pores reported in literature, for many, there is no experimental basis to document the stability and accessibility of the pores. Only a limited number of examples exist where the pores have been shown to be reversibly accessible.[116] Many three dimensional MOFs do not meet the criteria for porous materials, such as materials with isolated cavities in the framework that are classified as non-porous.[116]

Careful analysis is needed to establish the porosity of a material. Fluid exchange and isothermal sorption of gases prove permanent porosity for those porous MOFs.[117] Though extensive work has been done to deliberately design material with different pore sizes and shapes, very limited knowledge exists about the mechanism of formation.

## 2.8 Ligand Denticity and Dimensionality in Metal Organic Frameworks

Extensive studies on hybrid metal organic frameworks have improved the understanding of the relationship between ligand denticity and the final architecture of a MOF. Whereas the preferred coordination of the metal in the framework plays a significant role in the determination of MOF geometry, the denticity of the ligand and its binding modes greatly influence the MOF structure, generating intriguing networks of different dimensions. While a basic rationale between these factors exists, the prediction of MOF architecture remains the ultimate challenge.

Occasionally the functional groups on a ligand may be found in the open framework of the MOF structure. These functional groups could be modified to change the property of the MOF. It is of interest to note that the dimensionality of porous MOFs can be maintained even when the ligand bound functional groups in the cavities are carefully modified. The three-dimensional crystal structure of a gadolinium MOF ($\{[Gd_2(N\text{-}BDC)_3(dmf)_4]\}_n$, BDC = benzenedicarboxylate) remains unchanged when the amino functional groups in the cavities were chemically transformed to acetamide ($CH_3CONH$), urethane ($CH_3CH_2NHCONH$-) groups when ethylisocyanate ($CH_3CH_2NCO$) and acetic acid ($CH_3COOH$) are used respectively during the synthesis.[35] Though denticity influences framework dimensionality, synthetic conditions and routes also have a role to play.[77]

## 2.9 Hydrothermal and Solvothermal Synthesis

Hydrothermal synthesis is the preparation of crystalline products based on the increased solubility of inorganic substances in water at temperatures above the boiling

point. Typically, temperatures in the range of 100-350 $^{o}$C, and elevated pressure between 20-25 mTorr are utilized.[114] When the solvent is not water, the process is termed solvothermal. Since the products from a hydrothermal condition are dependent on pressure, temperature, pH, and concentration of the solution, it becomes difficult to predict or even rationalize product formation. The reaction is usually conducted in autoclaves. Autoclaves are steel pressure containers lined with Teflon (polytetrafluoroethylene). Special autoclaves used for hydrothermal synthesis are described as pressure container bombs, digestion tanks or polymerization reactors. Figure 2.3 displays an autoclave bomb.

**Figure 2.3.** Autoclave and Teflon liner for hydrothermal synthesis.[118]

The advantages in using these containers include low incidence of pollution because the solutions are tightly sealed, volatile compounds can dissolve quickly without any loss and the Teflon liner resists corrosion. The disadvantage in using an autoclave is that the reaction cannot be monitored to determine when crystallization occurs. To

circumvent this problem we have used sealed Carius tubes. The aim is to obtain single crystals suitable for X-ray diffraction. To ensure thorough mixing of reagents, aqueous solutions of each reagent were prepared separately prior to combining these.[119] The pressure is often within the tube may be as high as 22.5 mTorr, depending on fill volume and temperature, although due to safety reasons, pressures will be kept below 7.5 mTorr. As the water evaporates the pressure above the solution in the sealed Carius tube increases and this enhances solubility.

A new variant in hydrothermal synthesis involves the use of microwaves, as shown with the formation of nickel phosphonate.[120] Microwave-assisted hydrothermal synthesis reaches high temperatures in a shorter time and thereby reduces crystallization time.

## 2.10 Conclusions

Metal organic frameworks (MOFs) consist of metal centers that are associated through organic linkers that form three-dimensional structures. MOFs are typically robust, rigid and thermally stable; they have a wide range of applications. The properties and special characteristics of magnesium and calcium based MOFs may be explored for medicinal applications such as bone scaffolds. In this work the synthesis and characterization of phosphonate based calcium and magnesium frameworks are explored via hydrothermal and solvothermal synthesis.

## 2.11 References:


(1) Zacher, D.; Schmid, R.; Wöll, C.; Fischer, R. A. *Angew. Chem. Int. Ed.* **2011**, *50*, 176.
(2) Cheetham, A. K.; Rao, C. N. R.; Feller, R. K. *Chem. Commun.* **2006**, 4780.
(3) Zacher, D.; Shekhah, O.; Woll, C.; Fischer, R. A. *Chem. Soc. Rev.* **2009**, *38*, 1418.
(4) Millward, A. R.; Yaghi, O. M. *J. Am. Chem. Soc.* **2005**, *127*, 17998.
(5) Bennett, T. D.; Goodwin, A. L.; Dove, M. T.; Keen, D. A.; Tucker, M. G.; Barney, E. R.; Soper, A. K.; Bithell, E. G.; Tan, J.-C.; Cheetham, A. K. *Phys. Rev. Lett.* **2010**, *104*, 115503.
(6) Bunzli, J.-C. G.; Piguet, C. *Chem. Soc. Rev.* **2005**, *34*, 1048.
(7) Della Rocca, J.; Liu, D.; Lin, W. *Acc. Chem. Res.* **2011**, *44*, 957.
(8) Kreno, L. E.; Leong, K.; Farha, O. K.; Allendorf, M.; Van Duyne, R. P.; Hupp, J. T. *Chem. Rev.* **2011**, *112*, 1105.
(9) Devic, T.; Horcajada, P.; Serre, C.; Salles, F.; Maurin, G.; Moulin, B. a.; Heurtaux, D.; Clet, G.; Vimont, A.; Grenèche, J.-M.; Ouay, B. L.; Moreau, F.; Magnier, E.; Filinchuk, Y.; Marrot, J. m.; Lavalley, J.-C.; Daturi, M.; Férey, G. r. *J. Am. Chem. Soc.* **2009**, *132*, 1127.
(10) Farha, O. K.; Özgür Yazaydın, A.; Eryazici, I.; Malliakas, C. D.; Hauser, B. G.; Kanatzidis, M. G.; Nguyen, S. T.; Snurr, R. Q.; Hupp, J. T. *Nat Chem* **2010**, *2*, 944.
(11) Murray, L. J.; Dinca, M.; Long, J. R. *Chem. Soc. Rev.* **2009**, *38*, 1294.
(12) Long, J. R.; Yaghi, O. M. *Chem. Soc. Rev.* **2009**, *38*, 1213.
(13) Collins, D. J.; Zhou, H.-C. *J. Mater. Chem.* **2007**, *17*, 3154.
(14) Meng, S. M. a. L. In *Energy-related applications of functional porous metal–organic frameworks* Florida, 2011; Vol. 83.
(15) *Chemical Engineering & Technology* **2010**, *33*, 188.
(16) Lim, K. L.; Kazemian, H.; Yaakob, Z.; Daud, W. R. W. *Chemical Engineering & Technology* **2010**, *33*, 213.
(17) Guo, Z.; Wu, H.; Srinivas, G.; Zhou, Y.; Xiang, S.; Chen, Z.; Yang, Y.; Zhou, W.; O'Keeffe, M.; Chen, B. *Angew. Chem. Int. Ed.* **2011**, *50*, 3178.
(18) Jiang, H.-L.; Tsumori, N.; Xu, Q. *Inorg. Chem.* **2010**, *49*, 10001.
(19) Jiang, J.-J.; Pan, M.; Liu, J.-M.; Wang, W.; Su, C.-Y. *Inorg. Chem.* **2010**, *49*, 10166.
(20) Yang, Q.; Zhong, C. *The Journal of Physical Chemistry B* **2006**, *110*, 17776.
(21) Martin-Calvo, A.; Garcia-Perez, E.; Manuel Castillo, J.; Calero, S. *PCCP* **2008**, *10*, 7085.
(22) Cazorla, C.; Shevlin, S. A.; Guo, Z. X. *J. Phys. Chem. C* **2011**, *115*, 10990.
(23) Hayashi, H.; Cote, A. P.; Furukawa, H.; O/'Keeffe, M.; Yaghi, O. M. *Nat Mater* **2007**, *6*, 501.
(24) Mu, B.; Walton, K. *Adsorption* **2011**, *17*, 777.
(25) Feng, L.; Chen, Z.; Liao, T.; Li, P.; Jia, Y.; Liu, X.; Yang, Y.; Zhou, Y. *Crystal Growth Des.* **2009**, *9*, 1505.
(26) Guo, Z.; Li, G.; Zhou, L.; Su, S.; Lei, Y.; Dang, S.; Zhang, H. *Inorg. Chem.* **2009**, *48*, 8069.

(27) Liang, P.-C.; Liu, H.-K.; Yeh, C.-T.; Lin, C.-H.; Zima, V. t. z. *Cryst. Growth Des.* **2011**, *11*, 699.
(28) Lin, H.; Maggard, P. A. *Inorg. Chem.* **2009**, *48*, 8940.
(29) Savonnet, M.; Bazer-Bachi, D.; Bats, N.; Perez-Pellitero, J.; Jeanneau, E.; Lecocq, V.; Pinel, C.; Farrusseng, D. *J. Am. Chem. Soc.* **2010**, *132*, 4518.
(30) Hinterholzinger, F.; Scherb, C.; Ahnfeldt, T.; Stock, N.; Bein, T. *Phys. Chem. Chem. Phys.* **2010**, *12*, 4515.
(31) Garibay, S. J.; Wang, Z.; Cohen, S. M. *Inorg. Chem. (Washington, DC, U. S.)* **2010**, *49*, 8086.
(32) Wang, Z.; Tanabe, K. K.; Cohen, S. M. *Chem.--Eur. J.* **2010**, *16*, 212.
(33) Hao, X.-R.; Wang, X.-L.; Su, Z.-M.; Shao, K.-Z.; Zhao, Y.-H.; Lan, Y.-Q.; Fu, Y.-M. *Dalton Trans.* **2009**, 8562.
(34) Song, Y.-F.; Cronin, L. *Angew. Chem., Int. Ed.* **2008**, *47*, 4635.
(35) Costa, J. S.; Gamez, P.; Black, C. A.; Roubeau, O.; Teat, S. J.; Reedijk, J. *Eur. J. Inorg. Chem.* **2008**, 1551.
(36) Chen, Z.; Xiang, S.; Arman, H. D.; Li, P.; Zhao, D.; Chen, B. *Eur. J. Inorg. Chem.* **2011**, *2011*, 2227.
(37) Zhu, L.-N.; Liang, M.; Wang, Q.-L.; Wang, W.-Z.; Liao, D.-Z.; Jiang, Z.-H.; Yan, S.-P.; Cheng, P. *J. Mol. Struct.* **2003**, *657*, 157.
(38) Dang, F.; Wang, X.; Han, G.; Yao, Y. *Monatshefte für Chemie / Chemical Monthly* **2009**, *140*, 615.
(39) Schubert, D. M.; Visi, M. Z.; Knobler, C. B. *Main Group Chem.* **2008**, *7*, 311.
(40) Braun, M. E.; Steffek, C. D.; Kim, J.; Rasmussen, P. G.; Yaghi, O. M. *Chem. Commun.* **2001**, 2532.
(41) Mulfort, K. L.; Hupp, J. T. *J. Am. Chem. Soc.* **2007**, *129*, 9604.
(42) Sapchenko, S. A.; Samsonenko, D. G.; Dybtsev, D. N.; Melgunov, M. S.; Fedin, V. P. *Dalton Trans.* **2011**, *40*, 2196.
(43) Sun, Y.-Q.; Gao, D.-Z.; Xu, Y.-Y.; Zhang, G.-Y.; Fan, L.-L.; Li, C.-P.; Hu, T.-L.; Liao, D.-Z.; Zhang, C.-X. *Dalton Trans.* **2011**, *40*, 5528.
(44) Harvey, S. D.; Eckberg, A. D.; Thallapally, P. K. *J. Sep. Sci.* **2011**, *34*, 2418.
(45) Ingleson, M. J.; Barrio, J. P.; Bacsa, J.; Steiner, A.; Darling, G. R.; Jones, J. T. A.; Khimyak, Y. Z.; Rosseinsky, M. J. *Angew. Chem., Int. Ed.* **2009**, *48*, 2012.
(46) Amo-Ochoa, P.; Givaja, G.; Miguel, P. J. S.; Castillo, O.; Zamora, F. *Inorg. Chem. Commun.* **2007**, *10*, 921.
(47) Zhu, M.; Peng, J.; Pang, H.-J.; Zhang, P.-P.; Chen, Y.; Wang, D.-D.; Liu, M.-G.; Wang, Y.-H. *Inorg. Chim. Acta* **2011**, *370*, 260.
(48) Choi, H. J.; Dinca, M.; Dailly, A.; Long, J. R. *Energy and Environmental Science* **2010**, *3*, 117.
(49) Yoon, J. H.; Choi, S. B.; Oh, Y. J.; Seo, M. J.; Jhon, Y. H.; Lee, T.-B.; Kim, D.; Choi, S. H.; Kim, J. *Catal. Today* **2007**, *120*, 324.
(50) He, H.; Dai, F.; Sun, D. *Dalton Trans.* **2009**, 763.
(51) Braun, M. E.; Steffek, C. D.; Kim, J.; Rasmussen, P. G.; Yaghi, O. M. *Chem. Commun. (Cambridge, U. K.)* **2001**, 2532.
(52) Wang, X.-S.; Ma, S.; Yuan, D.; Yoon, J. W.; Hwang, Y. K.; Chang, J.-S.; Wang, X.; Jorgensen, M. R.; Chen, Y.-S.; Zhou, H.-C. *Inorg. Chem. (Washington, DC, U. S.)* **2009**, *48*, 7519.

(53) Lin, J.-D.; Wu, S.-T.; Li, Z.-H.; Du, S.-W. *Dalton Trans.* **2010**, *39*, 10719.
(54) Zhao, X.-Q.; Zuo, Y.; Gao, D.-L.; Zhao, B.; Shi, W.; Cheng, P. *Cryst. Growth Des.* **2009**, *9*, 3948.
(55) Noro, S.-i.; Kitagawa, S.; Kondo, M.; Seki, K. *Angew. Chem. Int. Ed.* **2000**, *39*, 2081.
(56) Salles, F.; Bourrelly, S.; Jobic, H.; Devic, T.; Guillerm, V.; Llewellyn, P.; Serre, C.; Ferey, G. r.; Maurin, G. *The Journal of Physical Chemistry C* **2011**, *115*, 10764.
(57) Chen, B.; Ma, S.; Zapata, F.; Fronczek, F. R.; Lobkovsky, E. B.; Zhou, H.-C. *Inorg. Chem.* **2007**, *46*, 1233.
(58) Katharina M, F. *Coord. Chem. Rev.* **2008**, *252*, 856.
(59) Zapf, P. J.; Rose, D. J.; Haushalter, R. C.; Zubieta, J. *J. Solid State Chem.* **1996**, *125*, 182.
(60) Yucesan, G.; Golub, V.; O'Connor, C. J.; Zubieta, J. *Dalton Trans.* **2005**, 2241.
(61) Salta, J. R.; Zubieta, J. A.; American Chemical Society: 1996, p INOR.
(62) Jones, S.; Zubieta, J.; Royal Society of Chemistry: 2012, p 192.
(63) Finn, R. C.; Zubieta, J. *Inorg. Chim. Acta* **2002**, *332*, 191.
(64) De, B. P.; Ouellette, W.; Liu, H.; O'Connor, C. J.; Zubieta, J. *CrystEngComm* **2010**, *12*, 446.
(65) Lei, C.; Mao, J.-G.; Sun, Y.-Q.; Zeng, H.-Y.; Clearfield, A. *Inorg. Chem.* **2003**, *42*, 6157.
(66) Shimizu, G. K. H.; Vaidhyanathan, R.; Taylor, J. M. *Chem. Soc. Rev.* **2009**, *38*, 1430.
(67) Clearfield, A. In *Prog. Inorg. Chem.*; John Wiley & Sons, Inc.: 2007, p 371.
(68) Costantino, F.; Ienco, A.; Midollini, S. *Cryst. Growth Des.* **2009**, *10*, 7.
(69) Clearfield, A. *Dalton Trans.* **2008**, 6089.
(70) Konar, S.; Zoń, J.; Prosvirin, A. V.; Dunbar, K. R.; Clearfield, A. *Inorg. Chem.* **2007**, *46*, 5229.
(71) Sergienko, V. S.; Afonin, E. G.; Aleksandrov, G. G. *Russ. J. Coord. Chem.* **1999**, *25*, 123.
(72) Mao, J.-G.; Wang, Z.; Clearfield, A. *Inorg. Chem.* **2002**, *41*, 2334.
(73) Mao, J.-G.; Wang, Z.; Clearfield, A. *J. Chem. Soc., Dalton Trans.* **2002**, 4457.
(74) Svoboda, J.; Zima, V.; Beneš, L.; Melánová, K.; Vlček, M. *Inorg. Chem.* **2005**, *44*, 9968.
(75) Svoboda, J.; Zima, V.; Beneš, L.; Melánová, K.; Trchová, M.; Vlček, M. *Solid State Sciences* **2008**, *10*, 1533.
(76) Chen, Z.; Zhou, Y.; Weng, L.; Yuan, C.; Zhao, D. *Chem.--Asian J.* **2007**, *2*, 1549.
(77) Bauer, S.; Bein, T.; Stock, N. *Inorg. Chem.* **2005**, *44*, 5882.
(78) Du, Z.-Y.; Wen, H.-R.; Xie, Y.-R. *J. Mol. Struct.* **2008**, *891*, 272.
(79) Du, Z.-Y.; Xu, H.-B.; Mao, J.-G. *Inorg. Chem.* **2006**, *45*, 9780.
(80) Du, Z.-Y.; Xu, H.-B.; Mao, J.-G. *Inorg. Chem.* **2006**, *45*, 6424.
(81) Yang, E.-C.; Liu, Z.-Y.; Shi, X.-J.; Liang, Q.-Q.; Zhao, X.-J. *Inorg. Chem.* **2010**, *49*, 7969.
(82) Liang, J.; Shimizu, G. K. H. *Inorg. Chem.* **2007**, *46*, 10449.

(83) Jaffres, P.-A.; Couthon-Gourves, H.; Haelters, J.-P.; Hix, G. B.; Perez, O.; Caignert, V.; Boudin, S.; Rueff, J.-M. *Phosphorus, Sulfur Silicon Relat. Elem.* **2011**, *186*, 906.
(84) Volkringer, C.; Loiseau, T.; Férey, G.; Warren, J. E.; Wragg, D. S.; Morris, R. E. *Solid State Sciences* **2007**, *9*, 455.
(85) Hanusa, T. P. *Chem. Rev.* **1993**, *93*, 1023.
(86) Dietzel, P. D. C.; Blom, R.; Fjellvaag, H. *Eur. J. Inorg. Chem.* **2008**, 3624.
(87) Wu, Z.-F.; Hu, B.; Feng, M.-L.; Huang, X.-Y.; Zhao, Y.-B. *Inorg. Chem. Commun.* **2011**, *14*, 1132.
(88) Zhang, D.-J.; Song, T.-Y.; Zhang, P.; Shi, J.; Wang, Y.; Wang, L.; Ma, K.-R.; Yin, W.-R.; Zhao, J.; Fan, Y.; Xu, J.-N. *Inorg. Chem. Commun.* **2007**, *10*, 876.
(89) Jiang, C.-H.; Song, L.-F.; Jiao, C.-L.; Zhang, J.; Sun, L.-X.; Xu, F.; Zhang, H.-Z.; Xu, Q.-Y.; Gabelica, Z. *J. Therm. Anal. Calorim.* **2011**, *103*, 1095.
(90) Chen, N.; Zhang, J.; Gao, Y.-C.; Yang, Z.-L.; Lu, H.-J.; Li, G. *J. Coord. Chem.* **2011**, *64*, 2554.
(91) Platero-Prats, A. E.; de, l. P.-O. s. V. A.; Snejko, N.; Monge, A.; Gutierrez-Puebla, E. *Chem.--Eur. J.* **2010**, *16*, 11632.
(92) Kim, M. K.; Bae, K.-L.; Ok, K. M. *Cryst. Growth Des.* **2011**, *11*, 930.
(93) Chen, S.; Shuai, Q.; Gao, S. *Z. Anorg. Allg. Chem.* **2008**, *634*, 1591.
(94) Lo, S.-H.; Liu, H.-K.; Zhan, J.-X.; Lin, W.-C.; Kao, C.-C.; Lin, C.-H.; Zima, V. *Inorg. Chem. Commun.* **2011**, *14*, 1602.
(95) Luo, F.; Che, Y.-x.; Zheng, J.-m. *Inorg. Chem. Commun.* **2008**, *11*, 142.
(96) Chen, S.; Shuai, Q.; Gao, S. *Z. Anorg. Allg. Chem.* **2008**, *634*, 1591.
(97) Chen, K.; Feng, X.; Liang, L.; Wang, Q.; Cong, H.; Tao, Z.; Xue, S.; Zhu, Q.; Guizhou University, Peop. Rep. China . 2011, p 17pp.
(98) Ma, K.-R.; Zhu, Y.-L.; Yin, Q.-F.; Hu, H.-Y.; Ma, F. *J. Chem. Res.* **2010**, *34*, 705.
(99) Mukherjee, R.; Bunge, S. D.; Brasch, N. E. *J. Coord. Chem.* **2010**, *63*, 2821.
(100) Wen, L.-L.; Wang, F.-M.; Leng, X.-K.; Wang, M.-M.; Meng, Q.-J.; Zhu, H.-Z. *J. Inorg. Organomet. Polym. Mater.* **2010**, *20*, 313.
(101) Xiao, D.; Chen, H.; Zhang, G.; Sun, D.; He, J.; Yuan, R.; Wang, E. *Cryst. Eng.* **2011**, *13*, 433.
(102) Briggman, B.; Oskarsson, A. *Acta Crystallographica Section B* **1978**, *34*, 3357.
(103) Karipides, A.; Reed, A. T. *Acta Crystallographica Section B* **1980**, *36*, 1377.
(104) Gil de Muro, I.; Insausti, M.; Lezama, L.; Pizarro, J. L.; Arriortua, M. I.; Rojo, T. *Eur. J. Inorg. Chem.* **1999**, *1999*, 935.
(105) Yokomori, Y.; Flaherty, K. A.; Hodgson, D. J. *Inorg. Chem.* **1988**, *27*, 2300.
(106) Karipides, A.; Ault, J.; Reed, A. T. *Inorg. Chem.* **1977**, *16*, 3299.
(107) Kam, K. C.; Young, K. L. M.; Cheetham, A. K. *Crystal Growth & Design* **2007**, *7*, 1522.
(108) Appelhans, L. N.; Kosa, M.; Radha, A. V.; Simoncic, P.; Navrotsky, A.; Parrinello, M.; Cheetham, A. K. *J. Am. Chem. Soc.* **2009**, *131*, 15375.
(109) Cao, G.; Lynch, V. M.; Swinnea, J. S.; Mallouk, T. E. *Inorg. Chem.* **1990**, *29*, 2112.
(110) Jiang, J.; Babarao, R.; Hu, Z. *Chem. Soc. Rev.* **2011**, *40*, 3599.
(111) S. M. Auerbach, K. A. C. In *Part V, Applications*; P. K. Dutta, M. D., Ed. New York, 2003, p 833.

(112) Rowsell, J. L. C.; Yaghi, O. M. *Microporous Mesoporous Mater.* **2004**, *73*, 3.
(113) Fang, Q. R.; Makal, T. A.; Young, M. D.; Zhou, H. C. *Comments Inorg. Chem.* **2010**, *31*, 165.
(114) Attfield, J. P. In *Encyclopedia of Inorganic Chemistry*; Second ed.; King, R. B., Ed.; John Wiley and Sons Ltd.: Chichester, 2005; Vol. VII.
(115) Arruebo, M. *Wiley Interdisciplinary Reviews: Nanomedicine and Nanobiotechnology* **2012**, *4*, 16.
(116) Fletcher, A. J.; Thomas, K. M.; Rosseinsky, M. J. *J. Solid State Chem.* **2005**, *178*, 2491.
(117) Barton, T. J.; Bull, L. M.; Klemperer, W. G.; Loy, D. A.; McEnaney, B.; Misono, M.; Monson, P. A.; Pez, G.; Scherer, G. W.; Vartuli, J. C.; Yaghi, O. M. *Chem. Mater.* **1999**, *11*, 2633.
(118) Institute of nano Technology Home Page; Going lead-free using hydrothermal synthesis, http://www.nano.org.uk/news/1096/ (accessed Feb, 2012).
(119) Li, J. Q.; Sun, W. A.; Ao, W. Q.; Tang, J. N. *J. Magn. Magn. Mater.* **2006**, *302*, 463.
(120) Newalkar, B.; Chiranjeevi, T.; Choudary, N.; Komarneni, S. *J. Porous Mater.* **2008**, *15*, 271.

# CHAPTER 3

# Ligand Systems

## 3.1 Introduction

Several phosphorus based compounds of magnesium and calcium with diverse structural motifs are described in this thesis. The target compounds are based on a group of phosphonate, phosphinate and phosphite ligands (Figure 3.1). Also included is one compound based on formic acid ($HCO_2H$) shown in Figure 3.2, obtained as a decomposition product from the solvent dimethyl formamide (DMF). This chapter provides a detailed discussion on the ligands utilized, including phenylphosphinic acid (HPPA), phenylphosphonic acid ($H_2PPA$), phosphonic acid ($H_3PO_3$), phosphoric acid ($H_3PO_4$), methylenediphosphonic acid ($H_4MDPA$), ethylenediphosphonic acid ($H_4EDPA$), propylenediphosphonic acid , 4,4′-biphenyldiphosphonic acid ($H_4BDPA$), 4-(4′-phosphonophenoxy) phenyl phosphonic acid ($H_4PPPA$), amino trimethylenephosphonic acid ($H_6ATMPA$) and ethylenediamine tetramethylene-phosphonic acid ($H_8EDTMPA$), as summarized in Table 3.1.

Two of the ligands, HPPA and $H_3PO_3$ were commercially obtained while $H_3PO_4$ was a decomposition product from ethylenediphosphonic acid. $H_4MDPA$ was a gift from the Zubieta laboratory, while $H_4EDPA$, $H_4PDPA$, $H_4BDPA$, $H_4PPPA$ $H_6ATMPA$ and $H_8EDTMPA$ ligands were synthesized. Two methods outlined below were employed for the syntheses of the ligands; the Michaelis-Arbuzov's reaction and a Mannich-type reaction. The ligands $H_4EDP$, $H_4PDPA$, $H_4BDPA$ and $H_4PPPA$ were synthesized by the Michaelis-Arbuzov reaction while $H_6ATMPA$ and $H_8EDTMPA$ ligands were synthesized by the Mannich reaction.

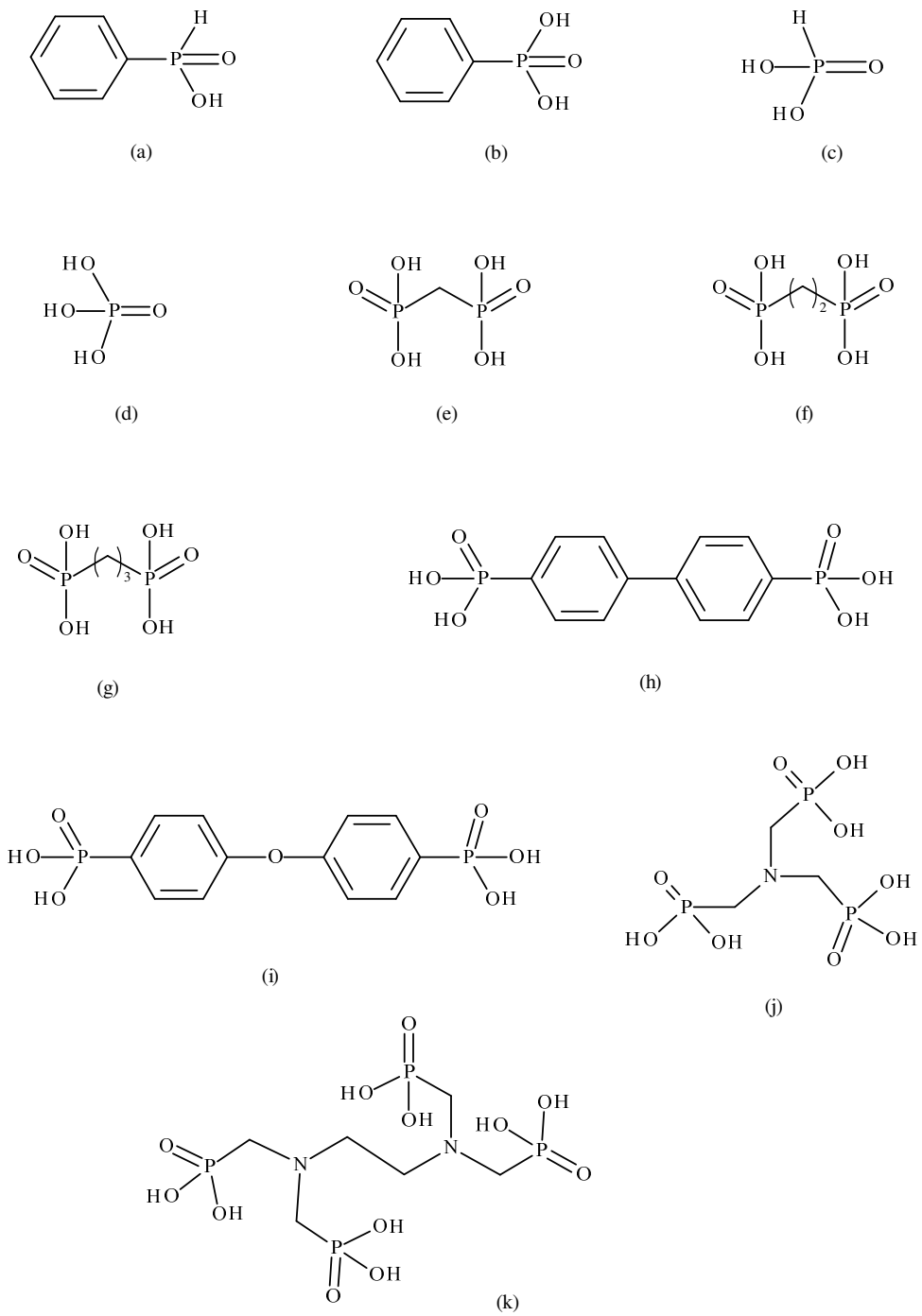


**Figure 3.1.** P-based ligands utilized in this work, **(a).** phenylphosphinic acid (HPPA), **(b).** phenylphosphonic acid ($H_2PPA$), **(c).** phosphonic acid ($H_3PO_3$), **(d).** phosphoric acid ($H_3PO_4$), **(e).** methylenediphosphonic acid ($H_4MDPA$), **(f).** ethylenediphosphonic acid ($H_4EDPA$), **(g).** propylenediphosphonic acid ($H_4PDPA$), **(h).** 4,4-biphenyldiphosphonic acid (H4BPDPA), **(i).** 4-(4′-phosphonophenoxy) phenylphosphonic acid ($H_4PPPA$), **(j).** amino trimethylenephosphonic acid ($H_6ATMPA$) and **(k).** ethylenediamine tetramethylenephosphonic acid ($H_8EDTMPA$).

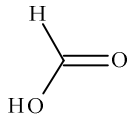


**Figure 3.2.** Formic acid ligand from decomposition of DMF solvent.

Several of the above mentioned phosphinic and phosphonic acids have important applications as drugs for calcium related disorders,[1-5] as well as scale and corrosion inhibition.[6-9]

In this chapter, some key properties of the ligands, such as the stepwise deprotonation of the diphosphonates and zwitterionic effect of the triphosphonates are also discussed.

## 3.2 Nomenclature of Phosphorus Containing Ligands

Phosphorus plays a major role in the biochemistry of all living organisms. Table 3.1 gives a summary of some of the most common phosphorus oxoacids along with their oxidation states.[10] Phosphonic and diphosphonic acids are called phosphonates in their deprotonated state while deprotonated phosphinic acid is termed phosphinate. Anions of phosphorus acid are termed phosphite and those of phosphoric acid are called phosphate. This is summarized in Table 3.2.

**Table 3.1**. Names of common phosphorus oxyacids

| Structure | Formula/Name | Oxidation state of P |
|---|---|---|
| 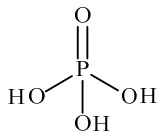 | Phosphoric acid<br>or<br>Orthophosphoric acid<br>($H_3PO_4$) | 5 |
| 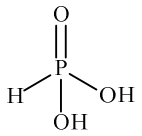 | Phosphorous acid<br>($H_3PO_3$) | 3 |
| 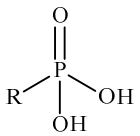 | Phosphonic acid<br>($RPO_3H_2$)<br>R = alkyl, aryl | 3 |
| 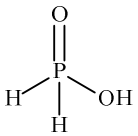 | Phosphinic acid<br>($H_3PO_2$) | 1 |
| 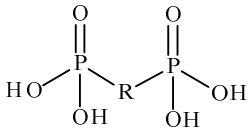 | Diphosphonic acid<br>($R(PO_3H_2)_2$)<br>R = alkyl, aryl | 3 |
| 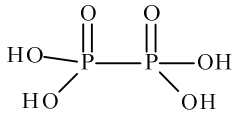 | Hypophosphoric acid<br>($H_4P_2O_6$) | 4 |
| 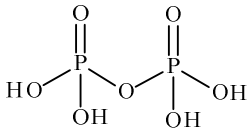 | Pyrophosphoric acid<br>($H_4P_2O_7$) | 5 |

**Table 3.2** Nomenclature of the deprotonated forms of P-based acids

| Name of acid | Name of deprotonated form |
|---|---|
| Phosphoric acid | Phosphate |
| Phosphorus acid | Phosphite |
| Phosphonic acid | Phosphonate |
| Diphosphonic acid | Diphosphonate |
| Phosphinic acid | Phosphinate |

### 3.3 Ligand Deprotonation

Significant literature exists on metal organic frameworks (MOFs) based on ethylenediphosphonic acid, $H_2O_3P(CH_2)_2PO_3H_2$.[11] This ligand system depicts a variety of metal binding modes and deprotonation types. The degree of deprotonation is pH dependent. The most common deprotonation state is based on a double deprotonation, involving a single deprotonation on each of the phosphonate units, leaving a symmetrical arrangement. More rare is a combination of single/double deprotonation, as seen in the novel $\{CaNa[(HO_3P(CH_2)_2PO_3H)(HO_3P(CH_2)_2PO_3H_2)_n]\}$compound **11** in chapter 7 and the literature examples of $(M^{III}(H_2O)(HO_3P(CH_2)_2PO_3)$ where M = Fe, Ga, Al.[12] Diphosphonates of the alkali metals typically exhibit single deprotonation of only one

phosphate group, an example includes $Na(HO_3P(CH_2)_2PO_3H_2)$.[13] Scheme 3.1 illustrates the stepwise deprotonation for ethylenediphosphonic acid .

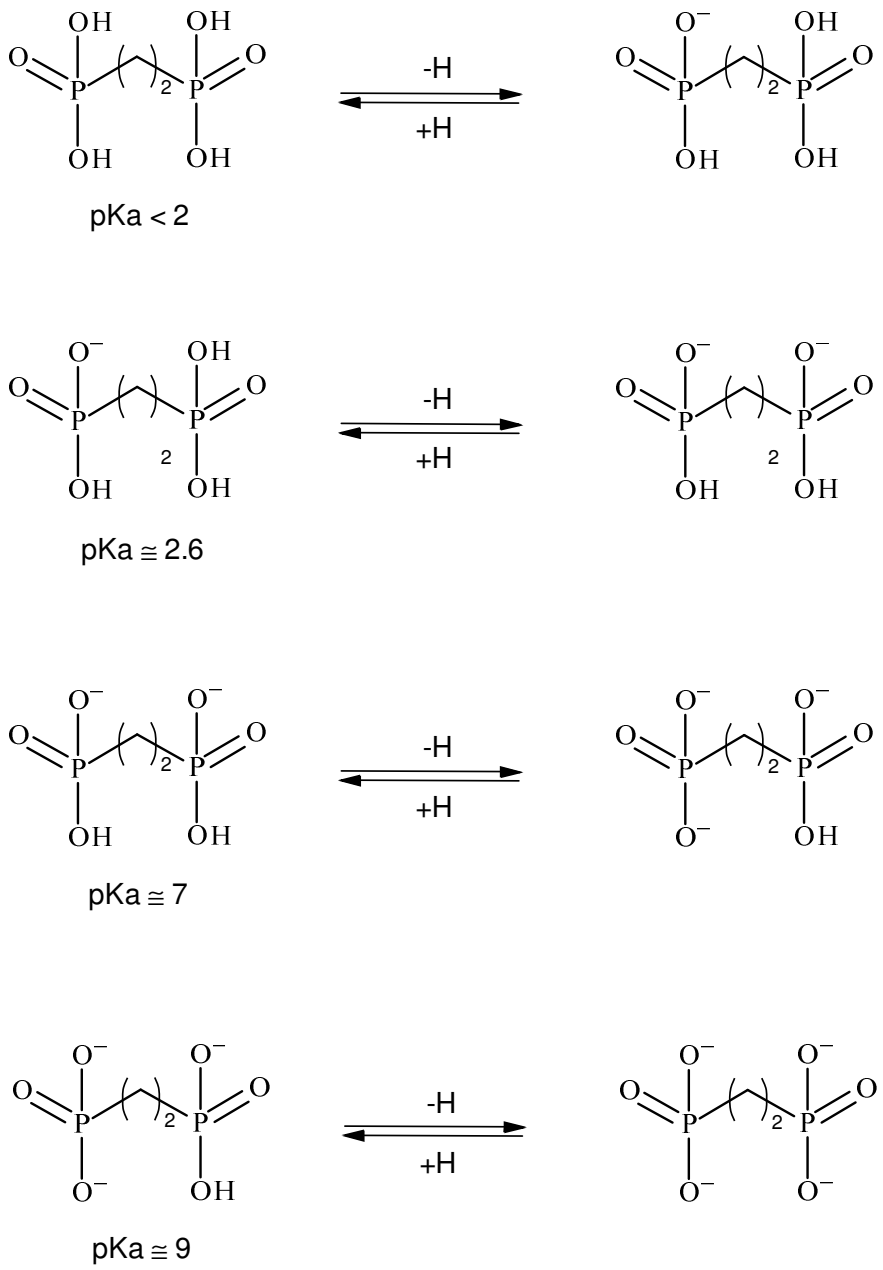


**Scheme 3.1.** Stepwise deprotonation of ethylenediphosphonic acid (f).

## 3.4. General Synthetic Routes

Two types of reaction routes were employed for the synthesis of ligands. These include Michealis- Arbuzov reaction for the synthesis of the esters of $H_4$EDP and $H_4$PDPA followed by acid hydrolysis to afford the corresponding acids. The Mannich reaction was used for the preparation of $H_4$BDPA, $H_4$PPPA and $H_6$ATMPA ligands.

### 3.4.1 Michealis-Arbuzov Reaction

The synthesis of phosphonates ($RPO(OR)_2$) by the treatment of trialkyl phosphate with alkyl halides was first discovered by Augustus Michaelis and further explored by Alexandra Arbuzov, hence the name Michealis-Arbuzov or simply Arbuzov reaction.[14,15] The reaction involves the formation of a carbon-phosphorus bond and is useful in the preparation of phosphinates ($R_2PO(OR)$) and phosphine oxide ($OPR_3$). The R group may be alkyl, aryl or an acyl group. The most commonly used alkyl halides RX are based on X = Cl, Br, I. A modified form of the Arbuzov reaction is employed for the synthesis of the alkylene diphosphonate compounds.[16] The reaction is shown in Scheme 3.2.

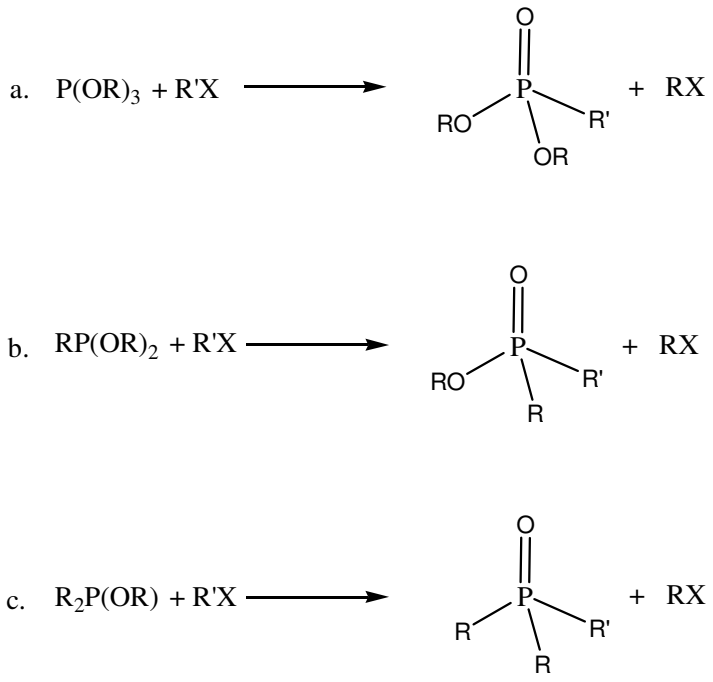


**Scheme 3.2.** Michealis-Arbuzov reaction for the synthesis of 3.2a. phosphonate, 3.2b. phosphinate, 3.2c. phosphine oxide

The mechanism of the reaction involves a $S_N2$ nucleophilic attack of the alkyl group in R'X by the lone pair of electrons on phosphorus to form an unstable intermediate. In a second step, dissociation of one alkyl group from the phosphite results in P=O bond formation yielding the phosphonate. The halide then attacks the alkyl to form the new alkyl halide RX (Scheme 3.3). [17] When phenyl groups are involved, a nickel catalyst is required for the formation of the phenyl phosphonate.[18]

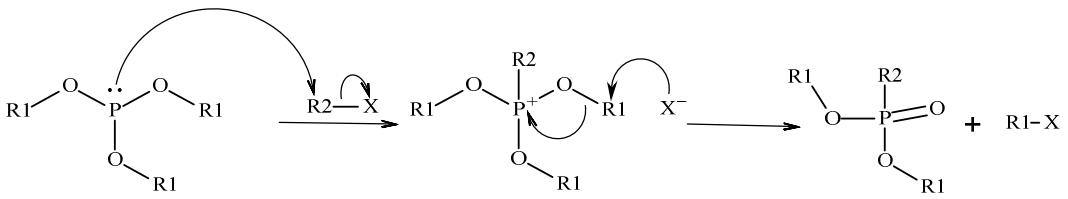


**Scheme 3.3.** Mechanism of Michealis-Arbuzov reaction

### 3.4.2 Mannich Reaction

In the Mannich reaction, ammonia or a primary or secondary amine reacts with a carbonyl group to form a Schiff's base, which under condensation affords a N-C bond.[19,20]

### 3.4.3 Acid Hydrolysis

In the preparation of the diphosphonates, hydrolysis of the four alkyl esters *via* concentrated HCl leads to the formation of the diphosphonic acids (Scheme 3.4).[21]

$$R_2O_3P(CH_2)_nPO_3R_2 + 4HCl \longrightarrow H_2O_3P(CH_2)_nPO_3H_2 + 4RCl$$

**Scheme 3.4.** Hydrolysis of tetraalkyldiphosphonate to form diphosphonic acid.

### 3.5. Hydrogen Bonding

The occurrence of hydroxyl groups on the ligand systems and water molecules in some of the compounds results in hydrogen bond formation. The hydrogen bonds play a major role in increasing the dimensionalities of the structures by connecting sheets into three-dimensional structures or linking chains into sheets. The presence of the hydrogen bonds necessitated special considerations during the structural determination of the compounds.

A hydrogen bond is an attractive interaction between hydrogen and an electronegative atom (acceptor atom, A) such as F, O, N.[22] The hydrogen atom is bonded to another electronegative atom (donor atom, D), typically represented as D-H···A. Hydrogen bonds are stronger than Van de Waals forces. Typical hydrogen bond interactions are 1.60-2.00 Å in length, with the H···A distance directly related to the strength of the interaction. Geometry also plays a major role; typically in the strongest bonds a linear D-H···A geometry is observed, but the angle is always above 110 $^{o}$.

All the ligand systems in this project bear at least one hydroxyl groups or an amino group that may be involved in hydrogen bonding. Among the compounds that are discussed, the majority has intermolecular hydrogen bonding that occur between the layers, or in some cases are solely responsible for the extension of dimensionality from two to three as seen in the magnesium hexaqua compound (**7**) or from one to two dimensions as seen in compound **8.** In a few compounds, such intermolecular hydrogen bonds occur within the sheets of the compound. In this latter case, (compound **3**, chapter 4) the dimension of the structure remains unchanged.

### 3.5.1 Crystallographic location of Hydrogen Atoms

Hydrogen atoms scatter X-rays weakly due to low electron density. Their location in an X-ray diffraction experiment poses significant limitations.[23] It is however important to determine the exact location of the H atom in order to reliably assign the chemical structures. There are two ways to include hydrogen atoms in the crystallographic experiment: hydrogen atoms are either added at calculated positions or they are located from the electron density map during structure refinement. The located hydrogen atoms are typically refined using restraints.

A careful examination of the Fourier difference map can help locate the position of the H atom but the distances are typically too short, due to the low nuclear charge and long distances between nucleus and electrons.[24] The application of restraints helps in representing a more accurate distance.

On the other hand, hydrogen atoms may also be placed in calculated positions, often the more accurate of the two methods, as the above problems are circumvented. In this case, the hydrogen atoms "ride" on the atoms to which they are bound.[25]

Different categories of hydrogen bonding are identified in this work that require different treatment; these include water ($O-H_2$), hydroxyl (P-O-H), phosphinates (P-H ) and amine(N-H) groups.[25] The use of calculated hydrogen positions in some of the cases is not possible due to a significant variation of location, as the case for waters of crystallization; therefore location of hydrogen atoms in a Fourier map is essential. Some of the hydrogen atoms involved in hydroxyl groups in this work are therefore located in Fourier difference maps and refined with restraints, in others cases, data quality did not permit their location, resulting in the placement of the atoms in calculated positions.

Finally, all the H atoms on nitrogen and phosphorus were located in the respective difference maps.

## 3.6 Conclusions

The structures, properties, nomenclature and preparation of the phosphorus containing ligands used in this work have been discussed. The ligands fall into the category of mono-, di- and triphosphonates. The ability of the ligands to form metal complexes is based on their acid/base chemistry, and the dimensions of the resulting compounds rely on the number of deprotonated oxygen atoms in the sample. The oxyacids are able to form hydrogen bonds especially if water molecules are present.

## 3.7 Experimental

### 3.7.1 Synthesis of Ethylenediphosphonic Acid, $H_4$EDPA:

A modified synthesis for ethylenediphosphonic acid was employed.[15] 1, 2-Dibromoethane (23.6 mL, 0.23 mol) and triethylphosphite (142 mL, 0.82 mol) were measured into a 500 mL three-necked flask equipped with a stir bar. The flask was fitted with a condenser, an addition funnel and connected to a Schlenk line. The flask was purged with $N_2$ and heated (using a heating mantle) with stirring to about 165 $^{o}$C. The resulting pale, oily product was vacuum dried, treated with 150 mL of concentrated HCl, and refluxed for three days. Rotary evaporation yielded a white, solid product which was washed with acetonitrile to yield colorless crystalline products. The colorless crystals were dried under vacuum and hot water bath. The reaction is summarized in Scheme 3.5. Yield: 26.8 g, 0.14 mol, 51.1 %; m.p. 223-225 $^{o}$C; $^{1}$H-NMR (300 MHz, [$D_6$]DMSO, 25

$^{o}$C): δ = 1.7 pm (d, $J_{P\text{-}C\text{-}H}$ = 6 Hz, 4H, CH); IR (Nujol): 3871.3(w), P-O 2721.7(m), PO-H 1461.2(s), 1373.7(s),1152.0 (m), 1017.8(m), 924.4(m), P-C 714.3(m), 486.7(w).

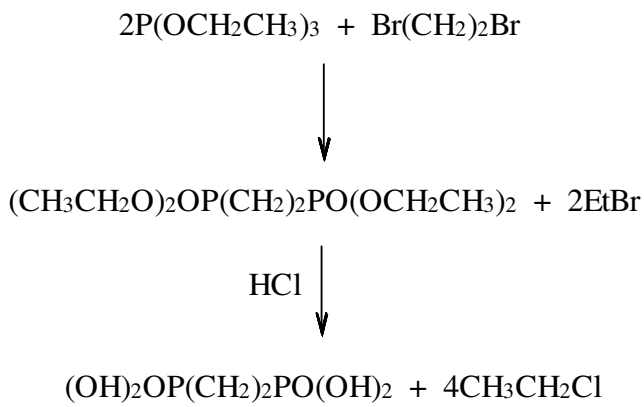


**Scheme 3.5.** Synthesis of ethylenediphosphonic acid, $H_4$EDPA.

### 3.7.2 Synthesis of Propylenediphosphonic Acid, $H_4$PDPA:

A modified synthesis for propylenediphosphonic acid was employed.[15] Into a 250 mL three necked flask equipped with a stir bar, 1, 3-dibromopropane (7.05 mL, 0.069 mol) and triethylphosphite (35.5 mL, 0.21 mol) were measured. The flask was fitted with a condenser, an addition funnel and connected to a Schlenk line. The flask was purged with $N_2$ and heated with a heating mantle to about 165 $^{o}$C. The resulting pale oily product was vacuum dried, treated with 50 mL concentrated HCl and refluxed for three days. Rotary evaporation yielded a white solid product which was washed with acetonitrile to yield colorless crystalline products. The colorless crystals were dried under vacuum using a hot water bath. The reaction is summarized in Scheme 3.6. Yield: 8.52g, 0.04 mol, 60.5 %; m.p. 175-178 $^{o}$C; $^{1}$H-NMR (300MHz, [$D_6$]DMSO, 25$^{o}$C): δ = 1.6 pm (m, 6H, CH); IR

(Nujol): 3871.3(w), PO-H 2721.7(m), 1461.2(s), 1373.7(s), 1152.0(m), 1018.8(m), 924.4(m), P-C 714.3(m), 487.7(w).

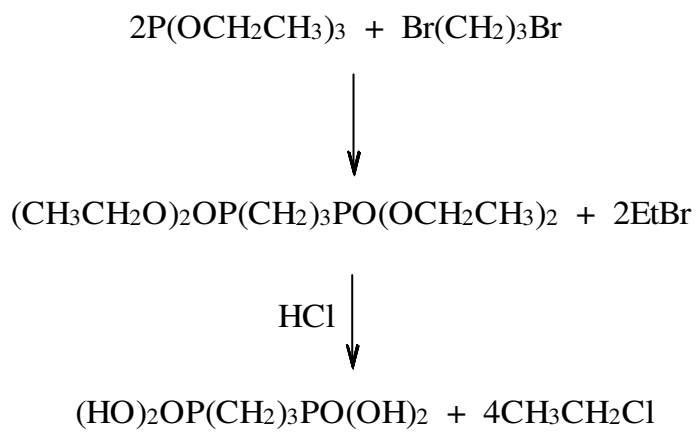


**Scheme 3.6.** Synthesis of propylenediphosphonic acid, $H_4PDPA$.

### 3.7.3 Synthesis of 4,4′-Biphenyl Diphosphonic Acid, $H_4BPDPA$:

The synthesis of 4,4′-biphenyl diphosphonic acid following a slight modification of a recorded procedure.[26] 4,4-Dibromophenyl (6.27 g, 0.02 mol) were placed into a 250mL flask equipped with a stir bar and containing 50 mL of 1,3-diisopropylbenzene. The mixture was heated to 185 $^{o}$C and $NiBr_2$ (0.5 g, 0.002 mol) was added with stirring. The flask was purged with $N_2$ while triethylphosphite ($P(OC_2H_5)_3$) (10 mL, 0.058 mol), was added slowly over a period of 6 hours. The brown mixture, which was refluxed for 24 hours turned black. An additional $NiBr_2$ (0.25 g, 0.001 mol) and $P(OC_2H_5)_3$ (5 mL, 0.029 mol) were added to the black mixture and heated for 24 hours. The resulting black solution was distilled to remove the diisopropylbenzene and excess $P(OC_2H_5)_3$. The

resulting black sticky product was extracted with 50 mL cyclohexane three times and the colorless solution was kept at room temperature over night. The solution was filtered to obtain a white solid which was recrystallized from petroleum ether. The crystals were dissolved in 40 mL concentrated HCl and refluxed for 12 hours, thereafter, 40 mL distilled $H_2O$ was added and stirred for 12 hours. The resulting precipitate was filtered, washed with distilled $H_2O$ and air dried to obtain a dirty white solid (Scheme 3.7). Yield: 1.55 g, 0.005 mol, 18 %; m.p.: 163 $^oC$ (decomposition); $^1H$-NMR (300MHz, $[D_6]$DMSO, 25$^oC$): $\delta$ = 7.40 pm (m, 8H, PhH); IR (Nujol): 2897.2(s), PO-H 2722.0(m), 2354.6(w), 1596.1(w), 1467.8(s), P=O 1152.7(s), 1024.3(m), 936.8(m), 814.3(w), P-C 709.1(m), 551.7(w), 452.1(w).

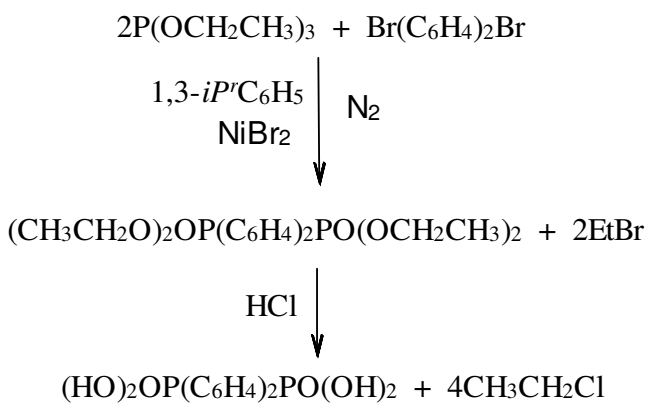


**Scheme 3.7.** Synthesis of 4,4′-biphenyl diphosphonic acid, $H_4$BPDPA.

### 3.7.4 Synthesis of 4-(4'-Phosphono phenoxy) Phenylphosphonic Acid, $H_4PPPA$:

The 4-(4'-Phosphono phenoxy) phenylphosphonic acid ligand was prepared by a modified synthetic route,[27] as shown in Scheme 3.8. Bis-(4-bromophenyl) ether (12.21g 0.04 mol) and 1,3-diisopropylbenzene (93 mL, 0.49 mol) of were measured into a 500 mL three-necked flask containing a stir bar. The flask was then fitted with a reflux condenser with nitrogen inlet, an addition funnel and a thermometer. The flask was purged with nitrogen and then heated to 70-80°C while stirring. The addition funnel was momentarily removed to add dry anhydrous nickel (II) chloride (0.485 g, 0.003 mol), which served as a catalyst. The brown mixture was refluxed under a stream of nitrogen gas at 180°C while triethylphosphite (18.6 mL, 0.12 mol) was added over a 3 hour period using the addition funnel. The mixture was heated for 24 hours maintaining a temperature of around 150°C. Then another portion of dry nickel (II) chloride (0.428 g, 0.003 mol) and triethylphosphite (18.6 mL, 0.12 mol) were added. The mixture was heated while stirring for another 24 hours and then allowed to cool overnight.

The solvent was removed from the resulting dark black solution by vacuum distillation and then kept at room temperature for two days until it became sticky and tar-like. The product was extracted with hexane in a Soxhlet extractor. The extraction was allowed to continue for four days, and then the hexane was removed by distillation affording an oily product.

The product was dissolved in ethanol (232 mL, 3.9 mol) and then transferred to a 500 mL three-neck flask fitted with a stir bar, a thermometer, addition funnel, and reflux condenser. The solution was heated to 80°C while stirring. Then concentrated HCl (93 mL, 1.08 mol) was added dropwise over a two hour period to hydrolyze the ester. After

the hydrochloric acid was added, the reflux set-up was replaced by a distillation apparatus to allow the collection of the ethyl chloride. The solution was heated at 80°C for 5 days and allowed to cool to room temperature. A white solid was obtained upon rotary evaporation which was washed with water and dried at 60 $^{o}$C. Yield: 5.26 g, .015 mol, 44%; m.p.: 271-275 $^{o}$C; $^{1}$H-NMR (300MHz, $CDCl_3$, 25$^{o}$C): δ = 7.80 pm (q, 4H, PhH), 7.13 pm (q, 4H, PhH); IR (Nujol): PO-H 1352.2(s), 1100.6(m), P-C 714.4(w).

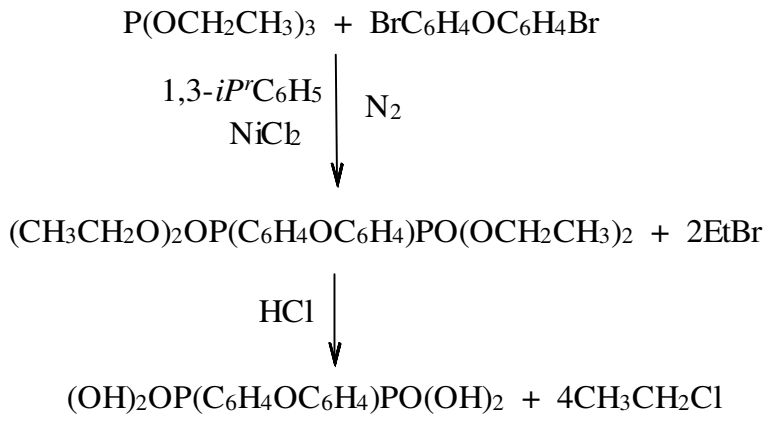


**Scheme 3.8.** Synthesis of 4-(4'-Phosphonophenoxy) phenylphosphonic acid, $H_4$PPPA

### 3.7.5 Synthesis of Amino trimethylenephosphonic Acid, $H_6$ATMPA:

The triphosphonate ligand was prepared by the Mannich reaction[10] with a few modifications, as shown in Scheme 3.9. Into a 1 L three-neck flask containing ammonium chloride (17.8 g, 0.33 mol) and a stir bar, $H_3PO_3$ (82.0 g, 1.00 mol) diluted in 100 mL distilled water was added. The clear solution was immediately acidified with 100 mL concentrated HCl while stirring and purging with $N_2$. The mixture was then refluxed for

an hour after which 160 mL 37 % (1.61 mol) aqueous formaldehyde ($H_2CO$) was added dropwise at a rate of about 2.6 mL/min with the aid of a dropping funnel. The mixture was refluxed for another hour and cooled to room temperature. Once the mixture was cool, the water was removed by rotary evaporation. The remaining colorless solution was left at room temperature until crystals formed after three weeks. The crystals were washed with a 5:1 acetone/water mixture. The white solid was air dried and weighed. Yield: 66.5 g, 0.20 mol, 67.4%; m.p. 210-212 $^oC$; $^1H$-NMR (300MHz, $D_2O$, 25$^oC$): $\delta$ = 3.74 pm (d, $J_{P\text{-}C\text{-}H}$ = 12 Hz, 6H, $CH_2$); IR (Nujol): 2726.9(s), P-OH 2640.6(s), P=O 1154.6(m), 1368.6(s), 1298.7(m), 930.1(w), 715.5(m), 722.5(s).

$$NH_4Cl + 3H_3PO_3 + 3CH_2O + 2HCl \xrightarrow[\text{reflux}]{H_2O} N(CH_2PO_3H_2)_3 + 3HClO + 3H_2$$

**Scheme 3.9.** Synthesis of amino tris(methylenephosphonic) acid, $H_6$ATMP.

### 3.7.6 Synthesis of ethylenediamine tetramethylenephosphonic acid, $H_8$EDTMPA:

A modified synthesis for ethylenediamine tetramethylenephosphonic acid was employed.[28] Phosphorous acid (20.5 g, 0.25 mol) were added to concentrated HCl (15.6 mL, 0.18 mol) in a 100 mL three-necked flask containing a stir bar. To this mixture, ethylenediamine (3.3 mL, 0.05 mol) was added slowly with stirring followed by reflux at 130 $^oC$ for ten minutes. To the resulting pale yellow solution, formaldehyde (19.8 mL, 0.54 mol) was added dropwise over a period of ten minutes. The resulting yellow solution was refluxed for another two hours, allowed to cool to room temperature and the solvent was reduced under vacuum. White crystalline product formed when the concentrated

solution was left at room temperature overnight. The solid was filtered, washed with cold water and allowed to air dry (Scheme 3.10). Yield: 15.1g, .004 mol, 78.4 %; m.p.: 216-220 $^{o}$C; $^{1}$H-NMR (300MHz, $D_2O$, 25$^{o}$C): δ = 3.80 pm (s, 4H, $CH_2$), 3.50 pm (d, $J_{P\text{-}C\text{-}H}$ = 12.3 Hz, 8 H, $CH_2$); IR (Nujol):1590.3(w), H-O 1450.2(s), N-C 1362.7(s), 1152.7(w), 732.6(m), 528.4(w).

$$H_2N(CH_2)_2NH_2 + 4H_2CO + 4H_3PO_3 \xrightarrow[\text{-}H_2O]{HCl} (H_2O_3PCH_2)_2N(CH_2)_2N(CH_2PO_3H_2)_2$$

**Scheme 3.10**. Synthesis of ethylenediamine tetramethylenephosphonic acid, $H_8$EDTMPA.

## 3.8 Experimental Details

Triethylphosphite, acetonitrile, 1, 2-dibromoethane, 1, 3- dibromopropane, 4,4′-dibromophenly, bis-(4-bromophenyl) ether, ammonium chloride, formic acid, hydrochloric acid, anhydrous nickel (II) chloride, anhydrous nickel (II) bromide, formaldehyde, ethylenediamine, phosphorous acid, 1,3-diisopropylbenzene, cyclohexane, petroleum ether, ethanol and acetone were obtained commercially. Triethylphosphite was distilled prior to use while others were used as purchased.

Products were analyzed by IR spectroscopy. A Perkin-Elmer PE 1600–FT-IR spectrometer was used to collect IR spectra as Nujol mulls between KBr plates. Melting points were determined using the Thermocouple VWR thermometer probe.

## 3.9 References:


(1) Athayde, A. d. M.; Libbs Farmaceutica Ltda, Brazil . 2003, p 19 pp.
(2) Benedict, J. J.; Perkins, C. M.; The Procter & Gamble Company, USA . 1996, p 12 pp.
(3) Camper, N.; Scott, C. J.; Migaud, M. E. *New J. Chem.* **2010**, *34*, 949.
(4) Long, K. A.; Jackson, J. K.; Yang, C.; Chehroudi, B.; Brunette, D. M.; Burt, H. M. *J. Biomater. Sci., Polym. Ed.* **2009**, *20*, 653.
(5) Rogers, M. J.; Crockett, J. C.; Coxon, F. P.; Monkkonen, J. *Bone (Amsterdam, Neth.)* **2011**, *49*, 34.
(6) Ishizaki, T.; Okido, M.; Masuda, Y.; Saito, N.; Sakamoto, M. *Langmuir* **2011**, *27*, 6009.
(7) Maxisch, M.; Thissen, P.; Giza, M.; Grundmeier, G. *Langmuir* **2011**, *27*, 6042.
(8) Zang, D.-M.; Cao, D.-K.; Zheng, L.-M. *Inorg. Chem. Commun.* **2011**, *14*, 1920.
(9) Jiang, J.; Xu, Y. *E-J. Chem.* **2011**, *8*, 1881.
(10) Greenwood, N. N.; Earnshaw, A. *Chemistry of the Elements,* 2nd Edition; Butterworth-Heinemann, 1997, p 510.
(11) Soghomonian, V.; Chen, Q.; Haushalter, R. C.; Zubieta, J. *Angewandte Chemie International Edition in English* **1995**, *34*, 223.
(12) Merrill, C. A.; Cheetham, A. K. *Inorg. Chem.* **2005**, *44*, 5273.
(13) Rao, K. P.; Vidyasagar, K. *Eur. J. Inorg. Chem.* **2005**, *2005*, 4936.
(14) Bhattacharya, A. K.; Thyagarajan, G. *Chem. Rev.* **1981**, *81*, 415.
(15) Michaelis-Arbuzov, P.-R. *Pure Appl. Chem.* **1964**, *9*.
(16) Steve J.Fitch, C. C. a. S. K. L. In *Monsanto Company*; Vinita Park: USA, 1966.
(17) Garner, A. Y.; Chapin, E. C.; Scanlon, P. M. *The Journal of Organic Chemistry* **1959**, *24*, 532.
(18) Balthazor, T. M.; Grabiak, R. C. *The Journal of Organic Chemistry* **1980**, *45*, 5425.
(19) Rodríguez, B.; Bolm, C. *The Journal of Organic Chemistry* **2006**, *71*, 2888.
(20) Song, J.; Wang, Y.; Deng, L. *J. Am. Chem. Soc.* **2006**, *128*, 6048.
(21) Moedritzer, K.; Irani, R. R. *J. Inorg. Nucl. Chem.* **1961**, *22*, 297.
(22) Emsley, J. *Chem. Soc. Rev.* **1980**, *9*, 91.
(23) Almlof, J.; Ottersen, T. *Acta Crystallographica Section A* **1979**, *35*, 137.
(24) Cooper, R. I.; Thompson, A. L.; Watkin, D. J. *J. Appl. Crystallogr.* **2010**, *43*, 1100.
(25) Muller, P. *Crystallogr. Rev.* **2009**, *15*, 57.
(26) Prochniak, G.; Zon, J.; Daszkiewicz, M.; Pietraszko, A.; Videnova-Adrabinska, V. *Acta Crystallogr., Sect. C: Cryst. Struct. Commun.* **2007**, *C63*, o434.
(27) Gómez-Alcántara, M. M.; Cabeza, A.; Martínez-Lara, M.; Aranda, M. A. G.; Suau, R.; Bhuvanesh, N.; Clearfield, A. *Inorg. Chem.* **2004**, *43*, 5283.
(28) Banerjee, S.; Samuel, G.; Kothari, K.; Unni, P. R.; Sarma, H. D.; Pillai, M. R. A. *Nuclear Medicine and Biology* **2001**, *28*, 205.

# CHAPTER 4

## Synthetic and Structural Studies on Calcium Phosphinate, Phosphonate, Phosphite and Phosphate Compounds.

### 4.1 Introduction

Interest in calcium phosphonate chemistry has risen due to the use of phosphonate–based drugs that are employed for treatment of bone diseases,[1-3] yet very little work has been done to understand the coordination chemistry of calcium with phosphonate based ligands. The paucity of information is due to difficulties in obtaining quality crystals of calcium phosphonates. The large radii of the heavy alkaline earth metal ions ($Ca^{2+}$ =1.14 Å, $Sr^{2+}$ = $1.27^{2+}$ Å and $Ba^{2+}$ = 1.49 Å) result in a significant tendency towards aggregation, rendering the resulting products insoluble.[4] Aggregation is one of the means to achieve coordinative saturation as is the coordination of co-ligands such as water.[4]

Hydrothermal and solvothermal synthetic routes which are used extensively for the preparation of transition metal phosphonates are explored in the synthesis of calcium, phosphinate, phosphite and phosphate compounds. To this effect, soluble calcium salts and ligands are allowed to react at elevated temperatures and pressures to enhance the solubility of the products and thus promote the crystallization process.

Phenylphosphinic acid has been successfully used in the synthesis of a number of phenylphosphinate metal compounds[5] with important applications as sorbents, ion exchangers in resins,[6,7] sensors and catalysts.[6] In addition, studies have demonstrated that the addition of phenylphosphonic and phenylphosphinic acids to hydroxyapatite (HA)

$Ca_{10}(PO_4)_6(OH)_2$, have increased its surface area and porosity[8] as the P-OH moieties on the HA surface are responsible for the adsorption of mineral and organic species.[9] HA is the major inorganic mineral in bone and therefore plays a major role in biomaterials[10] and in catalysis.[11]

The following ligands (Figure 1.4) are used in forming the compounds that will be discussed in this chapter, namely phenylphosphinic acid (HPPA) $C_6H_5PO(OH)H$ (a) in, phenylphosphonic acid ($H_2PPA$) $C_6H_5PO(OH)_2$ (b), phosphorous acid $H_3PO_3$ (c), and phosphoric acid $H_3PO_4$ (d), resulting from decomposition products of ethylenediphosphonic acid.

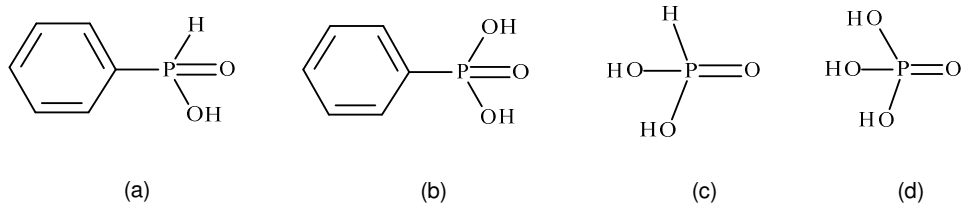


**Figure 4.1.** (**a**). Phenylphosphinic acid (HPPA) pKa 1.75[12] (**b**). Phenylphosphonic acid ($H_2PPA$) $pKa_1$ 1.83, $pKa_2$ 7.07[13], (**c**). Phosphonic acid ($H_3PO_3$) $pKa_1$ 1.3, $pKa_2$ 6.7 [14] (**d**). Phosphorus acid ($H_3PO_4$) $pKa_1$ 2.12 $pKa_2$ 7.21 $pKa_3$ 12.65[15]

With the exception of the HPPA ligand which is monobasic and therefore forms only monoanionic species, the $H_2PPA$, $H_3PO_3$ and $H_3PO_4$ ligands can exist as mono-, di- and trianionic species. The names of the acids and their respective are provided in Table 4.1.

**Table 4.1.** Nomenclature of some P-based oxoacids and their anions

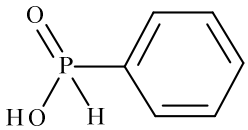

Phenylphosphinic acid

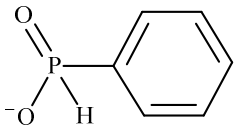

phenylphosphinate

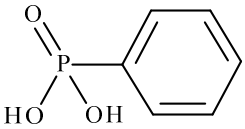

Phenylphosphonic acid

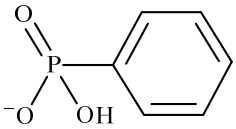

hydrogen phenylphosphonate

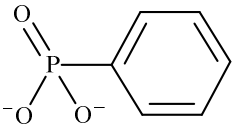

phenylphosphonate

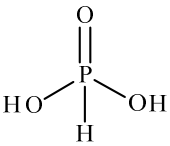

Phosphonic acid

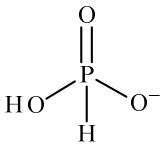

hydrogen phosphite

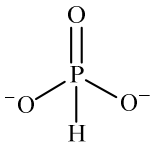

phosphite

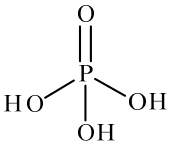

Phosphoric acid

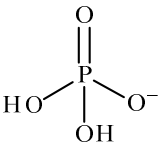

dihydrogen phosphate

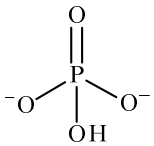

hydrogen phosphate

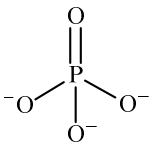

phosphate

Six compounds, **1-6** are hereby presented: calcium phenylphosphinate, **1** involving the HPPA ligand, calcium hydrogen phenylphosphonate, **2** based on the $H_2PPA$ ligand**,** anhydrous calcium hydrogen phosphite, **3** and calcium hydrogen phosphite monohydrate, **4**, involving the $H_3PO_3$ ligand in its monoanionic form ($H_2PO_3^-$), calcium phosphite monohydrate, **5**, involving $H_3PO_3$ ligand in its dianionic form ($HPO_3^{2-}$) and calcium hydrogen phosphate **6** containing $H_3PO_4$ in its dianionic form ($HPO_4^{2-}$). Among those, the remaining new compounds **1, 3** and **6** will be described in detail. Compound **1** and **3** are new compounds; no other alkaline earth metal phenylphosphinate compound has been reported. Compound **6** is however, a well known mineral but no structural data are available. Compounds **2, 4** and **5** have been reported previously so we only report an improved crystallographic analysis.[16-20]

### 4.2 Synthetic Considerations for compounds 1, 3, and 6.

To obtain single crystals suitable for single crystal X-ray diffraction, hydrothermal synthesis involving a calcium source in aqueous medium with the ligand followed by slow evaporation of solvent at room temperature is employed. Details on hydrothermal synthesis and its use in the preparation of metal organic frameworks is discussed in Chapter 3. Difficulties in obtaining crystalline samples of compounds **1**, **3**, and **6** resulted in extensive work to optimize crystallization conditions, such as the introduction of different calcium sources, different stoichiometric ratios of calcium salt to ligand etc., leading to specific synthetic and crystallization conditions for each compound as provided below.

### 4.2.1 Calcium Phenylphosphinate, $\{Ca[C_6H_5PH(O)_2]_2[C_6H_5PH(O)OH]_2\}_n$ (1):

Multiple avenues to obtain crystalline samples were explored, involving the treatment of the ligand with various calcium salts in water or DMF both at room temperature and under hydrothermal conditions. Of those, the reaction of $CaCl_2$ with the ligand under hydrothermal conditions afforded poorly diffracting samples. Introduction of terephthalic acid, phosphorous acid and the coligand 1,4-dioxane under hydrothermal conditions only afforded powdery samples. Crystalline samples were obtained in a reaction involving $CaCl_2$ and phenyl phosphinic acid, HPPA in the presence of ethylenediphosphonic acid, $H_4EDPA$, as shown in Scheme 4.1.

$$CaCl_2 + C_6H_5PH(O)OH \xrightarrow[80\ ^oC]{H_2O/C_2H_8O_6P_2} \{Ca[C_6H_5PH(O)_2]_2[(C_6H_5PH(O)OH]_2\}_n \quad \textbf{(1)}$$

**Scheme 4.1**. Synthesis of calcium phenylphosphinate, **1**.

### 4.2.2 Anhydrous Calcium Hydrogenphosphite, $[Ca_{0.5}(H_2PO_3]_n$ (3):

Little is known on the chemistry of the 4-(4'-phosphonophenoxy) phenyl phosphonic acid, ($H_4PPPA$) ligand (Figure 4.2), likely a consequence of its low solubility in water. Accordingly, any attempts to utilize this ligand failed. However, the presence of the ligand during the reaction of calcium chloride and phosphorous acid led to the unexpected formation of calcium hydrogenphosphite monohydrate (**4**). As this has been reported previously, its synthesis will not be discussed further in this work.[20,21]

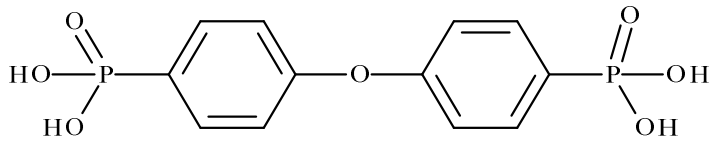

**Figure 4.2.** 4-(4'-phosphonophenoxy) phenyl phosphonic acid, $H_4$PPPA.

Since the $H_4$PPPA ligand was not contained in the final product, the reaction was repeated excluding the ligand to determine if it played any role in the formation of **4**. This resulted in the formation of anhydrous calcium hydrogenphosphite **(3)**. Compound **3** was therefore obtained by treating $CaCl_2$ with $H_3PO_3$ under solvothermal conditions in ethanol (Scheme 4.2)

$$CaCl_2 + H_3PO_3 \xrightarrow[150\ ^{o}C]{C_2H_5OH} [Ca_{0.5}(H_2PO_3)]_n \ \mathbf{(3)}$$

**Scheme 4.2.** Synthesis of anhydrous calcium hydrogen phosphite **3**.

### 4.2.3. Anhydrous Calcium Hydrogenphosphate, $[CaHPO_4]_n$ (6):

Anhydrous calcium hydrogenphosphate is a well known dibasic compound but its extended crystal structure has not been reported. Extensive crystallographic studies of the hydrated form, $CaHPO_4{\cdot}2H_2O$ exist due to its established role in the formation of kidney stones.[22] Thermogravimetric studies on calcium hydrogen phosphate dihydrate indicate dehydration upon heating to 294 $^{o}$C.[23] There are no previous crystallographic data on **6.**

Compound **6** was obtained from a likely decomposition of ethylenediphosphonic acid. After several unsuccessful attempts to coordinate ethylenediphosphonic acid ($H_4$EDPA) to calcium (Chapter 7), we decided to introduce ethylenediamine tetramethylenephosphonic acid ($H_8$EDTMPA) as co-ligand to a mixture of calcium

nitrate in water under hydrothermal conditions. The result was a 3D extended structure of **6** (Scheme 4.3).

$$Ca(NO_3)_2{\cdot}4H_2O + H_2O_3P(CH_2)_2PO_3H_2 \xrightarrow[H_2O,\,170\ ^{o}C]{(HO_3PCH_2)_2N(CH_2)_2N(CH_2PO_3H)_2} [CaHPO_4]_n \quad \textbf{(6)}$$

**Scheme 4.3.** Synthesis of anhydrous calcium hydrogen phosphate, **6**.

## 4.3 Structural Aspects

### 4.3.1 Calcium Phenylphosphinate, $\{Ca[C_6H_5PH(O)_2]_2[C_6H_5PH(OH)O]_2\}_n$, (1):

Compound **1** was obtained hydrothermally from the reaction of phenylphosphinic acid (HPPA), ethylenediphosphonic acid ($H_4EDA$) and calcium chloride in the ratio of 2:1:1. Interestingly, only the phenylphosphinic acid is found in the product. It is difficult to rationalize which factors may have influenced the deprotonation of one ligand over the other, but the two ligands have slightly different pKa values; phenylphosphinic acid (HPPA) and ethylenediphosphonic acid ($H_4EDA$)have respective values of 1.65±0.10 and 1.77±0.14 in DMSO at 25 ºC,[24] indicating that HPPA is slightly more acidic than $H_4EDA$. In addition the stoichiometric ratios of HPPA:$H_4EDPA$ were 2:1.

Compound **1** was structurally characterized by single crystal X-ray crystallography. The details of crystallographic data and structure refinement parameters are summarized in Table 4.2 in the experimental section of this chapter. Compound **1** crystallizes in the triclinic space group P-1 and represents the first alkaline earth phenylphosphinate. The structure of **1** is shown in Figures 4.3 and 4.4.

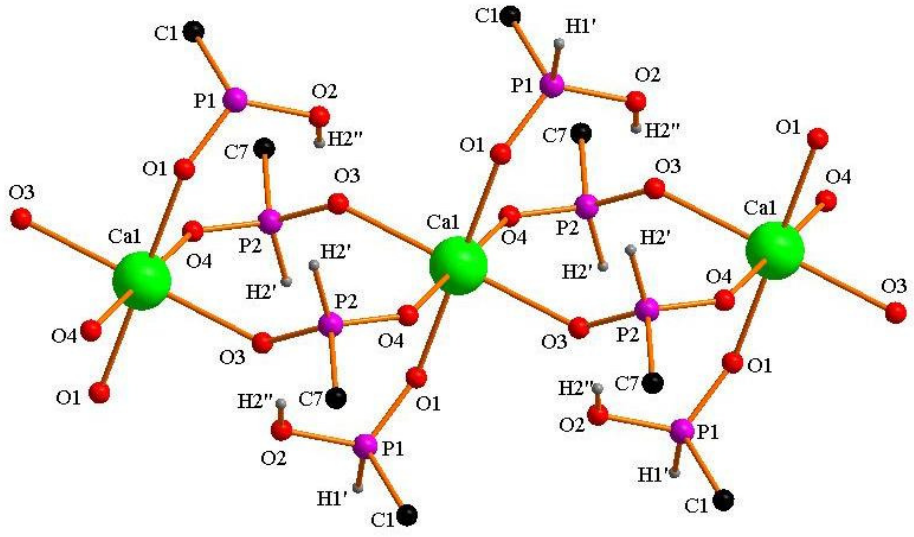


**Figure 4.3.** Labeling scheme of **1** showing the polymeric chain viewed from the y axis. The phenyl groups have been removed except the ipso carbon atoms shown in black.

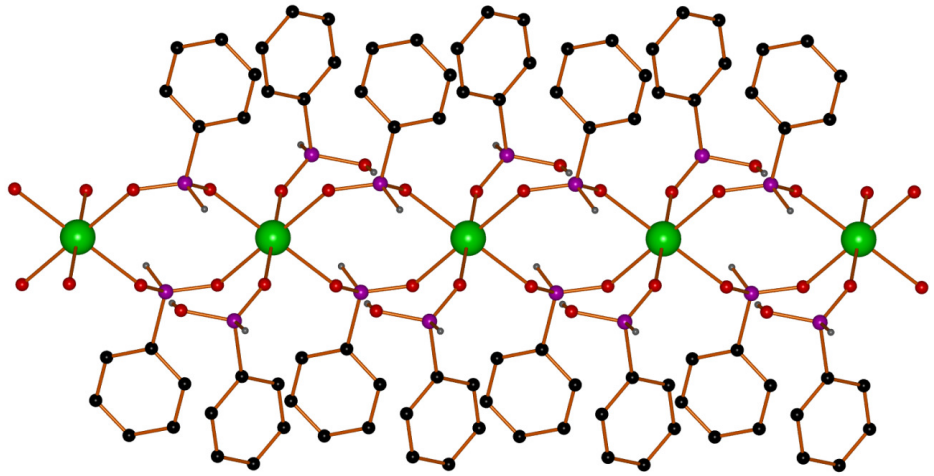

**Figure 4.4.** Graphical representation of compound **1.** The metal centers are represented by green spheres, oxygen (red), carbon (black), hydrogen (gray) and phosphorus by purple spheres.

The asymmetric unit of **1** consist of one calcium and two singly deprotonated ligands. The $Ca^{2+}$ ion is six-coordinated exhibiting a distorted octahedral geometry. There

are four singly deprotonated ligands shared between two $Ca^{2+}$ ions ensuring charge balance while two additional neutral ligands are also metal bound. In effect, the structure of **1** is constructed from HPPA in two binding modes to the $Ca^{2+}$ ion; whereas the deprotonated $PPA^-$ bridges two symmetrically related calcium centres, the neutral ligand coordinates to calcium center *via* the P=O moiety (Scheme 4.5).

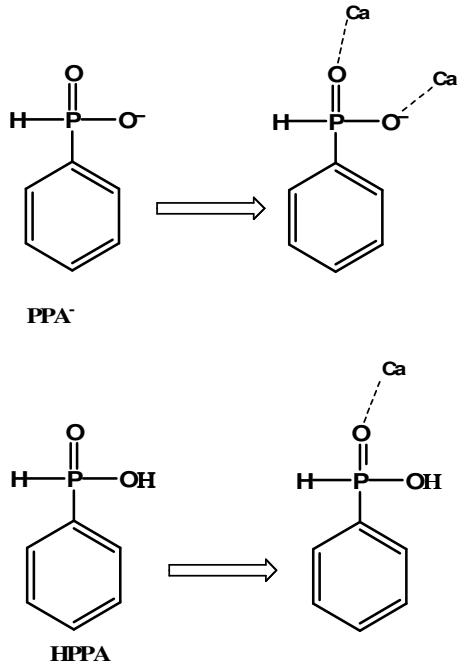


**Scheme 4.4**. Ligand in two deprotonated states with different binding modes in compound **1**.

The coordination environment of each $Ca^{2+}$ consists of six oxygen atoms comprising three pairs of symmetrically related oxygen atoms (O1, O3, O4) with calcium in an inversion center. The oxygen atoms of $PPA^-$ (O3 and O4), bridge the neighbouring $Ca^{2+}$ ions to give a chain structure. The P-O distances of O3 (P1-O3, 1.491(2) Å) and O4 (P2-O4, 1. 490(2) Å) are shorter compared to P-O distances of O1 (P2-O4, 1.524(2) Å and

O2 (P1-O2, 1.555(2) Å) but the longest P-O distance of 1.555(2) Å corresponds to the pendant P-OH (O2) moiety of the neutral ligand. The shortest P=O bond length of **1** 1.491(1) deviates only slightly from that of the neutral ligand (1.493(1) Å) shown in Figure 4.5.[25]

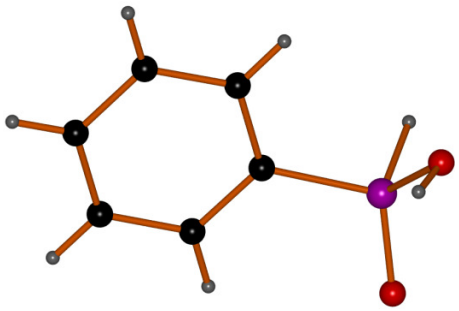

**Figure 4.5.** The structure of neutral phenylphosphinic acid,[25] showing phosphorus as a purple sphere, oxygen as red, carbon black and hydrogen atoms in grey spheres.

The P=O and P-O bond distances are usually affected by substituents on the phenyl group.[26] The H atoms on the P atom were located from the electron density map and refined freely at a distance of 1.278(3) Å and 1.288(3) Å from P1 and P2 respectively. Selected bond distances and bond angles are listed in Table 4.3.

**Table 4.3** Selected bond lengths [Å] and angles [°] for calcium phenylphosphinate **1**

| Bond distances | | Bond distances | | Bond angles | |
|---|---|---|---|---|---|
| Ca(1)-O(1) | 2.3055(2) | P(2)-O(4) | 1.4929(2) | O(1)-Ca(1)-O(3) | 92.53(6) |
| Ca(1)-O(1)#1 | 2.3055(2) | P(2)-O(1) | 1.5236(2) | O(1)-P(1)-O(2) | 116.42(1) |
| Ca(1)-O(4)#2 | 2.3443(2) | O(4)-Ca(1)#4 | 2.3443(2) | O(1)-P(1)-C(1) | 111.54(1) |
| Ca(1)-O(4)#3 | 2.3444(2) | P(2)-C(7) | 1.798(3) | O(2)-P(1)-C(1) | 107.21(1) |
| Ca(1)-O(3) | 2.3609(2) | P(1)-O(3) | 1.4905(2) | O(4)-P(2)-O(3) | 116.93(1) |
| Ca(1)-O(3)#1 | 2.3609(2) | P(1)-O(2) | 1.555(2) | O(4)-P(2)-C(7) | 109.87(1) |
| C(1)-C(6) | 1.393(4) | P(1)-C(1) | 1.801(3) | O(3)-P(2)-C(7) | 108.81(1) |
| P(1)-H1 | 1.278(2) | P(2)-H2 | 1.288(2) | | |

Symmetry transformations used to generate equivalent atoms:

#1 -x,-y,-z+2 #2 -x+1,-y,-z+2 #3 x-1,y,z #4 x+1,y,z

A number of alkali and alkaline earth phenylphosphonates are known, specific examples include $M[(C_6H_5)P(O)_2OH)]$ $[(C_6H_5)PO(OH)_2)]$ ) where M = Li, Na, K, Rb, Cs,[27] Mg ($Mg(O_3PC_6H_5)\cdot 2H_2O$) ,[28] $Ca\{[Ca[(C_6H_5)P(O)_2OH)]_2\}_n$ (**2**),[18,19,28,29] Sr ($Sr(C_6H_5)P(O)_2OH)_2$),[19,28-30] and Ba ($Ba(C_6H_5)P(O)_2OH)_2$).[28,29] The Mg compound is the only example of alkaline earth phenylphosphonate with a doubly deprotonated ligand.

Calcium hydrogen phenylphosphonate $\{[Ca[(C_6H_5)P(O)_2OH)]_2\}_n$ (**2**) [18,31] was synthesized by refluxing calcium nitrate and phenylphosphinic acid in water and crystallized under hydrothermal reaction conditions. Compound **2** forms a layer structure based on eight-coordinate calcium centers, as shown in Figures 4.6 and 4.7. There are three oxygen atoms per ligand which are all involved in metal coordination. The

deprotonated O1 bridges two metal centers, P=O3 acts as a donor atom to a single Ca center while O2 remains protonated as P-OH. The Ca-O bond lengths in **2** (2.346(3)-2.667(3) Å) compare to those in **1** (2.348(1)-2.521(1) Å).

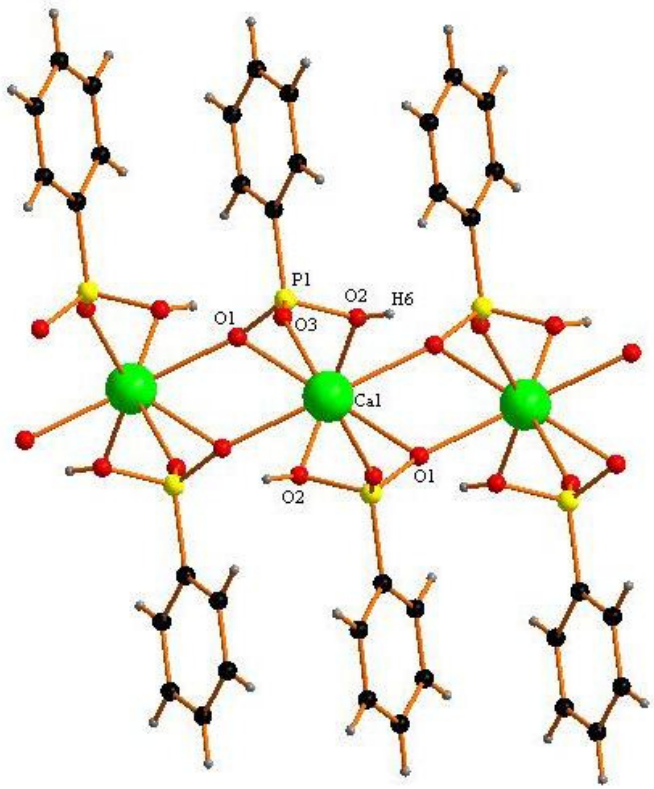


**Figure 4.6.** Structure of **2** viewed along the c-axis with partial labeling.

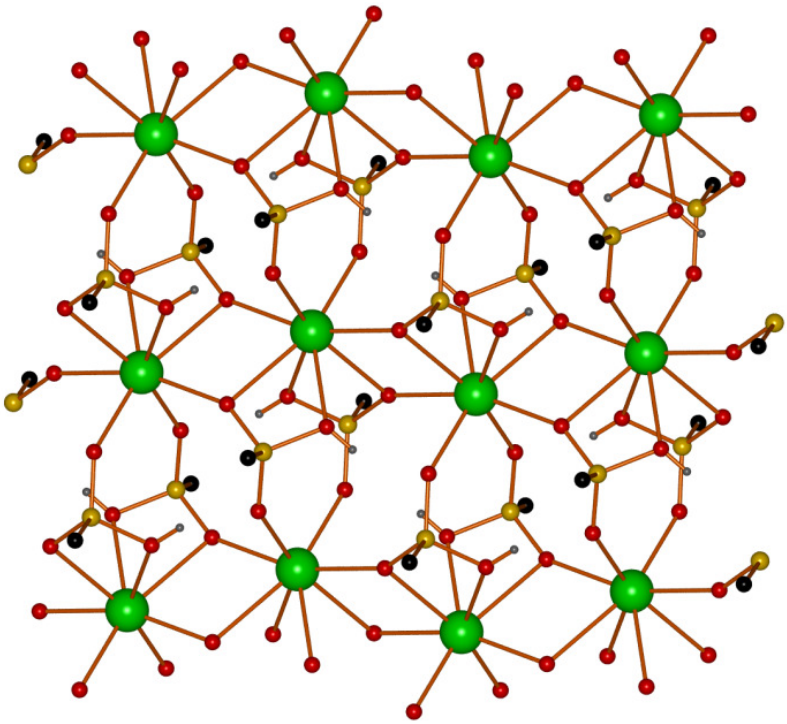

**Figure 4.7.** The layered structure of **2**, all atoms of the phenyl group except the ipso carbon atoms have been removed for clarity.

Significant differences between the structures of **1** and **2** exist; the most fundamental one is the metal coordination number and the dimensionality of the resulting solid. Both **1** and **2** form chains *via* bridging phosphinate and phosphonate oxygen atoms. In **2**, only O1 is involved in bridging the metal centers whereas in **1**, the metal centers are bridged by O-P-O moieties.

While compound **1** forms a chain, the corresponding calcium hydrogen phenylphosphonate compound **2** is a layer structure. Other phenyl hydrogen phosphonates such as $[Ca(HO_3PC_6H_5)_2]_n$,[19,29,31] $[Ca(O_3PC_6H_5)\cdot H_2O]_n$,[31] $[Ca(O_3PC_6H_5)\cdot 2H_2O]_n$ [31] and $[Ca_3(HO_3PC_6H_5)_2(O_3PC_6H_5)_2]_n$[31] form layered structures. Likewise, zinc phenylphosphinate $[Zn(O_2PHC_6H_5)_2]_n$, is a chain polymer[32,33] whereas the

corresponding phenylphosphonate $[Zn(HO_3PC_6H_5)_2]_n \cdot H_2O$[34] is a layered structure. This trend is not limited to the phenylphosphonate and phenylphosphinates, but other divalent monophosphonates[35] such as $Ca(O_3PCH_3).H_2O$, $Ca(HO_3PC_6H_{13})_2$,[36] and $Zn(O_3PCH_3).H_2O$ [37-39] have layered structures whereas the corresponding phosphinates of zinc[33] and manganese[40] are one-dimensional,[41] suggesting that the additional oxygen atom contributes to the extension of the structure in two dimensions.

Studies have indicated that in an acidic medium, $[Ca(O_3PC_6H_5)\cdot 2H_2O]_n$ is protonated to form $[Ca(HO_3PC_6H_5)_2]_n$ while the reverse occurs in weak basic medium.[31]

### 4.3.2 Anhydrous Calcium Hydrogenphosphite, $\{Ca[PH(O)_2OH]_2\}_n$ (3):

The novel anhydrous calcium hydrogenphosphite **3** was formed by the hydrothermal synthesis from $CaCl_2$ and phosphonic acid in a Carius tube at 150 $^oC$ for three days. The hot Carius tube was allowed to cool to room temperature and colorless hexagonal plates of crystals deposited overnight. Compound **3** was structurally characterized by single crystal X-ray crystallography. The details of crystallographic data and structure refinement parameters are summarized in Table 4.2 in the experimental section of this chapter.

Compound **3** crystallizes in the triclinic P-1 space group with a calcium ion in a distorted octahedral geometry. The $Ca^{2+}$ center is in a special position, with coordination to two singly deprotonated phosphonic acid ligands as shown in Figure 4.8. The overall structure is two-dimensional.

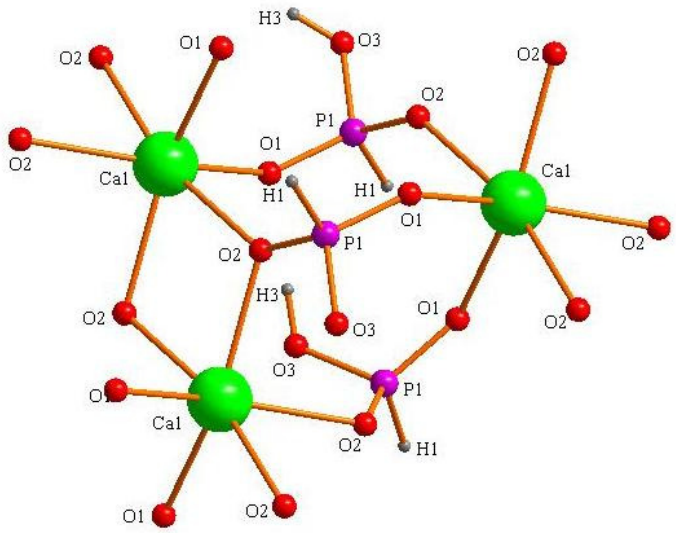


**Figure 4.8.** Schematic labelling of **3**

The P=O1 and P-O$^{-}$2 distances are similar (1.506(8) Å and 1.507(8) Å) while the P-O3H distance is slightly longer (1.570 (9) Å. Bond distances and angles for compound **3** are summarized in Table 4.4. The P-H distance of 1.389(1) Å compares well with those of other phosphite compounds. The distorted octahedral geometry is evident from the wide range of O-Ca-O angles (67.55 (3) Å-92.88 (3) Å).

**Table 4.4.** Selected Bond lengths [Å] and angles [°] for anhydrous calcium hydrogen phosphite **3**.

| Bond length | | Bond Angles | | Bond Angles | |
|---|---|---|---|---|---|
| Ca(1)-O(2)#1 | 2.358(8) | O(2)#1-Ca(1)-O(2)#2 | 166.00(4) | O(1)-P(1)-O(2) | 115.69(5) |
| Ca(1)-O(1)#3 | 2.368(8) | O(2)#1-Ca(1)-O(1)#3 | 86.37(3) | O(1)-P(1)-O(3) | 113.99(5) |
| Ca(1)-O(2)#5 | 2.403(8) | O(2)#2-Ca(1)-O(1)#3 | 84.74(3) | O(2)-P(1)-O(3) | 105.64(5) |
| Ca(1)-O(3)#5 | 2.979(1) | O(1)#3-Ca(1)-O(1)#4 | 101.08(4) | O(1)-P(1)-H(1) | 106.30(5) |
| P(1)-O(1) | 1.506(8) | O(2)#1-Ca(1)-O(2)#5 | 71.03(3) | O(2)-P(1)-H(1) | 111.30(6) |
| P(1)-O(2) | 1.507(8) | O(1)#4-Ca(1)-O(3)#5 | 153.18(3) | O(3)-P(1)-H(1) | 103.30(6) |
| P(1)-O(3) | 1.570(9) | O(2)#2-Ca(1)-O(2)#5 | 120.18(3) | P(1)-O(3)-H(3) | 121.50(2) |
| P(1)-H(1) | 1.389(1) | O(1)#3-Ca(1)-O(2)#5 | 92.88(3) | | |
| | | O(1)#4-Ca(1)-O(2)#5 | 151.21(3) | | |
| | | O(2)#1-Ca(1)-O(3)#5 | 122.05(2) | | |
| | | O(2)#2-Ca(1)-O(3)#5 | 67.55(3) | | |
| | | O(1)#3-Ca(1)-O(3)#5 | 83.30(3) | | |

Symmetry transformations used to generate equivalent atoms:

#1 x,-y+2,z+1/2 #2 -x,-y+2,-z #3 -x,y+1,-z+1/2

#4 x,y+1,z #5 -x,y,-z+1/2 #6 -x,-y+2,-z+1

#7 x,y-1,z

The sheet structure of **3** is propagated by O2 in a dual role; first by bridging two calcium centers along the b-axis and secondly by connecting the $Ca^{2+}$ centers through the O1-P-O2 moiety, thereby extending the structure along the c-axis, as shown in Figure 4.9. Apparently, the pendant P-OH (O3) group terminates the propagation, limiting the dimensionality of the structure to two.

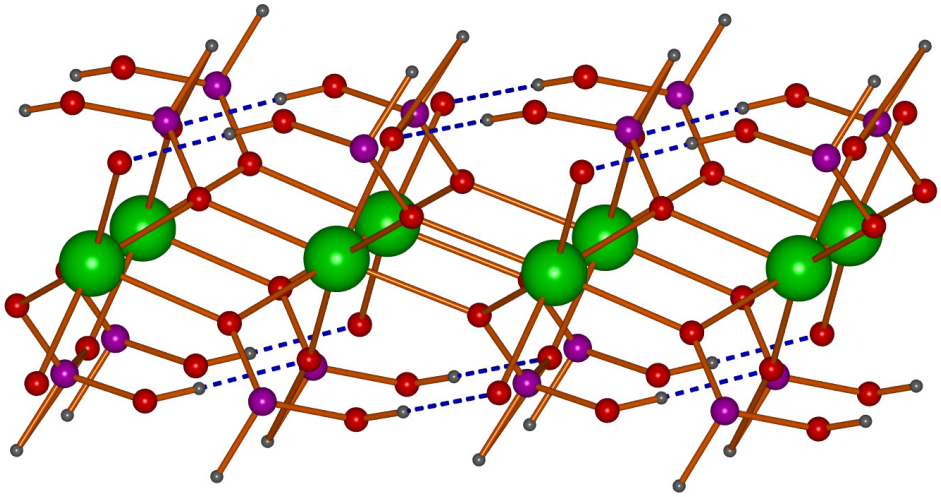

**Figure 4.9.** A sheet structure of **3** viewed down the b-axis, showing hydrogen bonding in blue dotted lines. The metal centers are represented by green spheres, oxygen (red), carbon (black), hydrogen (gray) and phosphorus by purple spheres.

Due to the presence of an uncoordinated P-OH group (O3) on each ligand, hydrogen bonds occur within the sheets as indicated in Figure 4.10, with a O3···O1 (donor-acceptor atoms D···A involved in hydrogen bonding) distance of 2.70 Å which is shorter than the sum of their Van der Waals radii (3.0 Å).

Two-dimensional, isostructural sheets of $Mg(HPO_3)\cdot 6H_2O$,[42,43] $Ca(HPO_3)\cdot H_2O$ (**5**) and $Sr(HPO_3)\cdot H_2O$[21] have also been reported. In these compounds, the phosphonic acid ligand is doubly deprotonated whereas it is singly deprotonated in **3** and in $\{Ca[PH(O)_2OH(H_2O)]_2\}_n$, **4**. The extent of deprotonation may be based on the different reaction conditions employed.

The main difference between **3** and **4** is that compound **4** has one coordinating water molecule, but compound **3** is anhydrous. The presence of the water molecule in **4**

leads to a seven-coordinated metal center versus six in **3**, and contributes to an increase in dimensionality through hydrogen bonding. In addition, one phosphonate O-H in **4** coordinates to the metal center. In contrast, in **3** none of the phosphonate O-H is involved in extending the structure, resulting in a lower overall dimensionality.

The crystal structure of **4** has already been reported by Larbot and Cot[20] and Mahmoudkani and Langer.[21] The literature preparation of **4** however involved a metathesis reaction between $CaCO_3$ and $H_3PO_3$.[44] The crystal structure of **4** was redetermined to draw a better comparison with compound **3**.

Compound **4** indicates a three-dimensional structure with seven coordinate $Ca^{2+}$ centers. The asymmetric unit of **4** (Figure 4.10) consists of one calcium ion center in coordinated to two singly deprotonated $H_3PO_3$ ligands and one water molecule (Figure 4.11).

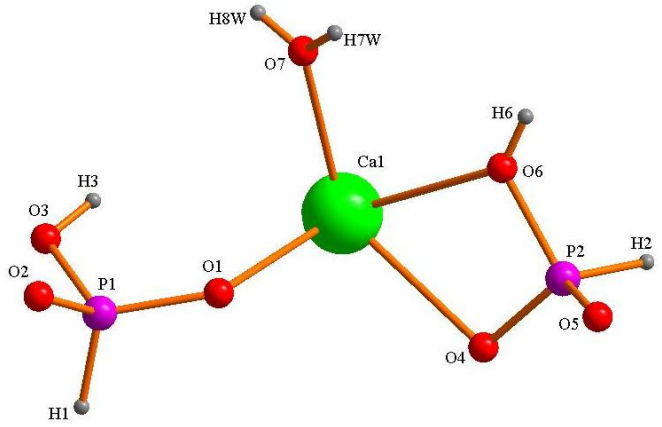


**Figure 4.10.** Schematic labeling of **4** showing the asymmetric unit of $[Ca(H_2PO_3)_2(H_2O)]_n$

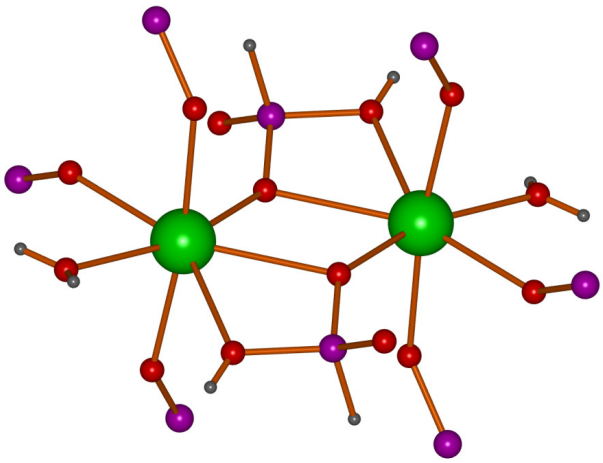

**Figure 4.11.** The calcium environment of **4**, showing seven coordination made of six phosphite oxygen atoms and one water molecule. The metal centers are represented by green spheres, oxygen (red), carbon (black), hydrogen (gray) and phosphorus by purple spheres.

The Ca-O bond distances in **4** range from 2.35(1) Å to 2.53(1) Å. The P-O bond distances 1.504(1)-1.570(2) are different from those in the phosphonates where typically three distinct P-O bond distances corresponding to P=O, P-$O^-$ and P-OH are observed. This is one of the special cases where in one ligand the oxygen with the acidic proton (O6, Figure 4.12) coordinates to the metal center, wheras in the second ligand there is a pendant P-OH (O3).

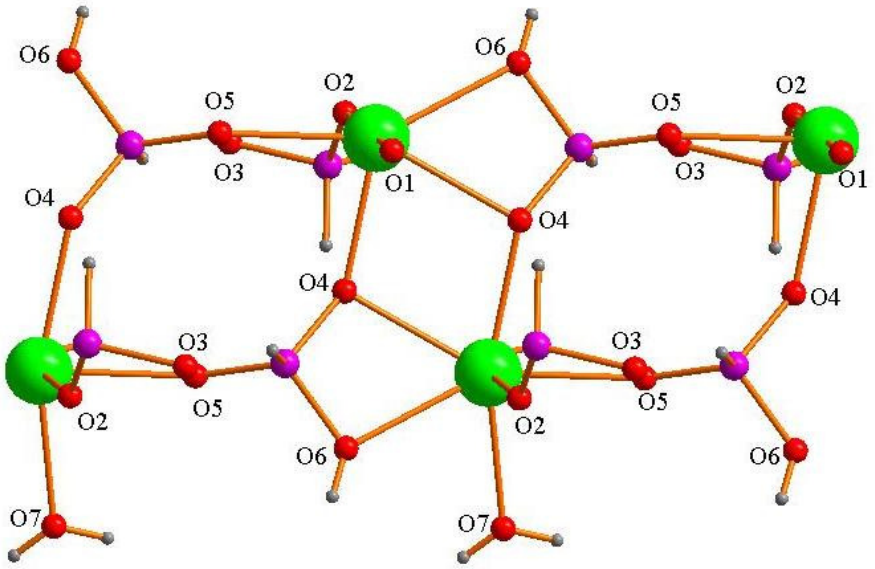


**Figure 4.12.** Sheet structure of **3** viewed along the b-axis, showing chelate formation by O4 and O6 and bridging involving O5-P-O4 in a eight-atom ring system.

The second ligand is metal-bound in a chelate fashion involving O4 and O6; the third oxygen O5 bridges two metal centers through a O4-P-O5 moiety to form an eight-membered ring system, (shown in Figure 4.9), typical of phosphinate (**1**) and phosphonates **10-13** (Chapter 6). The bridging motif in the ligand is shown in Figure 4.13, showing how the layers are connected, but leaving one non-coordinated P-OH on the ligand. Hydrogen bonds between water molecules and pendant P-OH groups hold sheets of **4** together to form a three dimensional structure. In addition, weak hydrogen bonds involving O3-H··· O5 exist within the sheets (Figure 4.14). The hydrogen bond distances are provided in Table 4.4.

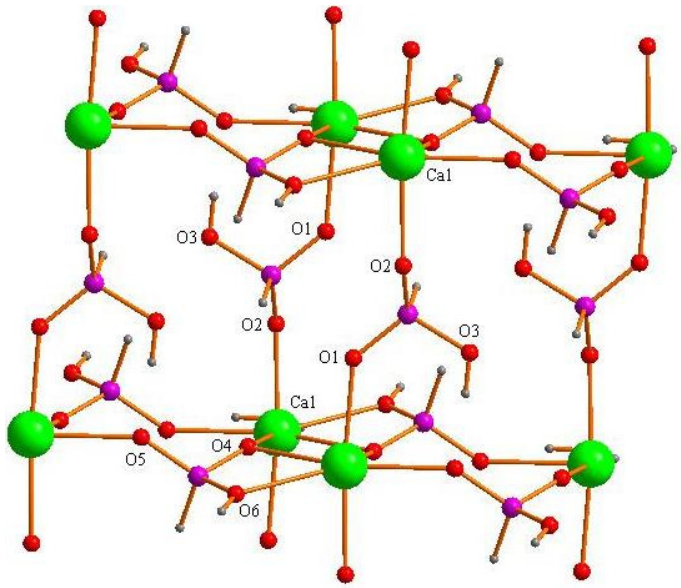


**Figure 4.13.** Structure of **4** viewed along the c axis showing O1-P-O2 linkage between sheets with partial labeling of the oxygen atoms.

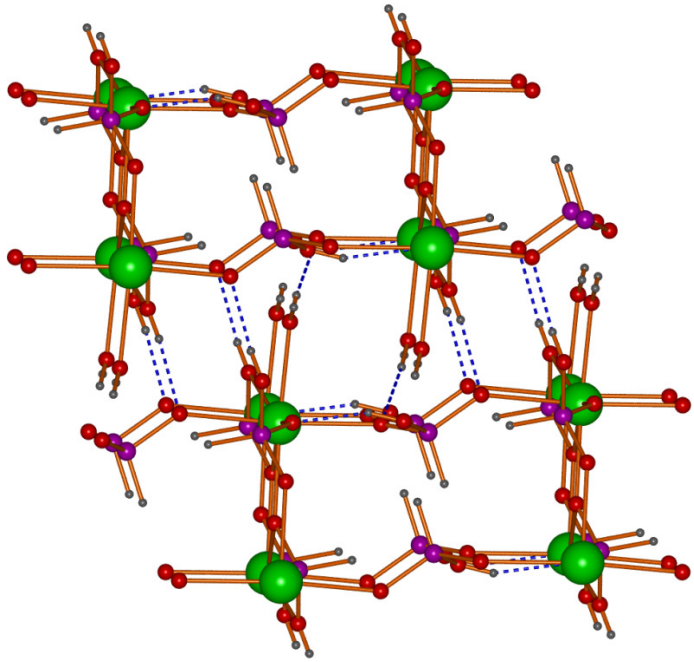

**Figure 4.14.** Structure showing extended view of **4**, with hydrogen bonds between layers (shown by vertical dotted blue lines) that hold the sheets into a 3D structure. Hydrogen atoms within the sheets are indicated by the horizontal dotted blue line.

### 4.3.3 Calcium Hydrogenphosphate, $[CaHPO_4]_n$ (6):

The novel calcium hydrogen phosphate, **6** was prepared by dissolving calcium nitrate and ethylenediphosphonic acid in water in the presence of tetramethylene-phosphonic acid. The mixture was placed in a Carius tube, sealed under vacuum and kept at 170 $^oC$ for 12 days during which colorless blocks of crystals formed. Compound **6** was structurally characterized by single crystal X-ray crystallography. The details of crystallographic data and structure refinement parameters are summarized in Table 4.2 in the experimental section of this chapter.

Compound **6** crystallizes in the triclinic space group P-1. It is a three-dimensional compound comprised of two hydrogen phosphate ions $HPO_4^{2-}$ and two crystallographically independent calcium ions in the asymmetric unit. Each ligand is therefore doubly deprotonated, O2 and O3 and O6 and O7 respectively belong to the two hydrogen phosphate ligands. Each ligand also contains a protonated P-OH functionality, these are O4 and O8 respectively. The P=O moieties are O1 and O5.

All phosphate oxygen atoms are involved in metal coordination and each calcium ion is coordinated by seven phosphate oxygen atoms (Figure 4.15).

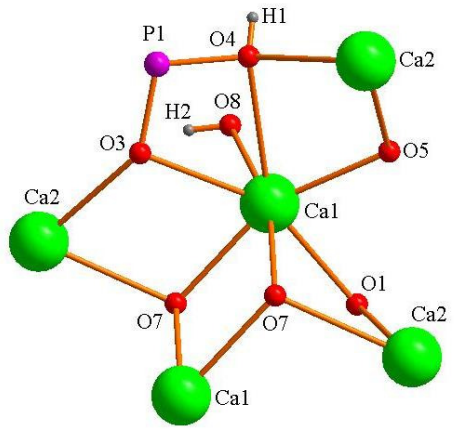


**Figure 4.15.** Calcium environment of the seven coordinate compound **6**.

However the two ligands display two binding modes, in one, O3 and O4 are involved in chelate formation, in addition, O1, O3 and O4 bridge between the metal centers. In the other ligand, chelate formation involves O5 and O7 whereas O7 bridges two Ca1 centers. O8 is responsible for the dense three-dimensional structure (Figure 4.16). The difference in binding modes of the phosphorus acid ligand is reflected in the wide range of P-O bond distances (1.509 (2) Å to 1.589 (2) Å).

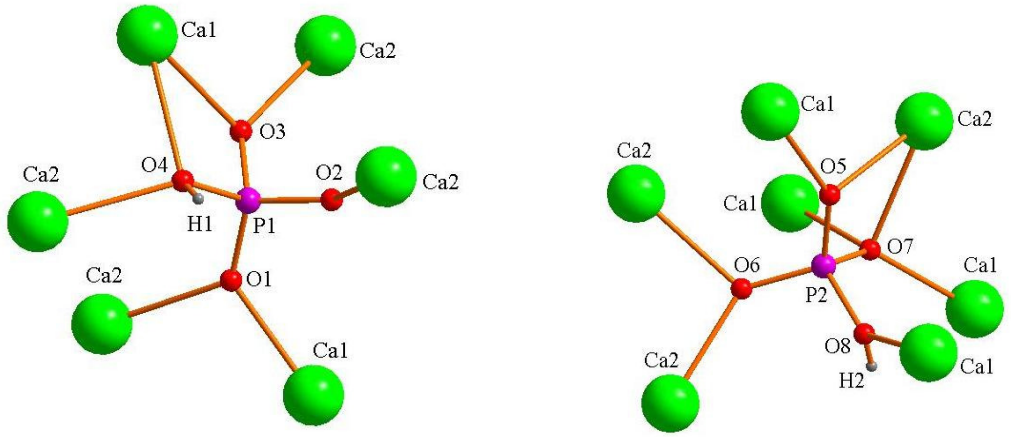


**Figure 4.16.** The binding modes of phosphorus acids in compound **6**

The Ca-O bond lengths range between 2.294 (2 ) and 2.684 (2) Å, the shortest being Ca(1)-O(5) while the longest correspond to Ca(1)-O(4). Selected bond distances and lengths are summarized in Table 4.5.

The previously reported $CaHPO_4$ was precipitated from a homogeneous solution *via* urea hydrolysis.[45] Alkaline earth phosphonates involving Mg have also been reported.[46]

**Table 4.5.** Bond lengths [Å] and angles [°] for anhydrous calcium hydrogen phosphate (**6**)

| | | | |
|---|---|---|---|
| Ca(1)-O(5)#1 | 2.294(2) | O(5)#1-Ca(1)-O(1)#2 | 78.77(8) |
| Ca(1)-O(1)# 2 | 2.348(2) | O(5)#1-Ca(1)-O(8)#3 | 104.94(8) |
| Ca(1)-O(8)# 3 | 2.407(2) | O(1)#2-Ca(1)-O(8)#3 | 110.43(8) |
| Ca(1)-O(7)#4 | 2.419(2) | O(5)#1-Ca(1)-O(7)#4 | 157.60(7) |
| Ca(1)-O(7) | 2.431(2) | O(1)#2-Ca(1)-O(7)#4 | 79.73(8) |
| Ca(1)-O(3) | 2.478(2) | O(8)#3-Ca(1)-O(7)#4 | 88.41(7) |
| Ca(1)-O(4) | 2.684(2) | O(5)#1-Ca(1)-O(7) | 89.60(7) |
| P(1)-O(1) | 1.509(2) | O(1)#2-Ca(1)-O(7) | 74.09(7) |
| P(1)-O(2) | 1.529(2) | O(8)#3-Ca(1)-O(7) | 165.30(7) |
| P(1)-O(3) | 1.554(2) | O(7)#4-Ca(1)-O(7) | 78.52(7) |
| P(1)-O(4) | 1.556(2) | O(5)#1-Ca(1)-O(3) | 123.58(7) |
| P(2)-O(5) | 1.518(2) | O(1)#2-Ca(1)-O(3) | 153.19(8) |
| P(2)-O(6) | 1.522(2) | O(8)#3-Ca(1)-O(3) | 80.01(8) |
| P(2)-O(7) | 1.543(2) | O(7)#4-Ca(1)-O(3) | 75.87(7) |
| P(2)-O(8) | 1.589(2) | O(7)-Ca(1)-O(3) | 90.19(7) |
| Ca(2)-O(6)#7 | 2.378(2) | O(5)#1-Ca(1)-O(4) | 70.22(7) |
| Ca(2)-O(2)#8 | 2.421(2) | O(1)#2-Ca(1)-O(4) | 148.77(8) |
| Ca(2)-O(1)#7 | 2.466(2) | O(8)#3-Ca(1)-O(4) | 75.16(7) |
| Ca(2)-O(5)#4 | 2.470(2) | O(7)#4-Ca(1)-O(4) | 131. 50(7) |
| Ca(2)-O(6)#9 | 2.473(2) | O(7)-Ca(1)-O(4) | 108.58(7) |
| Ca(2)-O(4)#9 | 2.533(2) | O(3)-Ca(1)-O(4) | 56.66(7) |
| Ca(2)-O(7)#4 | 2.565(2) | | |

Symmetry transformations used to generate equivalent atoms:

#1 -x+1,-y,-z+1 #2 x+1, y, z #3 x, y, z+1 #4 -x+1,-y+1,-z+ #5 x, y-1, z #6 x-1, y, z

#7 -x,-y+1,-z+1 #8 -x,-y+1,-z+2 #9 x,y+1,z #10 -x,-y+2,-z+1 #11 x,y,z-1

## 4.4 Conclusions

Three calcium compounds based on phosphorus oxoacids have been synthesized and structurally characterized. Of those, two are novel compounds, calcium phenylphosphinate (**1**) and the anhydrous calcium hydrogen phosphite (**3**)**.** Compound **6**

is a well known mineral but it was synthesized by a different route. We redetermined the crystal structure of **6** since this has not been reported. There is clear correlation between ligand type and compound dimensionality. The monophosphinates (with two oxygen donor atoms) were observed to form 1D chains, while the monophosphonates (with three oxygen donor atoms) formed 2D sheets. The phosphites and phosphates (with three and four oxygen donor atoms respectively) on the other hand display 2D or 3D arrays.

## 4.5 Experimental

### 4.5.1 Synthesis of Calcium Phenylphosphinate (1):

Phenylphosphinic acid, HPPA (0.28 g, 1.97 mmol), ethylenediphosphonic acid, EDPA (0.19 g, 1 mmol) and $CaCl_2$ (0.11 g, 0.99 mmol) were dissolved in 10 mL distilled water and refluxed overnight. The resulting clear solution was transferred to a Carius tube, sealed at 40 mTorr pressure and heated for five days at 150 ºC. The clear solution was filtered into a small vial and concentrated in a water bath at 80 ºC. Tiny colorless crystals formed on the sides of the vials within one hour. Yield 0.4 g, 0.66 mmol, 30.5 %; m.p. 454 $^{o}$C (decomposes), IR (Nujol): 3375.3(s), 3188.5(w), 2727.5(m), 1455.4(s), 1373.0(s), 1041.1(m) 930.2(m), 749.3(m), 550.9(w).

### 4.5.2 Synthesis of Anhydrous Calcium Hydrogenphosphite (3):

To 4 ml of ethanol, $CaCl_2$ (0.11g, 1 mmol), was added to form a cloudy mixture, to which 3.5 mL of 2M $H_3PO_3$ solution were added. The resulting cloudy mixture was sealed in a Carius tube at 40 mTorr pressure. The sealed tube was kept in a 150 $^{o}$C oven for 3 days. When the hot tube was removed from the oven, the entire solution was

vaporized. The tube was allowed to cool to room temperature overnight. Colorless hexagonal plates of crystals were found in solution the next day. Good quality crystals of **3** were also formed when the reaction was repeated using water as solvent and warming the solution at 80 $^{o}$C in a vial for 2 hours. The yield was 0.03g, 0.3 mmol, 30 % (g). m.p: 450 $^{o}$C (decomposes); IR (Nujol): 2900(s), 2742(w), 1475(s), 1388(s), 1305(w), 1154(w), 950(w), 722(s).

### 4.5.3 Synthesis of Anhydrous Calcium Hydrogenphosphate (6):

To 6 mL distilled water, $Ca(NO_3)_2{\cdot}4H_2O$ (0.48 g, 0.25 mmol) and tetramethylenephosphonic acid, $H_8$EDTPA (0.153 g, 0.025 mmol) were added to form a cloudy mixture which was sealed in a Carius tube at 40 mTorr pressure and kept in a 170 $^{o}$C oven for 12 days. The tube containing a cloudy white mixture was allowed to cool to room temperature. The cloudy mixture was filtered to obtain a small amount of colorless crystalline solid along with white powder and a clear filtrate. The crystalline solid was transferred into the clear filtrate as seed for crystal growth and left at room temperature for slow evaporation of solvent. After about two weeks when there was no further observable increase in the crystal size, the crystalline solid was collected by filtration and dried. The amount of crystalline solid is too small to reliably determine the yield or conduct further analysis beyond single crystal X-ray diffraction.

## 4.6 Experimental Details

Phenylphosphinic acid (HPPA), phosphonic acid ($H_3PO_3$), $CaCl_2$ and $C_2H_5OH$ were obtained commercially and used without further purification. The synthesis of ethylenediphosphonic acid and 4-(4'-phosphonophenoxy) phenyl phosphonic acid is described in Chapter 3. A Perkin-Elmer PE 1600–FT-IR spectrometer was used to collect IR spectra as Nujol mulls between KBr plates. Single crystals of compounds **1, 3**, and **6** were analyzed by single crystal X-ray diffraction, compounds **1** and **3** also by IR spectroscopy. Melting points were determined using a VWR Thermocouple device. Crystals were not soluble in common NMR solvents, hence no spectra could be obtained.

## 4.7. X-ray Crystallography

X-ray quality crystals of compounds **1, 3** and **6**, were grown as described above. Crystals were taken out of the solutions and covered with viscous hydrocarbon oil (Infineum). Using a microscope, suitable crystals were selected and attached to a glass fiber. The crystal was mounted onto a 3-circle goniometer under a low temperature nitrogen stream of the low temperature device. Crystallographic data of **1** and **6** were collected using a Bruker SMART diffractometer equipped with APEX I CCD system, while **3** was collected using a Bruker DUO APEX II CCD. In all cases, MoKα-radiation ($\lambda$ = 0.71073 Å) at 96(2) K (**1** and **6**) and 97(2) K (**3**) was used. Crystal data, details of data collection and refinement of compounds **1**, **3** and **6** are provided in Table 4.1. The structures of **1**, **3** and **6** were solved by the Direct Methods as included in the SHELXS-97 and the structures were refined with SHELXL-97 program package.[4747] All non-hydrogen atoms were refined with anisotropic displacement parameters. Positions of

hydrogen atoms of the hydroxyl groups were found at calculated positions. All the phosphonate hydrogen atoms in **3** were located from the Fourier difference map and refined freely, except H3 which was placed in a calculated position. All hydrogen atoms bonded to carbon in **1**, **3** and **6** were also placed in calculated positions based on geometric considerations and refined as riding atoms. The hydrogen atom bonded to phosphorus atom in **1** and **3** were located and refined freely.

**Table 4.2**. Crystal data and structure refinement for compounds **1**, **3** and **6**

| | **1** | **3** | **6** |
|---|---|---|---|
| Empirical formula | $C_{24}H_{26}CaO_8P_4$ | $H_2Ca_{0.5}O_3P$ | $Ca_2H_2O_8P_2$ |
| Formula weight | 606.4 | 101.03 | 272.12 |
| Temperature (K) | 97(2) | 96(2) | 96(2) |
| Wavelength (Å) | 0.71073 | 0.71073 | 0.71073 |
| Crystal system | Triclinic | Monoclinic | Triclinic |
| Space group | P-1 | C2/c | P-1 |
| a (Å) | 5.67(1) | 15.12(1) | 6.62(7) |
| b (Å) | 7.64(2) | 5.53(5) | 6.90(8) |
| c (Å) | 15.22(4) | 7.18(6) | 6.97(8) |
| α (°) | 86.5(5) | 90 | 76.31(1) |
| β (°) | 84.4(4) | 100.45(2) | 83.69(1) |
| γ (°) | 87.4(4) | 90 | 88.40(2) |
| Volume ($Å^3$) | 654.41(3) | 590.1(9) | 307.7(6) |
| Z | 1 | 8 | 2 |
| Dcal($mg/m^3$) | 1.540 | 2.274 | 2.937 |
| μ ($mm^{-1}$) | 0.532 | 1.564 | 2.379 |
| Crystal size( $mm^3$) | 0.40 | 0.32 | 0.45 |
| | 0.10 | 0.20 | 0.30 |
| | 0.05 | 0.16 | 0.20 |
| 2θ range (°) | 2.69-28.40 | 2.74-37.03 | 3.03-28.43 |
| Reflections collected | 6452 | 3699 | 2848 |
| Independent reflections | 3230 | 1420 | 1395 |
| R1 [I>2sigma(I)] | 0.0470 | 0.0238 | 0.0276 |
| wR2 [I>2sigma(I)] | 0.1142 | 0.1026 | 0.0704 |
| R1 (all data) | 0.0677 | 0.0246 | 0.0306 |
| wR2 (all data) | 0.1237 | 0.1044 | 0.0725 |

## 4.8 References


(1) Jansen, D. R.; Rijn, Z. J.; Denkova, A.; Kolar, Z. I.; Krijger, G. C. *Langmuir* **2009**, *25*, 2790.
(2) ALBEE, F. H.; MORRISON, H. F. *Annals of Surgery* **1920**, *71*, 32.
(3) Zhang, Y.; Leon, A.; Song, Y.; Studer, D.; Haase, C.; Koscielski, L. A.; Oldfield, E. *J. Med. Chem.* **2006**, *49*, 5804.
(4) Hitzbleck, J.; O'Brien, A. Y.; Deacon, G. B.; Ruhlandt-Senge, K. *Inorg. Chem.* **2006**, *45*, 10329.
(5) Morizzi, J.; Hobday, M.; Rix, C. *J. Mater. Chem.* **2000**, *10*, 1693.
(6) Alexandratos, S. D.; Strand, M. A.; Quillen, D. R.; Walder, A. J. *Macromolecules* **1985**, *18*, 829.
(7) Trochimczuk, A. W. *React. Funct. Polym.* **2001**, *48*, 141.
(8) El Hammari, L.; Laghzizil, A.; Saoiabi, A.; Barboux, P.; Meyer, M. *Colloids and Surf. A* **2006**, *289*, 84.
(9) El Shafei, G. M. S.; Moussa, N. A. *J. Colloid Interface Sci.* **2001**, *238*, 160.
(10) Aissa, A.; Debbabi, M.; Gruselle, M.; Thouvenot, R.; Gredin, P.; Traksmaa, R.; Tõnsuaadu, K. *J. Solid State Chem.* **2007**, *180*, 2273.
(11) Mori, K.; Oshiba, M.; Hara, T.; Mizugaki, T.; Ebitani, K.; Kaneda, K. *New J. Chem.* **2006**, *30*, 44.
(12) Quin, L. D.; Dysart, M. R. *J. Org. Chem.* **1962**, *27*, 1012.
(13) Jaffé, H. H.; Freedman, L. D.; Doak, G. O. *J. Am. Chem. Soc.* **1953**, *75*, 2209.
(14) Carter, R. P.; Carroll, R. L.; Irani, R. R. *Inorg. Chem.* **1967**, *6*, 939.
(15) Zumdahl, S. S. *Chemical Principles*; 6th ed.; Houghton Mifflin Company: Massachusetts, 2009.
(16) Lima, C. B. A.; Airoldi, C. *Solid State Sci.* **2002**, *4*, 1321.
(17) Svoboda, J.; Zima, V.; Benes, L.; Melanova, K.; Vlcek, M. *Inorg. Chem.* **2005**, *44*, 9968.
(18) Mahmoudkhani, A. H.; Langer, V. *Solid State Sciences* **2001**, *3*, 519.
(19) Stone, J.; Smith, M.; Loye, H.-C. *J. Chem. Crystallogr.* **2007**, *37*, 103.
(20) Larbot, A.; Durand, J.; Cot, L. *Z. Anorg. Allg. Chem.* **1984**, *508*, 154.
(21) Mahmoudkhani, A. H.; Langer, V. *Phosphorus, Sulfur Silicon Relat. Elem.* **2001**, *176*, 83.
(22) Bujan, M.; Sikirić, M.; Filipović-Vinceković, N.; Vdović, N.; Garti, N.; Füredi-Milhofer, H. *Langmuir* **2001**, *17*, 6461.
(23) Joshi, V. S., Joshi J. Mihir 2003, p 817.
(24) Freedman, L. D.; Doak, G. O. *Chem. Rev.* **1957**, *57*, 479.
(25) Burrow, R. A.; Farrar, D. H.; Lough, A. J.; Siqueira, M. R.; Squizani, F. *Acta Crystallogr., Sect. C: Cryst. Struct. Commun.* **2000**, *C56*, E357.
(26) Cornet, S. M.; Dillon, K. B.; Howard, J. A. K.; Monks, P. K.; Thompson, A. L. *Acta Crystallogr., Sect. C: Cryst. Struct. Commun.* **2009**, *C65*, o195.
(27) Rao, K. P.; Vidyasagar, K. *Eur. J. Inorg. Chem.* **2005**, *2005*, 4936.
(28) Xu, X.-J.; Zhou, L.-H.; Lu, C.-Z. *Mater. Lett.* **2007**, *61*, 4980.
(29) Gao, L.-L.; Song, S.-Y.; Ma, J.-F.; Yang, J. *Cryst. Growth Des.* **2007**, *7*, 895.
(30) Mahmoudkhani, A. H.; Langer, V.; Smrcok, L. *Solid State Sci.* **2002**, *4*, 873.

(31) Svoboda, J.; Zima, V.; Beneš, L.; Melánová, K.; Vlček, M. *Inorg. Chem.* **2005**, *44*, 9968.
(32) Galeffi, B.; Simard, M.; Wuest, J. D. *Inorg. Chem.* **1990**, *29*, 955.
(33) Shieh, M.; Martin, K. J.; Squattrito, P. J.; Clearfield, A. *Inorg. Chem.* **1990**, *29*, 958.
(34) Martin, K. J.; Squattrito, P. J.; Clearfield, A. *Inorg. Chim. Acta* **1989**, *155*, 7.
(35) Mahmoudkhani, A. H.; Langer, V. *J. Mol. Struct.* **2002**, *609*, 97.
(36) Cao, G.; Lynch, V. M.; Swinnea, J. S.; Mallouk, T. E. *Inorg. Chem.* **1990**, *29*, 2112.
(37) Huang, J.; Fu, X.; Wang, G.; Li, C.; Hu, X. *Dalton Trans.* **2011**, *40*, 3631.
(38) Lu, X.; Li, J.; Sun, Z.-G.; Dong, D.-P.; Hua, R.-N.; Zhang, N.; Liu, L.; Tong, F.; Wang, W.-N. *Z. Anorg. Allg. Chem.* **2009**, *635*, 2617.
(39) Tong, F.; Zhu, Y.; Sun, Z.; Wang, W.; Zhao, Y.; Xu, L.; Gong, J. *Inorg. Chim. Acta* **2011**, *368*, 200.
(40) Bernot, K.; Luzon, J.; Sessoli, R.; Vindigni, A.; Thion, J.; Richeter, S.; Leclercq, D.; Larionova, J.; van der Lee, A. *J. Am. Chem. Soc.* **2008**, *130*, 1619.
(41) Cunningham, D.; Hennelly, P. J. D.; Deeney, T. *Inorg. Chim. Acta* **1979**, *37*, 95.
(42) Corbridge, D. *Acta Crystallographica* **1956**, *9*, 991.
(43) Powell, D. R.; Smith, S. K.; Farrar, T. C.; Ross, F. K. *Acta Crystallogr. Sect. C* **1994**, *50*, 342.
(44) Tu, M.; Luo, C.; Dang, J.; Chen, J. *Wujiyan Gongye* **1998**, *30*, 6.
(45) Burrus, H. L. *Journal of Applied Chemistry* **1961**, *11*, 376.
(46) Tamimi, F.; Nihouannen, D. L.; Bassett, D. C.; Ibasco, S.; Gbureck, U.; Knowles, J.; Wright, A.; Flynn, A.; Komarova, S. V.; Barralet, J. E. *Acta Biomaterialia* **2011**, *7*, 2678.
(47) Chadwick, S.; Englich, U.; Ruhlandt-Senge, K. *Chem. Commun.* **1998**, 2149.

# CHAPTER 5

## Synthesis and structural description of Calcium Formate

### 5.1 Introduction

Water has been the main solvent during the synthesis of the phosphonate based metal organic frameworks in this project, since most of the ligands (phenylphosphinic acid, ethylenediphosphonic acid, propylenediphosphonic acid and amino trimethylenephosphonic acid), are water soluble. However, on a few occasions, the use of N,N′-dimethylformamide (DMF, $CH_3)_2NCHO$) has been advantageous, specifically in cases where ligands are not water soluble. It was one of such syntheses that yielded the unexpected three-dimensional calcium formate (**7**).

DMF is widely used as a polar solvent; it is hydrophilic, aprotic and boils at 153 $^{o}$C. DMF has been used in a wide range of catalytic reactions[1,2] and in industrial applications as a gas absorbent.[3] DMF has been shown to decompose to generate dimethylamine and carbon monoxide *in situ*, its role in the preparation of carbonyl complexes[2,4] and in the Heck carbonylation (palladium-catalyzed synthesis of aryl amides from aryl halides) has been widely described.[5] The decomposition of DMF may occur at elevated temperatures or in the presence of a strong acid or base.[6] In addition, the hydrolysis reaction of DMF yields formic acid (Scheme 5.1). Also, the formation of formic acid (Figure 5.1) resulting from the decomposition of DMF has been reported.[7,8]

$$HC(O)N(CH_3)_2 + H_2O \longrightarrow HCO_2H + HN(CH_3)_2$$

Scheme 5.1 Hydrolysis reaction of DMF

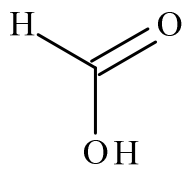


**Figure 5.1.** Formic acid pKa 3.77[9] (in $H_2O$).

The incorporation of decomposition products of DMF in coordination chemistry is a well described phenomenon.[10,11,12,13] In addition, In effect, DMF acts as both solvent and a reagent through the products of its decomposition.[6,10] In other instances, it may act as a ligand or a neutral donor molecule in coordination chemistry.[14-17]

The synthesis and structural analysis, along with structural studies on other of alkaline earth formate phases are described in this chapter.

## 5.2 Synthetic Considerations

Calcium formate, **7**, reported in this chapter is the result of DMF decomposition during attempts to prepare compounds based on biphenyl-4,4′-diphosphonic acid ligand, $H_4$BDPA (Figure 5.2).

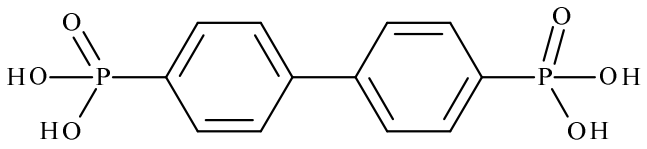


**Figure 5.2.** Biphenyl-4,4′-diphosphonic acid ($H_4$BDPA)

This ligand system is only scarcely explored in metal organic framework chemistry. Formates based on alkaline earth derivatives are not common, but there are few examples involving Mg,[18] Sr,[19] Ba compounds,[20] along with a few transition metal examples (V, Cu, Zn and Mo).[21-28]

Focusing on the lighter alkaline earth metals magnesium and calcium, various strategies were employed to prepare the $H_4BDPA$ target compounds and to obtain single crystals. Prime amongst those was the variation of solvent to identify one which allowed the highest solubility for the ligand. Various reactions were carried out in methanol, ethanol, ethanol/methanol mixtures, DMSO (dimethylsulfoxide), DMSO /ethanol and water/methanol mixtures, all of which were chosen based on literature examples,[22,23,29] which resulted in amorphous products. Furthermore, various coligands, including DABCO (diazabycyclo[2,2,2]-octane), 1,4-dioxane and diglyme did not result in crystalline products. On the other hand, treatment of $Ca(NO_3)_2{\cdot}4H_2O$ and $Mg(NO_3)_2{\cdot}6H_2O$ with $H_4BDPA$ ligand in dimethyl formamide (DMF), afforded crystals based on the decomposition of DMF. The solvothermal synthesis was conducted at 150 $^oC$ for five days. Crystalline colorless blocks in the tube (Scheme 5.2).

$$Ca(NO_3)_2{\cdot}4H_2O + Mg(NO_3)_2{\cdot}6H_2O + C_{12}H_{12}O_6P_2 \xrightarrow[150\ ^oC]{DMF} [Ca(HCO_2)_2]_n \quad \textbf{(7)}$$

**Scheme 5.2.** Synthesis of anhydrous calcium formate (**7**).

Since the ligand was not included in the final product, the reaction was repeated without the ligand. Subsequent solvothermal synthesis involving $MgCl_2$, $CaCl_2$ and $SrCl_2$ in DMF at 150 $^oC$ yielded crystals overnight that were identified, based on unit cell

parameters as the previously reported Mg formate,[8,18,30-34] Ca formate,[18,35,36] and Sr oxalate.[37]

A proposed mechanism of DMF decomposition /hydrolysis during the synthesis affording formate is given in Scheme 5.3 where bimolecular nucleophilic substitution ($S_N2$) results in the formation of formic acid. Formic acid then reacts with the metal salt yielding the metal formate compounds.

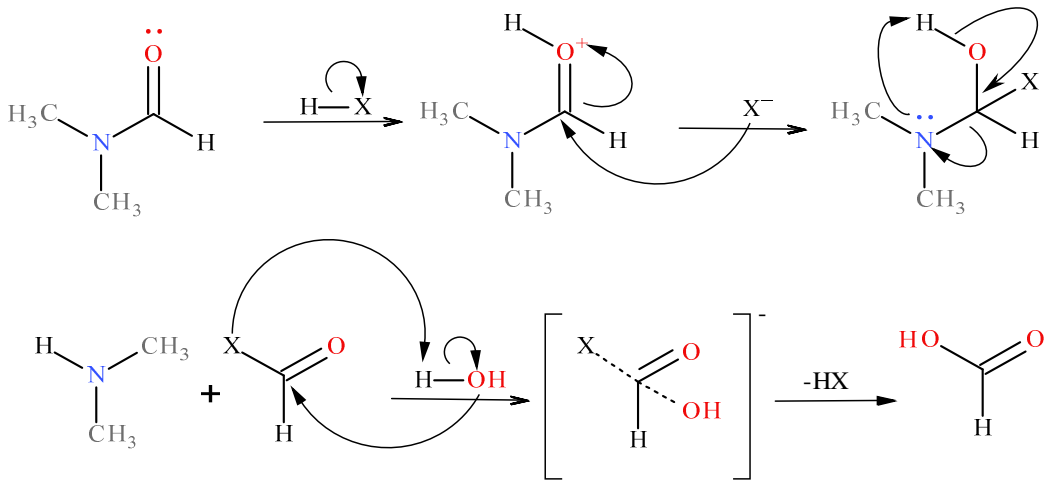


**Scheme 5.3** Mechanism of Acid hydrolysis of DMF to form formic acid.

### 5.3 Synthesis of Calcium Formate, $[Ca(HCO_2)_2]_n$ (7):

Compound **7** was obtained by treating a mixture of $Ca(NO_3)_2{\cdot}4H_2O$, $Mg(NO_3)_2{\cdot}6H_2O$ with biphenyl-4,4′-diphosphonic ($H_4BPDA$) acid in DMF in an evacuated Carius tube at 150 $^oC$ for five days. Colorless blocks of crystals formed in the tube. Compound **7** is structurally characterized by single crystal X-ray crystallography; it crystallizes in the orthorhombic Pbca space group. Detailed crystallographic data and

structure refinement parameters are summarized in Table 5.1 in the experimental section of this chapter.

Compound **7** is a three dimensional framework containing a $Ca^{2+}$ ion and two singly deprotonated formate ligands in the asymmetric unit. The calcium ion is coordinated to seven formate oxygen atoms, five of which coordinate in a monodentate fashion while the remaining two oxygen atoms are involved in chelate formation as shown in Figure 5.3.

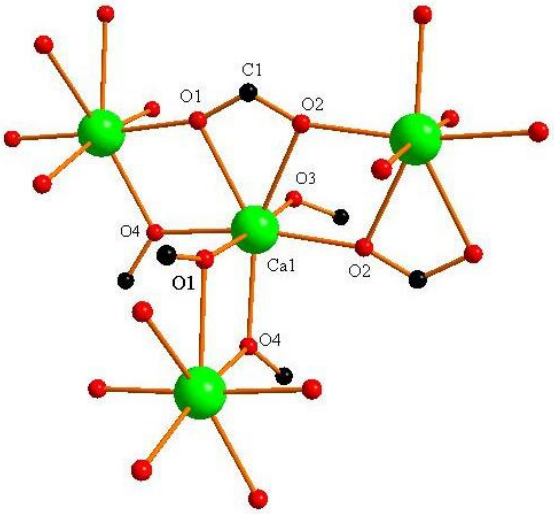


**Figure 5.3** Schematic labeling of calcium formate (**7**).

The chelating oxygen atoms (O1 and O2) also bridge the calcium centers to form a two-dimensional structure as displayed in Figure 5.4a. The sheets are held together by bridging formate oxygen atoms, leading to a three-dimensional propagation as shown in Figure 5.4b.

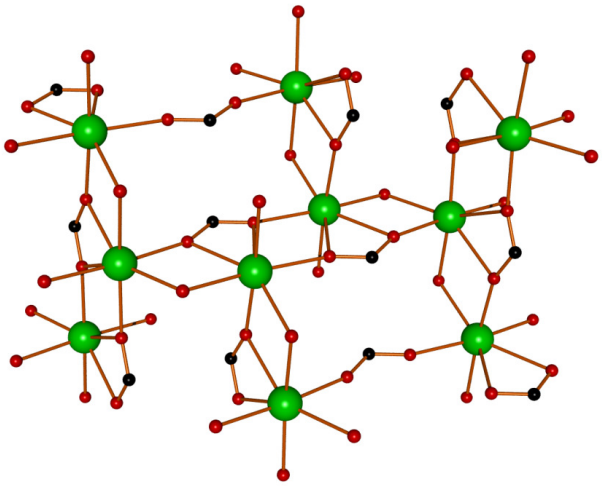

(**a**)

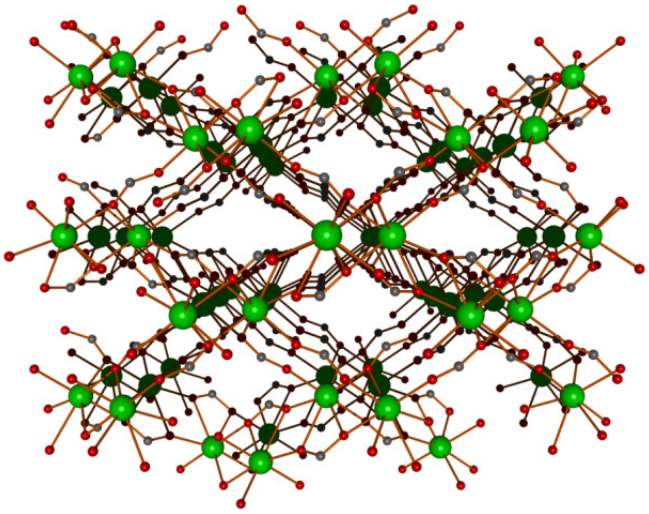

(**b**)

**Figure 5.4** Extended sheet structure of calcium formate **(7)** showing **a**. chelate and bridge formation, viewed from z-axis **b.** in three-dimensions. Green Sphere represent calcium, red oxygen and grey/black represent carbon. Hydrogen atoms on the carbon atoms are removed for clarity.

The average Ca-O distances of the chelating formates are longer (2.523(1) Å), compared to that of the monodentate ones, with average Ca-O distances of 2.370(5) Å. Not surprisingly, all the C-O distances fall within a narrow range of 1.245(2) - 1.267(2) Å. The values of the bond distances and angles are listed in Table 5.2. The bond distances

of compound **7** closely match those of α-calcium formate characterized by neutron diffraction. [38]

**Table 5.2.** Bond lengths [Å] and angles [°] for calcium formate

| Bond lengths | | Bond angles | | Bond angles | |
|---|---|---|---|---|---|
| Ca(1)-O(1) | 2.3204(9) | O(1)-Ca(1)-O(2)#1 | 95.39(3) | O(2)#1-Ca(1)-O(2)#3 | 70.46(4) |
| Ca(1)-O(3) | 2.3471(9) | O(1)-Ca(1)-O(3) | 176.20(3) | O(4)-Ca(1)-O(2)#3 | 121.51(3) |
| Ca(1)-O(2)#1 | 2.3494(9) | O(2)#1-Ca(1)-O(4) | 166.90(3) | O(4)#2-Ca(1)-O(2)#3 | 149.85(3) |
| Ca(1)-O(4) | 2.4053(9) | O(1)-Ca(1)-O(4)#2 | 74.22(3) | O(1)-Ca(1)-O(1)#3 | 84.65(3) |
| Ca(1)-O(4)#2 | 2.4274(9) | O(3)-Ca(1)-O(2)#1 | 87.84(3) | O(3)-Ca(1)-O(1)#3 | 91.95(3) |
| Ca(1)-O(2)#3 | 2.5102(1) | O(1)-Ca(1)-O(4) | 89.77(3) | O(2)#1-Ca(1)-O(1)#3 | 121.81(3) |
| Ca(1)-O(1)#3 | 2.5505(9) | O(3)-Ca(1)-O(4) | 87.48(3) | O(4)-Ca(1)-O(1)#3 | 70.59(3) |
| O(2)-Ca(1)#2 | 2.5101(1) | O(3)-Ca(1)-O(4)#2 | 108.17(3) | O(4)#2-Ca(1)-O(1)#3 | 148.27(3) |
| O(1)-C(1) | 1.2509(2) | O(2)#1-Ca(1)-O(4)#2 | 84.18(3) | O(2)#3-Ca(1)-O(1)#3 | 51.43(3) |
| O(2)-C(1) | 1.2540(2) | O(4)-Ca(1)-O(4)#2 | 85.67(3) | C(1)-O(1)-Ca(1)#2 | 92.12(7) |
| O(3)-C(2) | 1.2450(2) | O(1)-Ca(1)-O(2)#3 | 91.75(3) | O(1)-C(1)-O(2) | 122.50(1) |
| O(4)-C(2)#6 | 1.2673(2) | O(3)-Ca(1)-O(2)#3 | 87.44(3) | O(3)-C(2)-O(4)#7 | 125.23(1) |
| | | | | O(3)-C(2)-H(1) | 120.0(9) |
| | | | | O(4)#7-C(2)-H(1) | 114.7(9) |

Symmetry transformations used to generate equivalent atoms:
#1 x-1/2,-y+1/2,-z+1 #2 -x+3/2,y-1/2,z #3 -x+3/2,y+1/2,z
#4 -x+1,-y+1,-z+1 #5 x+1/2,-y+1/2,-z+1 #6 x+1/2,y,-z+3/2
#7 x-1/2,y,-z+3/2

There are close structural similarities between **7** and calcium hydrogen phosphite monohydrate, **4** (discussed in Chapter 4). Previous examples of alkaline earth metals include a three-dimensional magnesium formate, γ-$Mg_3(HCO_2)_6$ , where one oxygen bridges two metal centres ($\mu^2$) while the other binds in a monodentate fashion.[33]

Four forms of calcium formate have been reported; α-$Ca(HCO_2)_2$,[38] β-$Ca(HCO_2)_2$,[39] γ-$Ca(HCO_2)_2$,[19] and δ-$Ca(HCO_2)_2$,[39,40] structural information for all but the γ-phase[19] is available. The four forms of calcium formate (α, β, γ and δ) as well as three forms of strontium formates (α, β and δ) have been established using Differential Thermal Analysis (DTA).[19,40] At atmospheric pressure, the α-$Ca(HCO_2)_2$ phase exists at a temperature range of 298-493K, whereas β-$Ca(HCO_2)_2$ is stable between 298-453K, γ-$Ca(HCO_2)_2$ at 493-573K, and the δ-$Ca(HCO_2)_2$ between 573-633K.[40] Consequently, studies have shown phase transitions from α→β→ γ →δ on heating and cooling δ→ γ→ β → α among the calcium formate compounds,[19] for example the α-form transforms to β- $Ca(HCO_2)_2$ phase at temperatures above 338 K, whereas the β-polymorph converts back to the α-$Ca(HCO_2)_2$ on cooling in the presence of water vapor.[19,39]

The crystal structure of α-$Ca(HCO_2)_2$ was determined by neutron diffraction studies at 100 K, revealing a seven coordinate calcium center with Ca-O distances from of 2.322(8) to 2.558(6) Å. An additional weaker Ca-O interaction of 3.420(5) Å also exists. The ligand binding includes two chelating and four monodentate ligands.[38] The structures of β-$Ca(HCO_2)_2$[39] and δ-$Ca(HCO_2)_2$[19] were obtained by powder diffraction pattern at temperatures below 333K and at 603 K respectively.[19,39] β-$Ca(HCO_2)_2$ is six coordinate with Ca-O distances between 2.311(3) - 2.484(3) Å; two additional Ca-O distances of 2.944(3) Å are also observed.[39] δ-$Ca(HCO_2)_2$ display an eight coordinate calcium center with two types of Ca-O bonds; four of the Ca-O bond distances are the same (2.280(3) Å) while the remaining four are longer - 2.790(3) Å.[19]

There are also a few reported examples of Mg, Sr and Ba formates,[37,38,41-43] including a two dimensional $Mg(HCO_2)_2 \cdot 2H_2O$ which reversibly dehydrates to the

anhydrous three-dimensional form,[42,43] α-, β- and γ-$Mg(HCO_2)_2$ formates [33] and $Mg_3(HCO_2)_6$ formate. [18]

Four forms of Sr formate ($Sr(HCOO)_2 \cdot 2H_2O$, α-, β-, γ and δ-$Sr(HCOO)_2$) have been reported.[40] $Sr(HCOO)_2 \cdot 2H_2O$ dehydrates to α-$Sr(HCOO)_2$ at 403 K in an irreversible process, although the presence of water vapor, the δ→ β→α transitions occurs on cooling. β-$Sr(HCOO)_2$ is isomorphous to β-$Ca(HCOO)_2$.[40]

Transition metal formates include Cr,[44] Cd,[45] La,[46] Co,[47] V,[48] Zn,[49,50] Y[51] and Fe.[32] Recently in our laboratory, Sr formate as a result of DMF decomposition was also observed by another member of our research group.[52]

Similar to **7,** the above mentioned α-$Ca(HCO_2)_2$ crystallizes in the orthorhombic space group Pbca, with almost identical cell parameters, respectively (a = 10.168(4) Å, b = 13.407(2) Å, c = 6.278(2) Å) compared to (a = 10.230(2) Å, b = 6.260(7) Å, c = 13.325(1) Å). The slight contraction in volume may be due to temperature difference during structural analysis. Single X-ray quality crystals of **7** were obtained *via* the hydrothermal synthetic route; however only the crystalline powder of the compound has been reported, indicating the advantage of hydrothermal synthesis for crystallization of compounds.

## 5.4 Conclusions

Single X-ray quality crystals of **7** were obtained hydrothermally and characterised. The seven calcium coordinate is three-dimensional.

It is observed that phosphorous acid in **4** described in chapter 4 and formic acid in **7** exhibit very similar metal coordination motif.

## 5.5 Experimental

In an attempt to form calcium biphenyl-4,4′-diphosphonates, $H_4BDPA$ (0.10g, 0.31 mmol), $Mg(NO_3)_2{\cdot}6H_2O$ (0.08 g, 0.31 mmol) and $Ca(NO_3)_2{\cdot}4H_2O$ (0.14 g 0.59 mmol) were dissolved in 4 mL DMF. The cloudy suspension was sealed in a Carius tube at about 40 mTorr pressure and placed at 150 $^oC$ for five days. Single colorless blocks of crystals formed in the tube. Yield 0.018 g,0.14 mmol, 40 % based on $Ca(NO_3)_2{\cdot}4H_2O$; m.p.: 500 $^oC$; IR (Nujol): 2920.1(s), 2724.0(w), 1489.0(s), 1375.0(s), 1154.5(w), 722.5(s). The yields were too low to allow for further analysis.

## 5.6 Experimental Details

$Ca(NO_3)_2{\cdot}4H_2O$, $Mg(NO_3)_2{\cdot}6H_2O$, $C_2H_5OH$ and DMF, were obtained commercially. The reagents were used as purchased. A Perkin-Elmer PE 1600–FT-IR spectrometer was used to collect IR spectra as Nujol mulls between KBr plates. Single crystals of compound **7** were analyzed by X-ray diffraction and by IR spectroscopy. Crystals of **7** were not soluble in common NMR solvents hence no spectra was obtained.

## 5.7. X-ray crystallography

X-ray quality crystals of compound **7** were grown as described above. Crystals were taken out of the solutions and covered with viscous hydrocarbon oil (Infineum). Using a microscope, suitable crystals were selected and attached to a glass fiber. The crystal was mounted onto a 3-circle goniometer under a low temperature nitrogen stream of the low temperature device (93(2) K). Crystallographic data of **7** were collected using a Bruker diffractometer equipped with Duo Kappa system equipped with MoKα-radiation

($\lambda$ = 0.71073 Å). Crystal data, details of the data collection and refinement details are provided in Table 5.1. The structure of **7** was solved by Direct Methods with the aid of SHELXS-97, the structure was refined using SHELXL-97.[53] All non-hydrogen atoms were refined with anisotropic displacement parameters. All hydrogen atoms were placed on calculated positions.

**Table 5.1**. Crystal data and structure refinement for compound **7**

| | |
|---|---|
| Empirical formula | $C_2H_2CaO_4$ |
| Formula weight | 130.12 |
| Temperature (K) | 93(2) |
| Wavelength (Å) | 0.71073 |
| Crystal system | Orthorhombic |
| Space group | Pbca |
| a (Å) | 10.23(1) |
| b (Å) | 6.26(7) |
| c (Å) | 13.25(1) |
| α (°) | 90 |
| β (°) | 90 |
| γ (°) | 90 |
| Volume ($Å^3$) | 848.2(2) |
| Z | 8 |
| Dcal($mg/m^3$) | 2.038 |
| μ ($mm^{-1}$) | 1.362 |
| Crystal size( $mm^3$) | 0.45 x 0.35 x 0.30 |
| 2θ range (°) | 3.08-28.22 |
| Reflections collected | 6755 |
| Independent reflections | 1008 |
| R1 [I>2sigma(I)] | 0.0233 |
| wR2 [I>2sigma(I)] | 0.0606 |
| R1 (all data) | 0.0243 |
| wR2 (all data) | 0.0611 |

## 5.8 References:


(1) Spencer, A. *J. Organomet. Chem.* **1980**, *194*, 113.
(2) Serp, P.; Hernandez, M.; Richard, B.; Kalck, P. *Eur. J. Inorg. Chem.* **2001**, *2001*, 2327.
(3) Uchisawa, J.; Nanba, T.; Masukawa, S.; Obuchi, A. *Catal. Lett.* **2004**, *98*, 103.
(4) Rusina, A.; Vlcek, A. A. *Nature* **1965**, *206*, 295.
(5) Wan, Y.; Alterman, M.; Larhed, M.; Hallberg, A. *J. Org. Chem.* **2002**, *67*, 6232.
(6) Muzart, J. *Tetrahedron* **2009**, *65*, 8313.
(7) He, J.; Zhang, Y.; Pan, Q.; Yu, J.; Ding, H.; Xu, R. *Microporous Mesoporous Mater.* **2006**, *90*, 145.
(8) Rossin, A.; Fairen-Jimenez, D.; Düren, T.; Giambastiani, G.; Peruzzini, M.; Vitillo, J. G. *Langmuir* **2011**, *27*, 10124.
(9) Brown, H. C.; McDaniel, D. H.; Hafliger, O. *Determ. Org. Struct. Phys. Methods* **1955**, 567.
(10) Dickmeis, M.; Ritter, H. *Macromol. Chem. Phys.* **2009**, *210*, 776.
(11) Kahrovic, E.; Orioli, P.; Bruni, B.; Di Vaira, M.; Messori, L. *Inorg. Chim. Acta* **2003**, *355*, 420.
(12) Dakanali, M.; Tsikalas, G. K.; Krautscheid, H.; Katerinopoulos, H. E. *Tetrahedron Lett.* **2008**, *49*, 1648.
(13) Buchschacher, P.; Kalvoda, J.; Arigoni, D.; Jeger, O. *J. Am. Chem. Soc.* **1958**, *80*, 2905.
(14) Demessence, A.; D'Alessandro, D. M.; Foo, M. L.; Long, J. R. *J. Am. Chem. Soc.* **2009**, *131*, 8784.
(15) Liu, F.; Wang, L.; Yu, F.; Zhang, L.; Wu, Q.; Shi, Y.; Yang, X. *J. Chem. Eng. Data* **2010**, *55*, 1342.
(16) Suzuki, H.; Ishiguro, S.-I. *Acta Crystallogr. Sect. C* **1998**, *54*, 586.
(17) Yilmaz, V. T.; Topcu, Y. *Thermochim. Acta* **1997**, *307*, 143.
(18) Rood, J. A.; Noll, B. C.; Henderson, K. W. *Inorg. Chem.* **2006**, *45*, 5521.
(19) Comel, C.; Mentzen, B. F. *J. Solid State Chem.* **1974**, *9*, 210.
(20) Poojary, D. M.; Zhang, B.; Clearfield, A. *An. Quim. Int. Ed.* **1998**, *94*, 401.
(21) Poojary, D. M.; Zhang, B.; Bellinghausen, P.; Clearfield, A. *Inorg. Chem.* **1996**, *35*, 5254.
(22) Wang, Z.; Heising, J. M.; Clearfield, A. *J. Am. Chem. Soc.* **2003**, *125*, 10375.
(23) Clearfield, A.; Wang, Z. *J. Chem. Soc., Dalton Trans.* **2002**, 2937.
(24) DeBurgomaster, P.; Darling, K.; Jones, S.; Zubieta, J. *Inorg. Chim. Acta* **2010**, *364*, 150.
(25) Zhang, B.; Poojary, D. M.; Clearfield, A. *Inorg. Chem.* **1998**, *37*, 1844.
(26) Poojary, D. M.; Zhang, B.; Bellinghausen, P.; Clearfield, A. *Inorg. Chem.* **1996**, *35*, 4942.
(27) Breen, J. M.; Schmitt, W. *Angew. Chem. Int. Ed.* **2008**, *47*, 6904.
(28) Ouellette, W.; Wang, G.; Liu, H.; Yee, G. T.; O'Connor, C. J.; Zubieta, J. *Inorg. Chem.* **2008**, *48*, 953.
(29) Prochniak, G.; Zon, J.; Daszkiewicz, M.; Pietraszko, A.; Videnova-Adrabinska, V. *Acta Crystallogr., Sect. C: Cryst. Struct. Commun.* **2007**, *C63*, o434.

(30) Kim, H.; Samsonenko, D. G.; Yoon, M.; Yoon, J. W.; Hwang, Y. K.; Chang, J.-S.; Kim, K. *Chem. Commun.* **2008**, 4697.
(31) Samsonenko , D. G.; Kim, H.; Sun, Y.; Kim, G.-H.; Lee, H.-S.; Kim, K. *Chemistry – An Asian Journal* **2007**, *2*, 484.
(32) Viertelhaus, M.; Adler, P.; Clérac, R.; Anson, Christopher E.; Powell, Annie K. *Eur. J. Inorg. Chem.* **2005**, *2005*, 692.
(33) Mallick, A.; Saha, S.; Pachfule, P.; Roy, S.; Banerjee, R. *Inorg. Chem. (Washington, DC, U. S.)* **2011**, *50*, 1392.
(34) Rood, J. A.; Noll, B. C.; Henderson, K. W. *Inorg. Chem.* **2006**, *45*, 5521.
(35) Chukanov, N. V.; Malinko, S. V.; Lisitsyn, A. E.; Dubinchuk, V. T.; Kuz'mina, O. V.; Zadov, A. E. *Zap. Vseross. Mineral. O-va.* **1999**, *128*, 43.
(36) Fakeev, A. A.; Orlova, I. V.; Iskhakova, L. D.; Zhadanov, B. V. *Zh. Prikl. Khim. (S.-Peterburg)* **1997**, *70*, 1602.
(37) Christensen, A. N.; Hazell, R. G. *Acta Chem. Scand.* **1998**, *52*, 508.
(38) Burger, N.; Fuess, H.; Mason, S. A. *Acta Crystallographica Section B* **1977**, *33*, 1968.
(39) Matsui, M.; Watanabe, T.; Kamijo, N.; Lapp, R. L.; Jacobson, R. A. *Acta Crystallogr. Sect. B* **1980**, *36*, 1081.
(40) Mentzen, B. F.; Comel, C. *J. Solid State Chem.* **1974**, *9*, 214.
(41) Galigne, J. *Acta Crystallogr. Sect. B* **1971**, *27*, 2429.
(42) Malard, C.; Pezerat, H.; Herpin, P.; Toledano, P. *J. Solid State Chem.* **1982**, *41*, 67.
(43) Rossin, A.; Ienco, A.; Costantino, F.; Montini, T.; Di Credico, B.; Caporali, M.; Gonsalvi, L.; Fornasiero, P.; Peruzzini, M. *Crystal Growth & Design* **2008**, *8*, 3302.
(44) Cotton, F. A.; Rice, G. W. *Inorg. Chem.* **1978**, *17*, 688.
(45) Post, M. L.; Trotter, J. *Acta Crystallogr. Sect. B* **1974**, *30*, 1880.
(46) Kistaiah, P.; Sathyanarayana Murthy, K.; Iyengar, L.; Krishna Rao, K. V. *J. Mater. Sci.* **1981**, *16*, 2321.
(47) Kaufman, A.; Afshar, C.; Rossi, M.; Zacharias, D. E.; Glusker, J. P. *Struct. Chem.* **1993**, *4*, 191.
(48) Mootz, D.; Seidel, R. *Acta Crystallogr. Sect.C* **1987**, *43*, 1218.
(49) Stoilova, D.; Baggio, R.; Garland, M. T.; Marinova, D. *Vib. Spectrosc* **2007**, *43*, 387.
(50) Viertelhaus, M.; Anson, C. E.; Powell, A. K. *Z. Anorg. Allg. Chem.* **2005**, *631*, 2365.
(51) Trunov, V. A.; Kudryashev, V. A.; Bulkin, A. P.; Ulyanov, V. A.; Loshmanov, A. A.; Furmanova, N. G.; Antson, O.; Hiismäki, P.; Mutka, H.; Pöyry, H.; Tiitta, A. *Solid State Commun.* **1986**, *59*, 95.
(52) Peter Rosado, K. R.; Syracuse University.
(53) Chadwick, S.; Englich, U.; Ruhlandt-Senge, K. *Chem. Commun.* **1998**, 2149.

# CHAPTER 6

## Synthesis and Characterization of Magnesium Diphosphonates

### 6.1 Introduction

While the chemistry of transition metal phosphonates has seen remarkable growth with applications as diverse as gas separation, gas storage or catalytic systems,[1-4] the corresponding chemistry with s-block elements has received significantly less attention. Nevertheless, the vast array of three dimensional porous solids available for transition metals suggests a rich structural chemistry for the s-block analogues.

In our attempt to explore magnesium and calcium phosphonates with potential applications as biomimetic agents in bone therapy, we initiated a study to explore their structural chemistry in detail. Previous work on magnesium phosphonates has indicated challenges with respect to solubility and crystallization.[5,6] Hydrothermal synthesis has emerged as methodology of choice, as it promotes the solubility of products and thus aids in crystal growth.[7]

Magnesium is prevalent in many biological systems, for example the activation of enzymes for the synthesis of adenosine triphosphate (ATP) which is responsible for energy transfer in the cell.[8,9] Also, compounds such as 'Milk of Magnesia' $Mg(OH)_2$ and 'Epsom Salt' $MgSO_4{\cdot}7H_2O$ have valuable medicinal applications,[10] while MgO is used in animal feed.[11]

With a size of 86 pm,[12] the $Mg^{2+}$ ion has a high charge to size ratio, resulting in a tendency towards bond polarization and covalent bond character, as well as strong tendency towards donor coordination.[13,14] This is why $Mg^{2+}$ ions easily binds to

oxygen[15,16] and nitrogen based co-ligands,[17,18] and the majority of magnesium compounds prepared in aqueous media contain water,[19-29] as shown in the two-dimensional magnesium phosphonates $Mg(O_3PC_6H_5)(H_2O)$[6] and $\{Mg[(HO_3PCH(C_6H_5)]_2\}_{\infty}\cdot 8H_2O$.[30] In this work, the chemistry of magnesium phosphonates is explored to understand factors responsible for structural features.

Aside of its prevalence in biological systems, the low weight of magnesium makes it suitable for the preparation of low density metal organic frameworks (MOFs) with important applications in gas storage and separation of gas mixtures.[16,19,31-34] As discussed in Chapter 2 of this thesis, extensive work has been carried out on transition metal as compared to s-block metal organic frameworks (MOFs). Recent studies have also documented magnesium MOF's activity toward hydrogen, making them suitable candidates for gravimetric hydrogen uptake.[35] Common examples of three dimensional, porous magnesium based metal organic frameworks[35-37] are based on trinuclear carboxylate bound units.[38] In $[Mg_3(BPT)_2(H_2O)_4]_{\infty}$ (BPT = bipyridine tricarboxylate) for instance, trinuclear magnesium clusters are coordinated to the rigid organic linker BPT ligand through oxygen atoms forming three-dimensional framework.[35]

The detailed investigation on the relation between synthetic routes, ligand type and the resulting structural characteristics provide the foundation for the understanding of parameters governing the factors leading to framework geometry and dimensionality. This chapter describes the preparation and structural features of a three-dimensional magnesium ethylenediphosphonate **8** and two-dimensional magnesium propylenediphosphonate **9.** In both compounds, dimensionality is affected by hydrogen bonding, adding an additional parameter in the understanding of structural principles.

The chemistry of propylenediphosphonic acid is quite limited, and this is in strong contrast to the corresponding ethylenediphosphonates. Compound **9** therefore represents the only example for this ligand involving alkaline earth metals with the exception of the $[Ba_2(O_3P(CH_2)_3PO_3)\cdot 3H_2O)]_n$, reported by Tuikka *et al.*[39] Single crystals of the Ba species were formed by gel crystallization. The three-dimensional structure of $[Ba_2(O_3P(CH_2)_3PO_3)\cdot 3H_2O]_n$, is comprised of layers of eight coordinate barium centers that are pillared by the hydrocarbon chains of the fully deprotonated ligand ($PDPA^{4-}$). Three water molecules complete the coordination sphere of the $Ba^{2+}$ ion.[39] Other examples of compounds made with $H_4PDPA$ include Ti,[40] Ag,[41] Zn,[42] V,[43] Mo, Ni and Gd.[44,45]

In most magnesium based MOFs, there is at least one water molecule in the coordination sphere of the metal,[29,46,47] and compounds **8** and **9** are no exception. For some MOFs, the coordinated water molecules can be removed at elevated temperatures without decomposition of the MOF.[48] Examples of three-dimensional MOFs with such characteristics include $[Mg(3,5\text{-pdc})H_2O)]$ (pdc = pyridine dicarboxylate),[27] $[Mg_2(btc)(CH_3COO)(C_4H_9NO)_3\cdot H_2O]_n$ (btc = 1,3,5-benzenetricarboxylate),[49] and $[Mg(H_2dhtp)(H_2O)_2]_n$ ($H_4dhtp$ = 2,5-dihydroxy terephthalic acid).[14] After removal of water molecule(s) the open magnesium sites of these compounds are available for binding to various gas molecules such as $H_2$ and $CO_2$.[27]

In this chapter, the synthesis and characterization of two magnesium diphosphonates, one with an ethylene linker, $H_4EDPA$ (Figure 6.1a), the other with a propylene linker, $H_4PDPA$ (Figure 6.1b) are described.

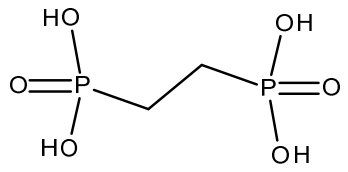


Ethylenediphosphonic acid ($H_4EDPA$)

($pKa_1$ 1.5, $pKa_2$ 3.18, $pKa_3$ 7.62, $pKa_4$ 9.28)[50]

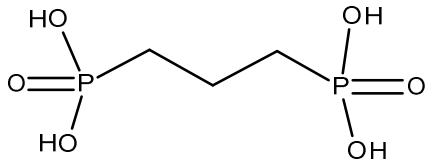


Propylenediphosphonic acid ($H_4PDPA$)

($pKa_1$ 1.6, $pKa_2$ 3.06, $pKa_3$ 7.65, $pKa_4$ 8.63)[50]

**Figure 6.1.** Diphosphonic acid ligands used to prepare compounds **8** and **9**.

Diphosphonic acids have been shown to initiate a wide variety of compounds due to their ability to carry multiple degree of deprotonation but also due to the variety of metal binding modes.

## 6.2 Synthetic Considerations

With scarce knowledge on the preferred synthetic pathways for alkaline earth metal phosphonate complexes, a number of synthetic procedures were evaluated in order to prepare the target compounds and obtain single crystals. In analogy with transition metal MOFs, the synthesis of magnesium and calcium phosphonates is based on ligand

acidity. As shown in detail in this chapter, slight changes in reaction conditions often lead to significant structural changes. Also, the framework geometry is influenced by several factors, chiefly the ligand and solvent characteristics; of particular importance is the pH of the solution, the temperature, and pressure and crystallization conditions.

Demonstrating the challenges in designing feasible systematic route, but perhaps even more importantly, challenges in predicting structural parameters, the two ligands used in this chapter differ only by one carbon in the linker. Nevertheless, their crystallization required dramatically different approaches, and their structural parameters could not be more different.

The ligand characteristics influence the mode of metal binding, with factors such as denticity, linker length and degree of deprotonation. The basicity of the solvent also plays a major role as there is competition between solvation and ligation.[19] Compounds **8** and **9** have been prepared using water as solvent as it is non-toxic, non-flammable and most relevant to biological systems.

Single crystals of compounds **8** and **9** were analyzed by X-ray diffraction. Thermogravimetric studies were also conducted to determine the temperatures at which coordinated water is lost. The characterization of compounds **8** and **9** is limited to solid state methods due to their insolubility in common NMR solvents, as is the case of most metal organic frameworks (MOFs) with extended structures.[51]

### 6.2.1 Magnesium Ethylenediphosphonate (8):

Attempts to crystallize magnesium ethylenediphosphonates from water or DMF at room temperatures and under hydrothermal or solvothermal conditions failed. Hence

the introduction of donors and coligands was explored, based on work by Best *et al*.[52] The introduction of the coligand phenylphosphinic acid resulted in the formation of Xray quality crystals of **8**.

Compound **8** was prepared by refluxing magnesium nitrate, ethylene-diphosphonic acid and phenylphosphinic acid in dimethyl formamide (DMF) overnight. The resulting clear solution was sealed in a Carius tube at 40 mTorr. The sealed tubes were kept in an oven at 150 $^{o}$C for seven days. After slow cooling, the tubes were opened and the resulting colorless solution transferred into a small glass vial and covered with Parafilm. Several holes were punctured in the Parafilm to allow slow evaporation of solvent. The vial was left at room temperature until colorless crystal appeared after two weeks (Scheme 6.1).

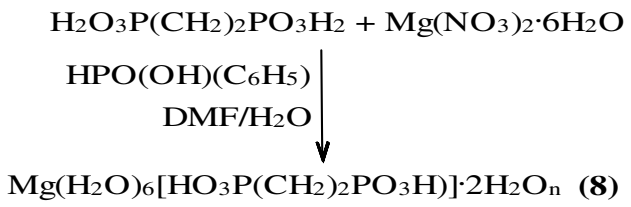


**Scheme 6.1.** Synthesis of compound magnesium ethylenediphosphonate **8.**

Based on the success of promoting crystal formation by the introduction of coligands, the introduction of DABCO (1,4-diazobicyclo[2.2.2]octane), promoted crystal growth within a few hours, even so that neither of the coligands is contained in the final product.

The reaction was repeated using water as solvent under the same hydrothermal conditions, affording crystals with identical unit cell parameters as **8** (Table 6.1, experimental section), indicating that the solvent type does not affect product formation.

En route to explore product formation and crystallization conditions to optimize compound yields, a variety of magnesium salts, $MgCl_2$, $Mg(CH_3CO_2)_2$ and $Mg(NO_3)_2{\cdot}6H_2O$ were used. All of them yielded powdery products. Furthermore, different ligand to metal salt ratios were utilized. While the ratios did not affect compound formation, a dependency on crystallization speed was observed, with the crystal formation being fastest with a ligand to salt ratio of 1:2.

### 6.2.2 Magnesium Propylenediphosphonate, (9):

To determine the effect of carbon chain length on structural parameters of the product, propylenediphosphonic acid $H_4PDPA$ was introduced. X-ray quality crystals were obtained by treatment of $Mg(NO_3){\cdot}6H_2O$ with $H_4PDPA$ in water in a small vial at 80 $^oC$. (Scheme 6.2).

$$H_2PO_3(CH_2)_3PO_3H_2 \; + \; Mg(NO_3)_2{\cdot}6H_2O \xrightarrow[80\ ^oC]{H_2O} Mg(HO_3P(CH_2)_3PO_3H_2)_2(H_2O)_{2n} \; \mathbf{(9)}$$

**Scheme 6.2.** Synthesis of magnesium propylenediphosphonate **9.**

## 6.3 Structural Aspects:

### 6.3.1 Magnesium Ethylenediphosphonate, $\{Mg(H_2O)_6(HO_3P(CH_2)_2PO_3H)\cdot 2H_2O\}_n$ (8):

Compound **8** crystallizes in the triclinic space group *P*-1. Crystal data, details of data collection and refinement of compounds **8** are provided in Table 6.1 in the experimental section of this chapter. The compound is made up of a doubly deprotonated ligand and $Mg^{2+}$ along with coordinated water molecules and waters of crystallization. There is no direct metal-ligand bond; instead, the association of cations and anions in **8** is achieved exclusively through hydrogen bonding *via* water molecules, resulting in the formation of a two-dimensional sheet structure.

The magnesium centers are coordinated in an octahedral fashion by six water molecules resulting in the well documented $[Mg(OH_2)_6]^{2+}$ cation. Extensive hydrogen bonding from coordinated water molecules to the diphosphonate ligands propagated the structure. Additional hydrogen bonding is provided by two waters of crystallization. The various O-H···O hydrogen bonds system in **8** have H···O distances of 1.925-2.066 Å, hydrogen bonding interactions, most of which are weak. As hydrogen positions are associated with a significant positional uncertainty, O-O distances are often used to determine their strength. O-O distances of 2.73-2.81 Å, along with a mean O-H-O angle of 176° which is near linear geometry, indicate strong hydrogen bonding. These values are summarized in Table 6.2.

**Table 6.2**. Hydrogen bonding geometry for compound **8**

| D-H…A | d(D-H) | d(H..A) | <D-H..A | d(D..A) |
|---|---|---|---|---|
| O1-H1O1…O5 | 0.797 | 2.014 | 172.65 | 2.806 |
| O1-H2O1…O4 | 0.774 | 2.042 | 175.87 | 2.814 |
| O2-H1O2…O5 | 0.727 | 2.066 | 166.71 | 2.778 |
| O2-H2O2…O7W | 0.839 | 1.925 | 170.24 | 2.755 |
| O3-H1O3…O7W | 0.800 | 1.928 | 176.37 | 2.727 |
| O3-H2O3 …O5 | 0.797 | 1.995 | 175.48 | 2.790 |
| O7W-H1W1…O4 | 0.727 | 2.066 | 177.53 | 2.792 |
| O7W-H2W1…O6 | 0.749 | 2.059 | 168.98 | 2.797 |

Since each magnesium ion is located on a center of symmetry, only three of the metal coordinated water molecules are symmetry independent. The metal is surrounded in a slightly distorted octahedral fashion by six water molecules, with O-Mg-O angles ranging from 87.46 (4) ° to 92.54 (4) ° (Figure 6.2).

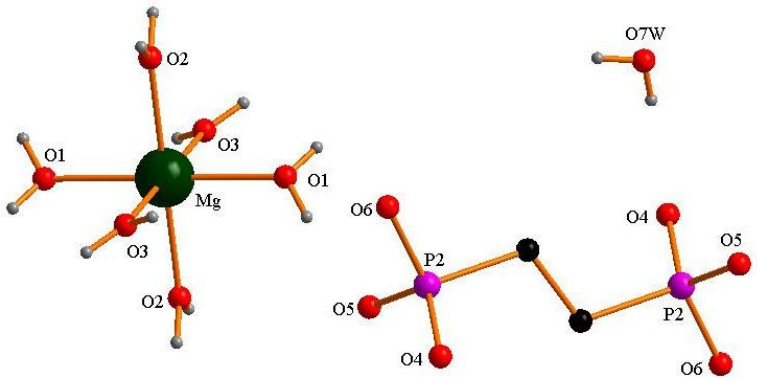


**Figure 6.2.** Graphical representation of compound **8** indicating atom labelling, Hydrogen atoms on carbon atom and hydrogen bonding are omitted for clarity.

The Mg-O distances differ slightly, with O1 in the trans position (2.080(1) Å) being slightly longer than the equatorial positions (2.048(1) Å, 2.056 (1) Å). These values are summarized in Table 6.3. The average Mg-$OH_2$ bond length in compound **8** is 2.06(1) Å, this value compares well with the average Mg-$OH_2$ bond distance of 2.06(2) Å, as determined from the average of 50 $[Mg(H_2O)_6]^{2+}$ structures by Dale S.H. et *al*.[53]

**Table 6.3.** Selected bond lengths [Å] and angles [°] of magnesium ethylenediphosphonate **8**

| Bond distances | | Bond angles | |
|---|---|---|---|
| P-O(5) | 1.5054(9) | O(5)-P-O(4) | 114.06(5) |
| P-O(4) | 1.5260(8) | O(5)-P-O(6) | 107.21(6) |
| P-O(6) | 1.5847(9) | O(4)-P-O(6) | 109.48(5) |
| P-C | 1.8017(1) | O(3)-Mg-O(1) | 87.46(4) |
| Mg-O(3) | 2.0471(1) | O(3)-Mg-O(1)#1 | 92.54(4) |
| Mg-O(2) | 2.0560(1) | O(2)-Mg-O(1) | 91.87(4) |
| Mg-O(1) | 2.0804(1) | O(3)#1-Mg-O(2)#1 | 89.82(5) |
| O5-$H_a$W | 2.002(1) | O(3)-Mg-O(2)#1 | 90.18(5) |
| O- $H_e$W | 2.036(1) | O(2)-Mg-O(1) | 88.13(4) |
| O-$H_e$W | 1.893(1) | C#2-C-P | 113.00(10) |

Symmetry transformations used to generate equivalent atoms:

#1 -x+1,-y+2,-z #2 -x,-y+1,-z+1

Each of the six metal-coordinated water molecules is doubly hydrogen bridged. Of these, the water molecules in the equatorial positions are connected to one ligand and one lattice water. The two axial water molecules bridge two ligands. This arrangement is illustrated in Figure 6.3a with oxygen atoms of water molecules represented by yellow spheres. Figure 6.4 illustrates the hydrogen bonding network.

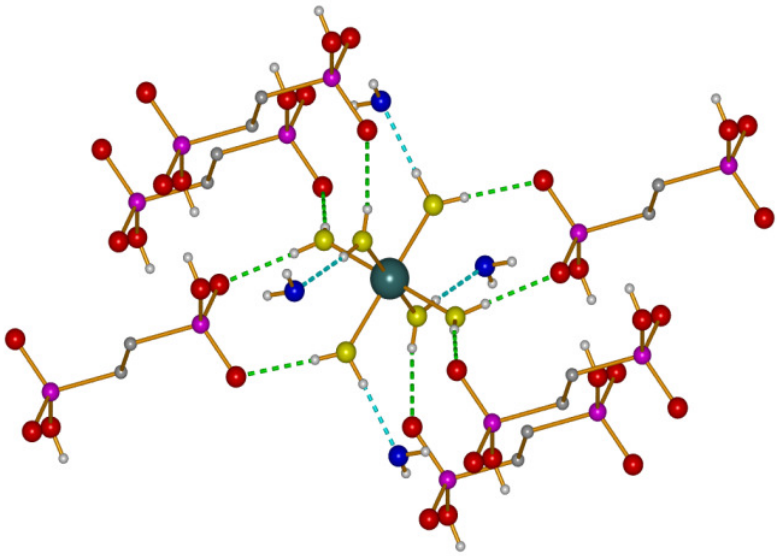

**(a)**

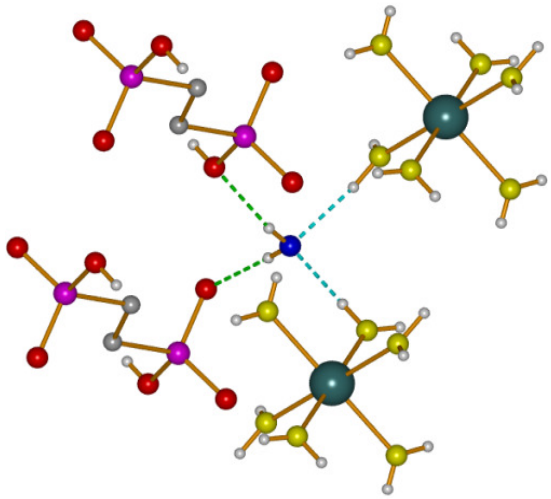

**(b)**

**Figure 6.3.** Hydrogen bonding in compound **8**. Blue spheres represent lattice water molecule while the yellow spheres represent metal coordinated water molecules. Phosphorus is in purple, phosphate oxygen atom is red while carbon is represented by grey spheres. All hydrogen atoms are represented by white spheres. **a.** shows the hydrogen bonding around the metal in compound **8** while **b.** depicts hydrogen bonding of one water molecule.

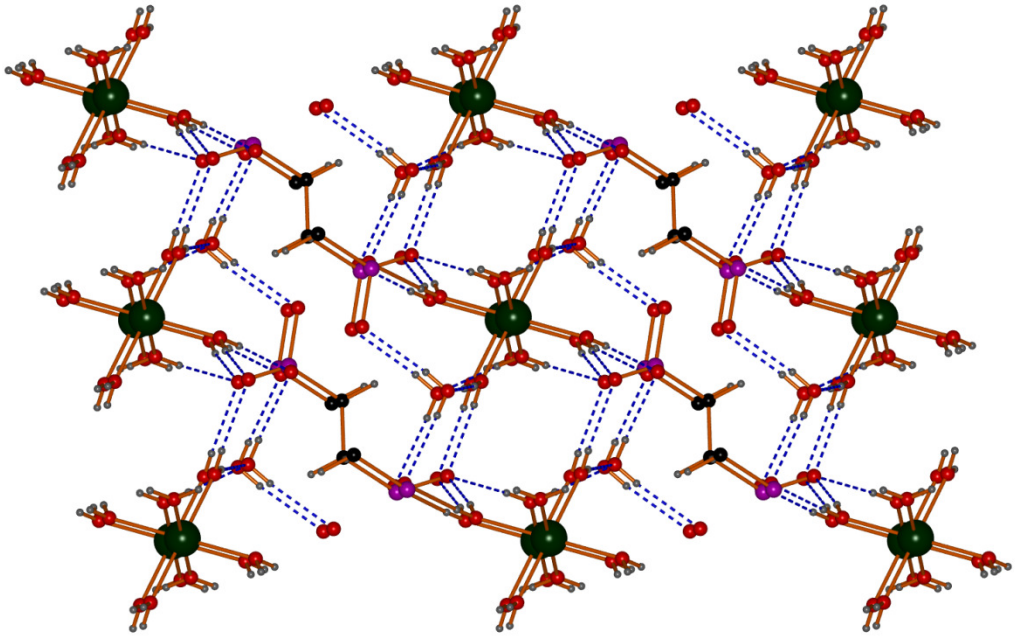

**Figure 6.4.** The two dimensional sheet of **8** showing alternating $[Mg(OH_2)_6]^{2+}$ ions and diphosphonate layers. Waters of crystallization are represented by blue spheres. Dark green spheres represent magnesium, while the purple sphere represent phosphorus. The red spheres represent oxygen, black, carbon, while the grey spheres represent hydrogen atoms.

Magnesium's position on an inversion center (and thus half occupancy), requires only one half of the doubly deprotonated diphosphonate ligand in the asymmetric unit. The assignment of P=O, P-O and P-O$^-$ moieties is straightforward and confirms the dianionic state of the ligand. The longest distance being P-OH (involving O6 with 1.5847(9) Å), with the P-O$^-$ moiety (involving O4) displaying shorter P-O bonds (1.5260(8) Å). In line with prior results, the P=O moiety (involving O5) has the shortest (1.5054(9) Å) bond.

As compound **8** contains both metal bound water, as well as lattice waters, a thermogravimetric analysis was undertaken to analyze the ease of water loss.

The TGA trace (Figure 6.5) does not show areas of distinct water loss, rather a gradual process, starting around 100 ºC. The weight loss at 494 $^{o}$C temperature is 38.21%, a value in good agreement with the calculated value of 40.41% coinciding with the complete loss of eight water molecules and formation of $\{Mg(H(HO_3P(CH_2)_2PO_3H)_n$. Further heating results in ligand degradation. The reversible uptake of water by **8** is not expected due to the nature of the structure supporting function of the water molecules.

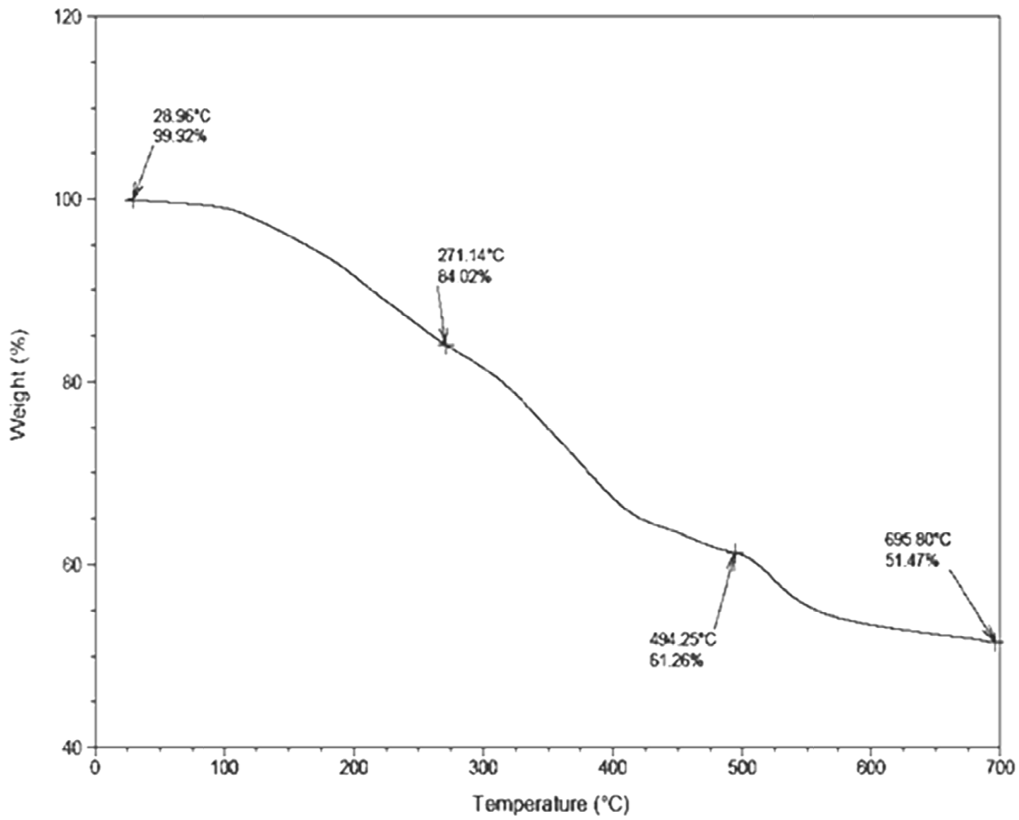


**Figure 6.5.** Thermogravimetric analyses of compound **8.**

Compound **8** has structural characteristics that are found in other magnesium compounds; namely the highly symmetrical hexaqua magnesium cation $[Mg(H_2O)_6]^{2+}$

with water molecules engaged in extensive hydrogen bonding.[54-62] As an example, phenylphosphonate $\{Mg\ [(HO_3PCH(C_6H_5)]_2\}_2(H_2O)_6{\cdot}2H_2O\}_n$[30] also has a hydrogen bonded $[Mg(H_2O)_6]^{2+}$ cation that result in a propagated arrangement. Other examples include $[Mg(H_2O)_6][(C_{10}H_4O_8)]$ (Figure 6.6),[53] $[Mg(H_2O)_6][2\text{-}AEPH^-]_2{\cdot}2H_2O$[56] (where AEPH = 2-aminoethylphosphonic acid) and $[Mg(H_2O)_6][\ CO_2(CH_2)_2CO_2]$.[63] Another example includes $[Mg(H_2O)_6][Cu_2C_8H_2NO_7)]{\cdot}2H_2O$,[18] with hydrogen bond length 1.96 (9)-2.24 (1) Å.

Water coordination involving the heavier alkaline earth cations is not uncommon, with the formation of $[Ae(H_2O)_6]_n$ Ae = Ca[64] Sr[20,65] and Ba[65-67] with n usually 6-7 for Ca, and 8-9 for Sr and Ba respectively, depicting the effect of increasing metal ion size.

Several hydrogen bonds exist between the $[Mg(H_2O)_6]^{2+}$ cation coordinating water molecules and oxygen atoms from the adjacent ligands. Typical hydrogen bond lengths (H···A) involving the hexaqua species range from 1.19(2)-2.01(7) Å.[18,53,63] Compound **8** has hydrogen bond lengths of 1.92(1)-2.06(1) Å indicating they fall into the weaker range of those reported.

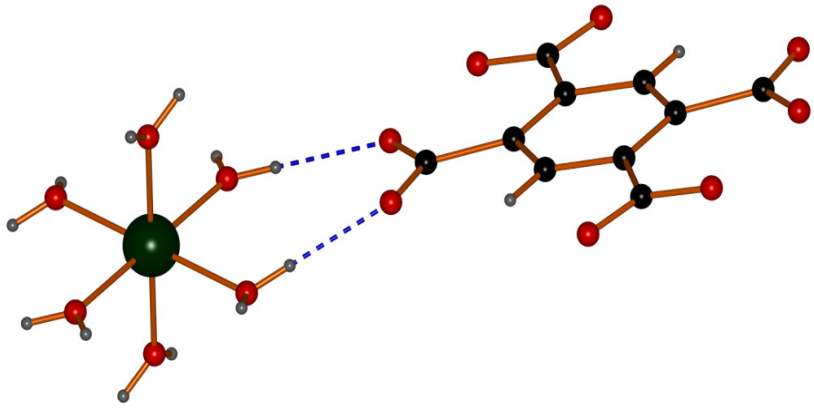

**Figure 6.6.** Schematic diagram of $[Mg(H_2O)_6(C_{10}H_4O_8)]$[53], showing hydrogen bonding between the carboxylate ion and $[Mg(H_2O)_6]^{2+}$ cation . The dark green sphere represents magnesium ion, red oxygen, black carbon and grey hydrogen atoms.

In $\{[Mg(H_2O)_6][Mg(Cl_2CP_2O_6(H_2O)]\cdot 7H_2O\}_n$,[68] two types of magnesium environments are observed; a hexaqua magnesium and a magnesium ion coordinated by ligand oxygen atoms and two water molecules. The Mg-$H_2O$ distances within $[Mg(H_2O)_6]^{2+}$ are 2.013(2)-2.121(2) Å, a value that compares well with **8**. Mg-O distances to the ligand are 2.020(2)-2.308(2) Å.

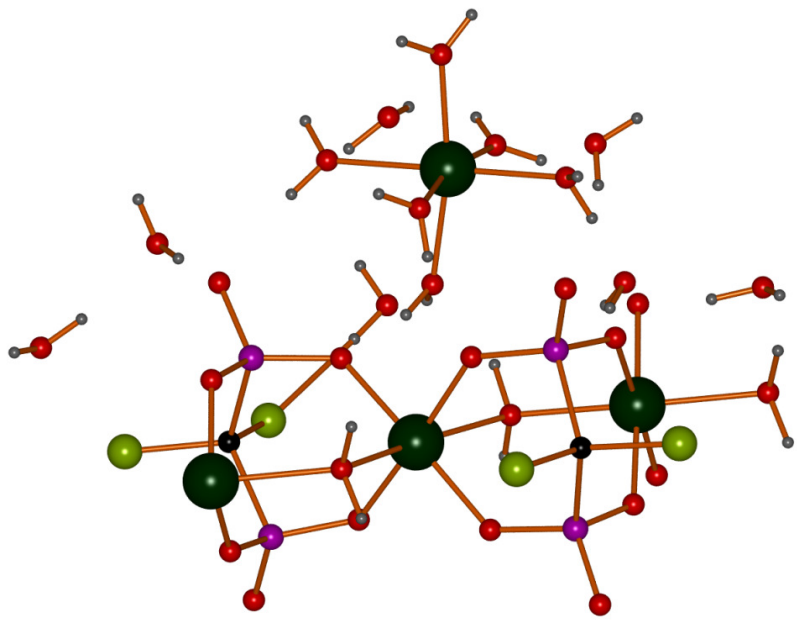

**Figure 6.7** Structure of $\{[Mg(H_2O)_6][Mg(Cl_2CP_2O_6(H_2O)]\cdot 7H_2O\}_n$,[68] showing the two magnesium environments. The dark green sphere represents magnesium, red oxygen, light green chlorine, purple phosphorus, black carbon and grey hydrogen atoms.

### 6.3.2 Magnesium Propylenediphosphonate, $[Mg(HO_3P(CH_2)_3PO_3H_2)_2(H_2O)_2]_n$ (9):

Compound **9** crystallizes in the monoclinic space group *P*2(1)/c as a 2D structure. Crystal data, details of data collection and refinement of compounds **9** are provided in Table 6.1 in the experimental section of this chapter. The O-Mg-O angles (87.44(4) ° - 92.55(4) °) indicate a slightly distorted octahedral magnesium environment. In the

asymmetric unit, one singly deprotonated ligand is coordinated to one Mg center with an occupancy of 0.5. The P-O bond lengths of 1.5263(1) Å correspond to the deprotonated P-O$^-$ while the longest P-O distances (1.546(1) Å, to 1.588(1) Å) involve the P-OH moiety. The shortest P-O bond distances (1.506(1) Å), correspond to the P=O distances. The bond lengths and angles are summarized in Table 6.4.

**Table 6.4.** Bond lengths [Å] and angles [°] for magnesium propylenediphosphonate **9**

| Bond lengths | | Bond angles | |
|---|---|---|---|
| Mg(1)-O(1W)#1 | 2.0588(13) | O(1)-Mg(1)-O(5) | 92.55(4) |
| Mg(1)-O(1W) | 2.0588(13) | O(1)-Mg(1)-O(5)#1 | 87.44(4) |
| Mg(1)-O(1) | 2.0658(11) | O(5)-Mg(1)-O(5)#1 | 180.0 |
| Mg(1)-O(1)#1 | 2.0658(11) | O(1)-P(1)-O(2) | 113.83(7) |
| Mg(1)-O(5) | 2.0998(11) | O(1)-P(1)-O(3) | 109.57(7) |
| Mg(1)-O(5)#1 | 2.0999(11) | O(2)-P(1)-O(3) | 108.49(7) |
| P(1)-O(1) | 1.5061(12) | O(1W)-Mg(1)-O(1) | 90.08(5) |
| P(1)-O(2) | 1.5458(13) | O(1W)-Mg(1)-O(5) | 88.32(5) |
| P(1)-O(3) | 1.5629(13) | O(1W)#1-Mg(1)-O(1) | 89.93(5) |
| P(1)-C(1) | 1.7764(16) | O(1W)#1-Mg(1)-O(5) | 91.68(5) |
| P(2)-O(4) | 1.5059(12) | | |
| P(2)-O(5) | 1.5263(12) | | |
| P(2)-O(6) | 1.5877(13) | | |
| P(2)-C(3) | 1.7939(17) | | |
| C(1)-C(2) | 1.538(2) | | |

Symmetry transformations used to generate equivalent atoms:

#1 -x+2,-y,-z+1 #2 -x+2,-y+1,-z+1

Each magnesium coordination sphere is saturated by four phosphonate oxygen atoms from two propylenediphosphonic forming a chain. The chains are propagated into sheets by hydrogen bonding, as shown in Figure 6.8.

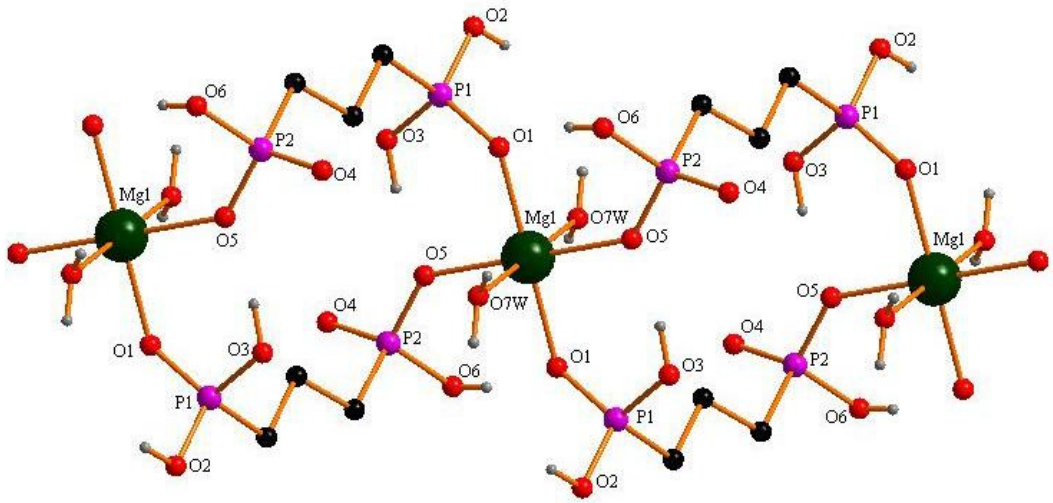


**Figure 6.8.** Schematic atom labeling of magnesium propylenediphosphonate **9**, showing the sheet structure.

Hydrogen bonding in **9** involves the hydroxyl groups on the phosphonate ligand and the two coordinating water molecules on magnesium as shown in Figures 6.9 and 6.10. The long interlayer distance of 4.001 (2) Å (between O2 on one chain and H1 on the adjacent chain) limits the compound to a two-dimensional structure. However, there is weak interaction between O6 in one layer and H3 on the adjacent layer.

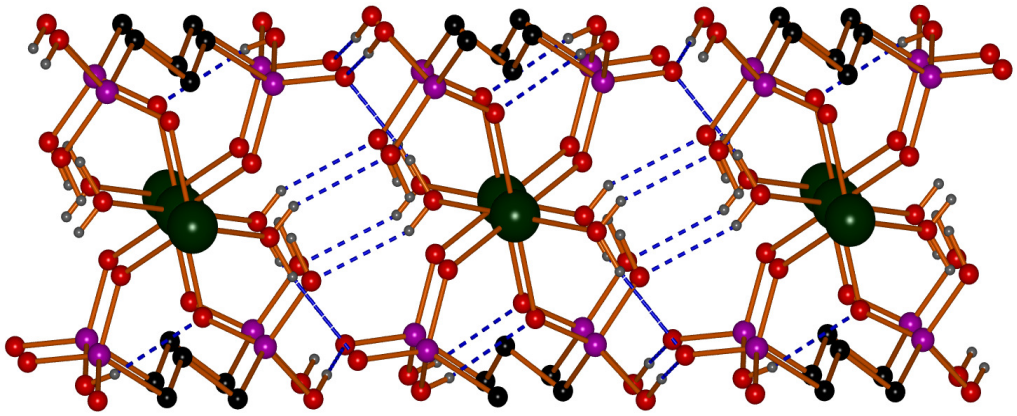

**Figure 6.9.** Chains of magnesium propylenediphosphonate **9** viewed from the y-axis and propagated through organic linkers. Blue dotted lines indicate hydrogen bonding. Hydrogen atoms, except those involved in hydrogen bonding, are omitted for clarity. The dark green spheres represent magnesium, red oxygen, purple phosphorus, black carbon and grey hydrogen atoms.

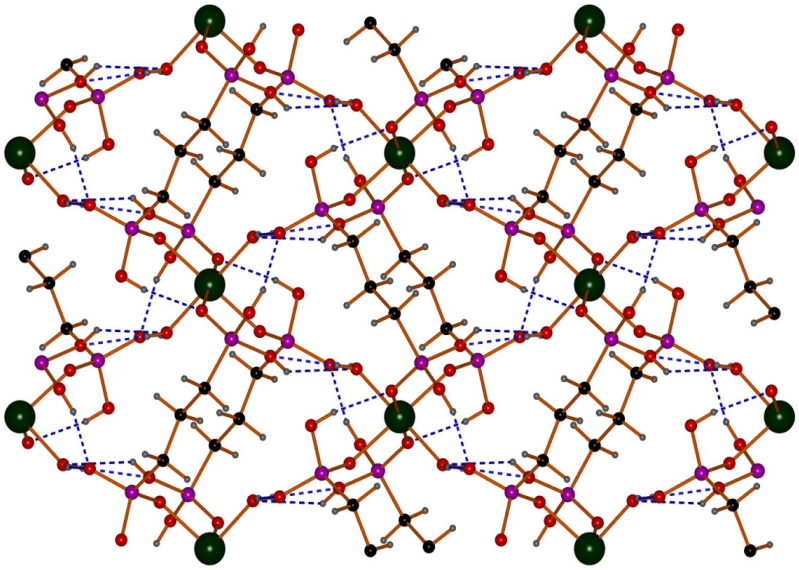

**Figure 6.10.** Magnesium propylenediphosphonates **9** viewed from the x-axis and showing adjacent chains of **9** connected by hydrogen bonds. The dark green spheres represent magnesium, red oxygen, purple phosphorus, black carbon and grey hydrogen atoms.

The O-O distances related to hydrogen bonding range between 2.57-2.78 Å, well below the sum of van der Waals radii (3.04 Å) for oxygen.[69] Figure 6.11. Hydrogen bonding values are summarized in Table 6.5.

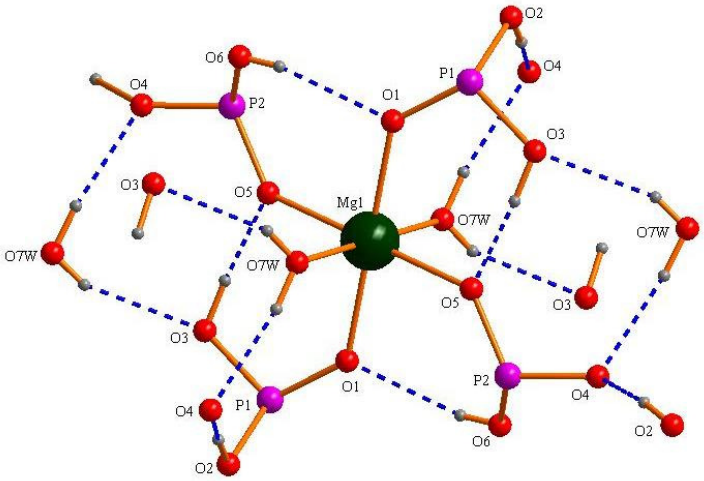


**Figure 6.11.** Hydrogen-bonding in compound **9**, methylene groups are eliminated for clarity.

**Table 6.5**. Hydrogen bonding geometry for compound **9**

| D-H…A | d(D-H) | d(H..A) | <DHA | d(D..A) A |
|---|---|---|---|---|
| O3-H3…O6 | 0.820 | 2.653 | 158.29 | 3.428 |
| O6-H6 …O1 | 0.820 | 1.988 | 147.73 | 2.717 |
| O7W-H7W…O4 | 0.786 | 2.005 | 171.89 | 2.785 |
| O7W-H8W…O3 | 0.711 | 2.091 | 154.95 | 2.751 |
| O2-H2…O4 | 0.820 | 1.773 | 163.51 | 2.570 |

Thermogravimetric analysis of **9,** the trace of which is shown in Figure 6.12, indicates a gradual process of a mass loss of 8% starting at about 90 °C to 190 $^{o}$C. This corresponds to the removal of two water molecules to yield the anhydrous

$\{Mg(HO_3P(CH_2)_3PO_3H_2)_2\}_n$. Beyond 190 °C, there is a gradual loss of mass, at 500 °C there is a sharp drop in mass, indicating decomposition.

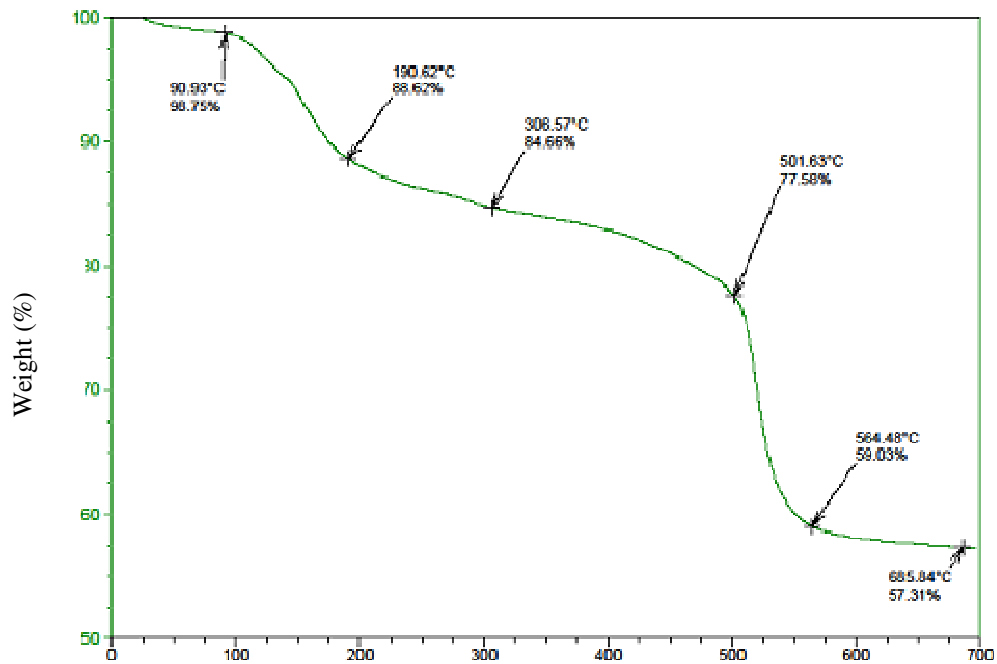


**Figure 6.12**. Thermogravimetric analyses of compound **9.**

Compound **8** is a sheet structure held together by hydrogen bonding into a three-dimensional structure. In contrast, no metal bound water is present in **9**. Curiously, compounds **8** and **9** have been prepared by similar synthetic strategies, with quite similar ligand systems, but their overall structural features could not be more different.

The comparison of acidity constants on diphosphonates ($H_2O_3P(CH_2)_nPO_3H_2$) involving different linker length indicate a tendency towards metal coordination. In diphosphonates with shorter linker lengths, the two phosphonate moieties influence each

other, and thus, a decreased tendency towards metal coordination is observed.[50] This is supported by $^{31}P$ NMR studies indicating the shielding effect of the two P atoms.[70] This effect diminishes with increasing chain length.[71] These studies provide a rationale of the large structural differences between the two diphosphonate ligands.

## 6.4 Conclusions

Two novel magnesium phosphonates have been synthesized. Both compounds form sheets involving $Mg^{2+}$ centers with coordination environment of six oxygen atoms. However, significant structural differences exist for **8** and **9**, with the formation of $[Mg(H_2O)_6]^{2+}$ cations and no metal ligand interaction in **8**, whereas **9** has no metal-water coordination. This work clearly shows the drastic effects small changes in ligand geometry as well as reaction conditions can have on compound formation. These results highlight the challenge to predict solid state structures as small changes in parameters will result in drastic structural effects.

## 6.5 Experimental

### 6.5.1 Synthesis of Magnesium Ethylenediphosphonate, $\{Mg(H_2O)_6[HO_3P(CH_2)_2PO_3H)]_2H_2O\}n$ (8):

Phenylphosphinic acid (0.14 g, 1 mmol), ethylenediphosphonic acid (0.19 g, 1 mmol), and $Mg(NO_3)_2.6H_2O$ (0.13 g, 0.5 mmol) of were combined in 10 mL of N, N – dimethyl formamide (DMF), resulting in a white precipitate. The cloudy mixture was refluxed overnight yielding a clear solution. This solution was then transferred into a Carius tube and sealed at 40 mTorr pressure. The tube was heated at 150 ºC for seven

days. The resulting clear solution was filtered into small vials. The vials were covered with perforated Parafilm and kept at room temperature, yielding colorless crystals within two weeks at room temperature. Yield: 0.09 g, 0.25 mmol, 50.6 %. IR (Nujol): O-H 3404(s), 3229.82(m), C-H 2903.08(s), P-OH 2700(w,br), 1631.12(m), O-H 1461.91(s), O-H 1362.72 (s), 1146.84(w), P=O 930.96(w).

### 6.5.2 Synthesis of Magnesium Propylenediphosphonate, $\{Mg(HO_3P(CH_2)_3PO_3H_2)]_2(H_2O)_2n$ (9):

Propylene diphosphonic acid (0.2 g, 0.98 mmol) and magnesium nitrate hexahydrate (0.13 g, 0.51 mmol) were dissolved in 6 mL of distilled water. The clear colorless solution was transferred into a vial and kept at 80 $^oC$ for three days. The clear solution was allowed to cool to room temperature, covered with perforated Parafilm and left at room temperature to slowly evaporate. After a month, single colorless crystals were obtained. Yield: 0.071g, 0.30 mmol, 58.9%. IR (Nujol): C-H 1461.9(s), O-H 1376.57 (s), P=O 940.3 (m).

## 6.6 Experimental Details

Phenylphosphinic acid, $Mg(NO_3)_2.6H_2O$, $MgAc_2$ $MgCl_2$, NaOH and DMF, were obtained commercially. The reagents were used as purchased. Thermogravimetric analysis was performed using a Q-500 Quantachrome Analyzer (TA-Instruments) with $N_2$ as a carrier gas with a heating ramp of 10$^oC$/min. A Perkin-Elmer PE 1600–FT-IR spectrometer was used to collect IR spectra as Nujol mulls between KBr plates. Single crystals of compounds **8** and **9** were analyzed by single X-ray diffraction and by FT-IR

spectroscopy. Crystals of **8** and **9** were not soluble in common NMR solvents hence no spectra could be obtained

### 6.7. X-ray crystallography

For compounds **8** and **9**, X-ray quality crystals were grown as described above. Crystals were taken out of the solutions and covered with viscous hydrocarbon oil (Infineum). Using a microscope, suitable crystals were selected and attached to a glass fiber. The crystals were mounted onto a 3-circle goniometer under the nitrogen stream of the low temperature device. Crystallographic data of **8** and **9** were collected using Bruker diffractometer equipped with a SMART CCD system, and using MoKα-radiation ($\lambda$ = 0.71073 Å) at 97(2) K. Crystal data, details of data collection and refinement of compounds **8** and **9** are provided in Table 6.1. The structures of **8** and **9** were solved by Direct Methods with the aid of SHELXS-97. The structures were refined with SHELXL-97.[72] Positions of hydrogen atoms of the hydroxyl groups on the phosphonate ligands were calculated and refined isotropically. Hydrogen atoms on water molecules in **8** were located from the Fourier difference map and refined with constraints. All other hydrogens were placed in calculated positions based on geometric considerations**.**

**Table 6.1.** Crystal data and structure refinement for compounds **8** and **9**

| | **8** | **9** |
|---|---|---|
| Empirical formula | $C_2H_{22}MgO_{14}P_2$ | $C_3H_{11}Mg_{0.5}O_7P_2$ |
| Formula weight | 356.45 | 233.21 |
| Temperature (K) | 97(2) | 97(2) |
| Crystal system | Triclinic | Monoclinic |
| Space group | P-1 | P2(1)/c |
| a (Å) | 6.53(1) | 9.95(6) |
| b (Å) | 6.57(1) | 7.66(4) |
| c (Å) | 10.04(2) | 12.41(7) |
| α (°) | 89.37(3) | 90 |
| β (°) | 74.13(3) | 109.10(1) |
| γ (°) | 62.56(3) | 90 |
| Volume ($Å^3$) | 364.6(1) | 896.7(2) |
| Z | 1 | 4 |
| dcalc($mg/m^3$) | 1.624 | 1.733 |
| μ ($mm^{-1}$) | 0.41 | 0.52 |
| Crystal size($mm^3$) | 0.20 | 0.30 |
| | 0.10 | 0.15 |
| | 0.05 | 0.10 |
| 2θ range (°) | 3.50-28.28 | 2.17-29.84 |
| Reflections collected | 3670 | 8847 |
| Independent reflections | 1787 | 2391 |
| R1 [I>2sigma(I)] | 0.0294 | 0.0341 |
| wR2 [I>2sigma(I)] | 0.0831 | 0.0098 |
| R1 (all data) | 0.0327 | 0.0389 |
| wR2 (all data) | 0.0861 | 0.1038 |

## 6.8 Thermogravimetric Analysis (TGA)

The TA Q 500 Instrument was used to perform the analyses. About 13 mg of white powder of compound was loaded on a platinum pan. Purified nitrogen gas was used with a balance purge rate of 40 mL/min and a sample purge rate of 60 mL/min. The temperature was ramped at 10°C per minute until a final temperature of 700°C was reached. After 68 minutes, about 50% of weight loss was recorded and a black residue remained in the pan.

## 6.9 References:


(1) Hu, J.; Zhao, J. a.; Hou, H.; Fan, Y. *Inorg. Chem. Commun.* **2008**, *11*, 1110.
(2) Mao, J.-G.; Wang, Z.; Clearfield, A. *Inorg. Chem.* **2002**, *41*, 3713.
(3) Merrill, C. A.; Cheetham, A. K. *Inorg. Chem.* **2006**, *46*, 278.
(4) Poojary, D. M.; Zhang, B.; Clearfield, A. *J. Am. Chem. Soc.* **1997**, *119*, 12550.
(5) Demadis, K. D.; Katarachia, S. D.; Raptis, R. G.; Zhao, H.; Baran, P. *Cryst. Growth Des.* **2006**, *6*, 836.
(6) Gao, L.-L.; Song, S.-Y.; Ma, J.-F.; Yang, J. *Cryst. Growth Des.* **2007**, *7*, 895.
(7) Stone, J.; Smith, M.; Loye, H.-C. *J. Chem. Crystallogr.* **2007**, *37*, 103.
(8) Nancollas, G. H.; Tomson, M. B.; Battaglia, G.; Wawrousek, H.; Zuckerman, M.; Ann Arbor Sci.: 1978, p 17.
(9) Li, F.-Y.; Chaigne-Delalande, B.; Kanellopoulou, C.; Davis, J. C.; Matthews, H. F.; Douek, D. C.; Cohen, J. I.; Uzel, G.; Su, H. C.; Lenardo, M. J. *Nature (London, U. K.)* **2011**, *475*, 471.
(10) Peter Atkins, T. O., Jonathan Rourke, Mark Weller,Fraser Armstrong; Edition, F., Ed.; W. H. Freeman and Company: New York, 2006.
(11) Gammon, D. D. E. a. S. D. *General Chemistry*; Eighth Edition ed.; Houghton Mifflin Company: New York Boston, 2005.
(12) Slater, J. C. *J. Chem. Phys.* **1964**, *41*, 3199.
(13) Gadipelli, S.; Ford, J.; Zhou, W.; Wu, H.; Udovic, T. J.; Yildirim, T. *Chem.--Eur. J.* **2011**, *17*, 6043.
(14) Dietzel, P. D. C.; Blom, R.; Fjellvaag, H. *Eur. J. Inorg. Chem.* **2008**, 3624.
(15) Williams, C. A.; Blake, A. J.; Wilson, C.; Hubberstey, P.; Schröder, M. *Cryst. Growth Des.* **2008**, *8*, 911.
(16) Sumida, K.; Brown, C. M.; Herm, Z. R.; Chavan, S.; Bordiga, S.; Long, J. R. *Chem. Commun. (Cambridge, U. K.)* **2011**, *47*, 1157.
(17) Freire, E.; Vega, D. R.; Baggio, R. *Acta Crystallogr., Sect. C: Cryst. Struct. Commun.* **2010**, *C66*, m166.
(18) Li, S.-J.; Song, W.-D.; Miao, D.-L.; Ma, D.-Y. *Acta Crystallogr C* **2011**, *67*, m105.
(19) Banerjee, D.; Finkelstein, J.; Smirnov, A.; Forster, P. M.; Borkowski, L. A.; Teat, S. J.; Parise, J. B. *Cryst. Growth Des.* **2011**, *11*, 2572.
(20) Arlin, J.-B.; Florence, A. J.; Johnston, A.; Kennedy, A. R.; Miller, G. J.; Patterson, K. *Cryst. Growth Des.* **2011**, *11*, 1318.
(21) Genceli Guner, F. E.; Lutz, M.; Sakurai, T.; Spek, A. L.; Hondoh, T. *Cryst. Growth Des.* **2010**, *10*, 4327.
(22) Wang, J.-P.; Lu, Z.-J.; Zhu, Q.-Y.; Zhang, Y.-P.; Qin, Y.-R.; Bian, G.-Q.; Dai, J. *Cryst. Growth Des.* **2010**, *10*, 2090.
(23) Kam, K. C.; Young, K. L. M.; Cheetham, A. K. *Cryst. Growth Des.* **2007**, *7*, 1522.
(24) Mastropietro, T. F.; Armentano, D.; Marino, N.; De Munno, G.; Anastassopoulou, J.; Theophanides, T. *Cryst. Growth Des.* **2007**, *7*, 609.
(25) Kinzhybalo, V.; Janczak, J. *J. Mol. Struct.* **2011**, *996*, 64.
(26) Chen, A.-x.; Liu, G.; Li, H.; Wang, J.-d.; Yue, F. *J. Chem. Crystallogr.* **2011**, *41*, 143.

(27) Mallick, A.; Saha, S.; Pachfule, P.; Roy, S.; Banerjee, R. *J. Mater. Chem.* **2010**, *20*, 9073.
(28) Köse, D. A.; Zümreoglu-Karan, B.; Hökelek, T. *Inorg. Chim. Acta* **2011**, *375*, 236.
(29) Reiss, G. J.; Boldog, I.; Janiak, C. *Acta Crystallographica Section E* **2011**, *67*, m1109.
(30) Lee, H.; Lynch, V. M.; Cao, G.; Mallouk, T. E. *Acta Crystallogr., Sect. C: Cryst. Struct. Commun.* **1988**, *C44*, 365.
(31) Shivaram, B. S.; Phillips, A. B.; University of Virginia Patent Foundation, USA . 2008, p 57pp.
(32) Trukhan, N.; Mueller, U.; Schubert, M.; Basf Se, Germany . 2008, p 33 pp.
(33) Maark, T. A.; Pal, S. *Int. J. Hydrogen Energy* **2010**, *35*, 12846.
(34) Stergiannakos, T.; Tylianakis, E.; Klontzas, E.; Froudakis, G. E. *J. Physical Chem. C* **2010**, *114*, 16855.
(35) Guo, Z.; Li, G.; Zhou, L.; Su, S.; Lei, Y.; Dang, S.; Zhang, H. *Inorg. Chem.* **2009**, *48*, 8069.
(36) Senkovska, I.; Kaskel, S. *Eur. J. Inorg. Chem.* **2006**, *2006*, 4564.
(37) Dincă, M.; Long, J. R. *J. Am. Chem. Soc.* **2005**, *127*, 9376.
(38) Rood, J. A.; Noll, B. C.; Henderson, K. W. *Main Group Chem.* **2006**, *5*, 21.
(39) Tuikka, M.; Haukka, M.; Ahlgrén, M. *Solid State Sci.* **2007**, *9*, 535.
(40) Serre, C.; Férey, G. *Inorg. Chem.* **2001**, *40*, 5350.
(41) Zhou, G.; Qian, G.; Ma, L.; Cheng, Y.; Xie, Z.; Wang, L.; Jing, X.; Wang, F. *Macromolecules* **2005**, *38*, 5416.
(42) Poojary, D. M.; Zhang, B.; Clearfield, A. *Chem. Mater.* **1999**, *11*, 421.
(43) Soghomonian, V.; Chen, Q.; Haushalter, R. C.; Zubieta, J. *Angew. Chem. Int. Ed.* **1995**, *34*, 223.
(44) Serpaggi, F.; Ferey, G. *J. Mater. Chem.* **1998**, *8*, 2749.
(45) Conary, G. S.; McCabe, D. J.; Meline, R. L.; Duesler, E. N.; Paine, R. T. *Inorg. Chim. Acta* **1993**, *203*, 11.
(46) Mesbah, A.; Aranda, L.; Steinmetz, J.; Rocca, E.; François, M. *Solid State Sci.* **2011**, *13*, 1438.
(47) Guo, X.-X.; Lin, J.-l. *Acta Crystallogr. Sect. E* **2011**, *67*, m665.
(48) Katharina M, F. *Coord. Chem. Rev.* **2008**, *252*, 856.
(49) Ma, S.; Fillinger, J. A.; Ambrogio, M. W.; Zuo, J.-L.; Zhou, H.-C. *Inorg. Chem. Commun.* **2007**, *10*, 220.
(50) Irani, R. R.; Moedritzer, K. *J. Phys. Chem.* **1962**, *66*, 1349.
(51) Rosi, N. L.; Eddaoudi, M.; Kim, J.; O'Keeffe, M.; Yaghi, O. M. *Cryst. Eng.* **2002**, *4*, 401.
(52) Shepherd, J. H.; Best, S. M. *JOM* **2011**, *63*, 83.
(53) Dale, S. H.; Elsegood, M. R. J.; Kainth, S. *Acta Crystallogr., Sect. C: Cryst. Struct. Commun.* **2003**, *C59*, m505.
(54) Kariuki, B. M.; Jones, W. *Acta Crystallographica Section C* **1989**, *45*, 1297.
(55) Kiseleva, E. A.; Troyanov, S. I.; Korenev, Y. M. *Russ. J. Coord. Chem.* **2007**, *33*, 85.
(56) Schier, A.; Gamper, S.; Müller, G. *Inorg. Chim. Acta* **1990**, *177*, 179.
(57) Baier, J.; Thewalt, U. *Z. Anorg. Allg. Chem.* **2002**, *628*, 1890.

(58) Matović, Z. D.; Meetsma, A.; Miletić, V. D.; van Koningsbruggen, P. J. *Inorg. Chim. Acta* **2007**, *360*, 2420.
(59) Thakur, A.; Yadav, A. *Acta Cienc. Indica, Phys.* **1993**, *19*, 19.
(60) Thakur, A.; Yadav, A. *Acta Cienc. Indica, Phys.* **1993**, *19*, 17.
(61) Cai, J.; Chen, C.-H.; Liao, C.-Z.; Feng, X.-L.; Chen, X.-M. *Acta Crystallogr. Sect. B* **2001**, *57*, 520.
(62) Perrin, C. L.; Lau, J. S.; Kim, Y.-J.; Karri, P.; Moore, C.; Rheingold, A. L. *J. Am. Chem. Soc.* **2009**, *131*, 13548.
(63) Vanhouteghem, F.; Lenstra, A. T. H.; Schweiss, P. *Acta Crystallogr., Sect. B: Struct. Sci.* **1987**, *B43*, 523.
(64) Colodrero, R. M. P.; Cabeza, A.; Olivera-Pastor, P.; Papadaki, M.; Rius, J.; Choquesillo-Lazarte, D.; García-Ruiz, J. M.; Demadis, K. D.; Aranda, M. A. G. *Cryst. Growth Des.* **2011**, *11*, 1713.
(65) Demadis, K. D.; Barouda, E.; Raptis, R. G.; Zhao, H. *Inorg. Chem.* **2008**, *48*, 819.
(66) Barouda, E.; Demadis, K. D.; Freeman, S. R.; Jones, F.; Ogden, M. I. *Cryst. Growth Des.* **2007**, *7*, 321.
(67) Murugavel, R.; Kuppuswamy, S.; Randoll, S. *Inorg. Chem.* **2008**, *47*, 6028.
(68) Kontturi, M.; Kunnas-Hiltunen, S.; Vepsäläinen, J. J.; Ahlgrén, M. *Solid State Sci* **2006**, *8*, 1098.
(69) Bondi, A. *The Journal of Physical Chemistry* **1964**, *68*, 441.
(70) Van Wazer, J. R.; Callis, C. F.; Shoolery, J. N.; Jones, R. C. *J. Am. Chem. Soc.* **1956**, *78*, 5715.
(71) Moedritzer, K.; Irani, R. R. *J. Inorg. Nucl. Chem.* **1961**, *22*, 297.
(72) Chadwick, S.; Englich, U.; Ruhlandt-Senge, K. *Chem. Commun.* **1998**, 2149.

# CHAPTER 7

# Calcium Alkylene Diphosphonates

## 7.1 Introduction

Studies on phosphinates, phosphonates, phosphite and phosphates described in Chapter 4 suggest that as the number of oxygen atoms in a ligand increase, structures with a higher dimensionality are obtained. This chapter explores diphosphonic acids as ligands[1,2] and examines how the linker length affects the overall structure of calcium alkylene diphosphonates. The diphosphonates utilize linkers with one, two and three carbon atoms as indicated in Figure 7.1. The compounds were phosphonate based metal organic frameworks to be used as scaffold material for bone in growth.

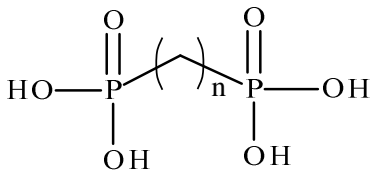


**Figure 7.1** Alkylenediphosphonic acids: (n = 1) methylenediphosphonic acid $H_4$MDPA, (n = 2) ethylenediphosphonic acid $H_4$EDPA and (n = 3) propylenediphosphonic acid $H_4$PDPA.

Bisphosphonates have found widespread use in medicinal applications and are the basis of the widely used drugs Boniva®, Fosamax®, Reclast®, Zoledronate®, Didronel®, Ibandronate®, Etidronate®, and Alendronate® [3-5] which are designed to treat bone diseases such as osteoporosis and bone cancer. [6-14] Bisphosphonates have found applications in industrial processes as ion exchangers, catalysts and sorption purposes.[15]

The majority of the diphosphonates are based on transition metals,[16-22] in contrast, relatively very few complexes with main group metals [23-25] and lanthanides[26,27] are reported. Several attempts to obtain single crystals of calcium ethylenediphosphonates failed, explaining why only limited work is available on alkaline earth metal phosphonates. So far, 3D $Ba[HO_3P(CH_2)_2PO_3H]$ [28] is the only reported example, for which single X-ray quality crystals were obtained by gel crystallization.[28]

This chapter discusses synthetic pathways towards four novel three-dimensional calcium based diphosphonates, namely calcium methylenediphosphonate (**10**), calcium sodium ethylenediphosphonate (**11**), calcium nitrate ethylenediphosphonate (**12**), and calcium propylenediphosphonate (**13**).

## 7.2 Synthetic Considerations

The synthesis of compounds **10** and **13** was straightforward, crystals of the compounds formed after combining calcium nitrate and $H_4$MDPA( for **10**) and $H_4$PDPA (for **13**) in aqueous solutions as shown in Scheme 7.1 and 7.2 respectively.

$$Ca(NO_3)_2{\cdot}4H_2O + H_2PO_3CH_2PO_3H_2 \xrightarrow[150\ ^oC]{H_2O,\ HPO(OH)(C_6H_5)} [CaCH_2(PO_3H)_2]_n \quad \textbf{(10)}$$

**Scheme 7.1.** Synthesis of compound **10**.

$$Ca(NO_3)_2{\cdot}4H_2O + H_2PO_3(CH_2)_3PO_3H_2 \xrightarrow[85\ ^oC]{H_2O} [Ca(HO_3P(CH_2)_3PO_3H)]_n \quad \textbf{(13)}$$

**Scheme 7.2.** Synthesis of compound **13**.

In contrast, the crystallization of calcium ethylenediphosphonate was very challenging. A wider range of crystallization methods were explored including simple precipitation,[29] slow evaporation of concentrated solutions as used during the crystallization of substituted bisphosphonic acid based compounds. [11,30,31]

En route to the target species, two crystalline products were obtained; a Ca/Na heterobimetallic ethylenediphosphonate (**11**) by hydrothermal synthesis as shown in Scheme 7.3 and a species which contained remaining nitrate moieties (**12**), the crystals of which were obtained by crystallization from a silicate gel as indicated in Scheme 7.4. The gel method produces large crystals which are usually unattainable by slow evaporation of solvent or under hydrothermal condition; however, these crystals are difficult to separate from the gel.[12,15,28,32]

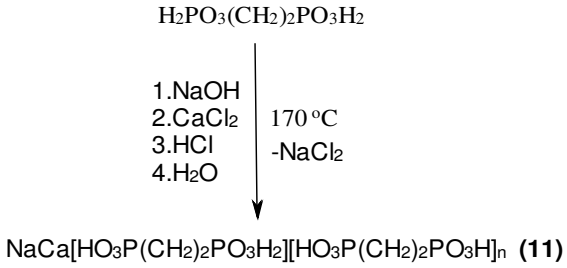


**Scheme 7.3.** Synthesis of compound **11**.

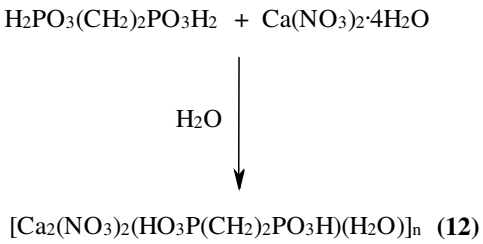


**Scheme 7.4.** Synthesis of compound **12**

## 7.3 Structural Aspects

### 7.3.1 Calcium methylenediphosphonate, $[Ca(HO_3PCH_2PO_3H)]_n$ (10):

Compound **10** is a three dimensional compound which crystallizes as monoclinic space group C2/c. Single crystals were obtained by hydrothermal synthesis of methylenediphosphonic acid and calcium nitrate. Crystal data, details of data collection and refinement of **10** are provided in Table 7.1 in the experimental section of this chapter.

The octahedral environment of $Ca^{2+}$ is comprised of six phosphonate oxygen atoms from a doubly deprotonated ligand (O2). Each ligand therefore retains one protonated P-OH (O3) species per phosphonate moiety as shown in Figure 7.2. The asymmetric unit consists of a Ca ion in an inversion center coordinated to one half of the doubly deprotonated ligand.

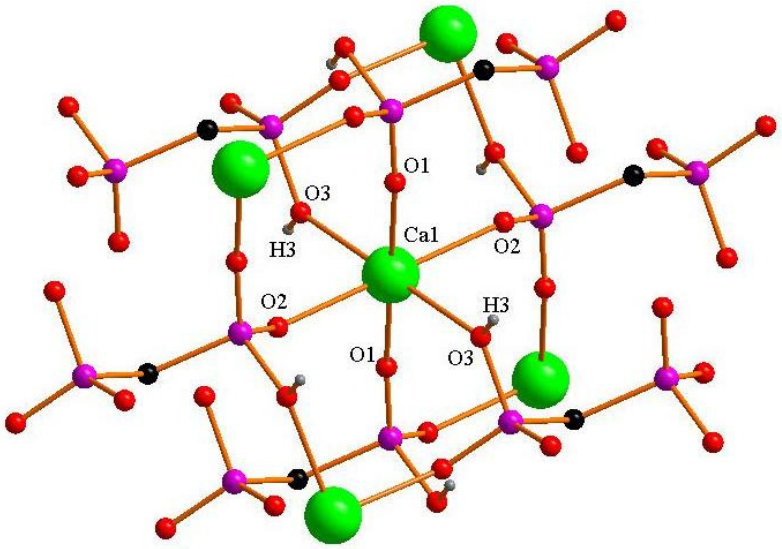


**Figure 7.2.** Structure showing the coordination environment of calcium in **10**, the hydrogen atoms on the carbon atoms are omitted for clarity

The P-O distances vary in length based on the P-O bond order and whether P-OH is deprotonated or not. The shortest, 1.418 (1) Å is associated with P=O (O1). The intermediate bond length 1.516 (1) Å corresponds to P-O$^-$ (O2), whereas the longest bond 1.519 (1) Å is associated with that of P-OH. The Ca-O bond lengths are between 2.264 (1) Å–2.447 (1) Å. Selected bond length and angles are given in Table 7.2.

**Table 7.2.** Selected bond lengths [Å] and angles [°] calcium methylenediphosphonate, **10**.

| | | | |
|---|---|---|---|
| P(1)-O(1) | 1.4918(1) | O(1)-P(1)-O(2) | 116.47(7) |
| P(1)-O(2) | 1.5159(1) | O(1)-P(1)-O(3) | 110.16(6) |
| P(1)-O(3) | 1.5967(1) | O(2)-P(1)-O(3) | 105.81(7) |
| P(1)-C(1) | 1.8005(1) | O(1)-P(1)-C(1) | 111.80(7) |
| Ca(1)-O(1) | 2.2636(1) | O(2)-P(1)-C(1) | 107.08(8) |
| Ca(1)-O(1)#1 | 2.2637(1) | O(3)-P(1)-C(1) | 104.72(5) |
| Ca(1)-O(2)#2 | 2.3486(1) | O(1)-Ca(1)-O(1)#1 | 180.0 |
| Ca(1)-O(2)#3 | 2.3486(1) | O(1)-Ca(1)-O(2)#2 | 86.48(4) |
| Ca(1)-O(3)#4 | 2.4472(1) | O(1)#1-Ca(1)-O(2)#2 | 93.52(4) |
| Ca(1)-O(3)#5 | 2.4472(1) | O(1)-Ca(1)-O(3)#4 | 82.61(4) |
| O(2)-Ca(1)#6 | 2.3486(1) | O(1)#1-Ca(1)-O(3)#4 | 97.39(4) |
| O(3)-Ca(1)#8 | 2.4472(1) | O(2)#2-Ca(1)-O(3)#4 | 81.27(5) |
| C(1)-P(1)#7 | 1.8005(1) | O(2)#3-Ca(1)-O(3)#4 | 98.73(5) |

Symmetry transformations used to generate equivalent atoms:

#1 -x,-y,-z #2 x-1/2,y-1/2,z #3 -x+1/2,-y+1/2,-z

All the six phosphonate oxygen atoms on the ligand coordinate to a metal center, (Figure 7.3) achieving the three-dimensional structure of **10** *via* bridging O-P-O groups, as shown in Figure 7.4.

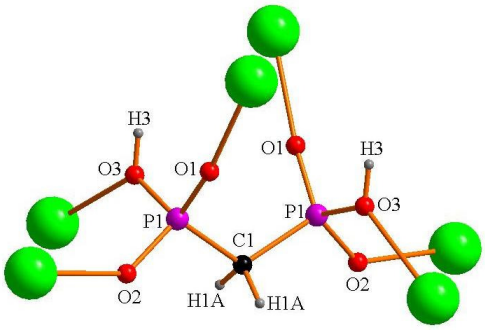


**Figure 7.3**. Structure of **10**, showing the coordination environment of the ligand, the green spheres represent the $Ca^{2+}$ centers.

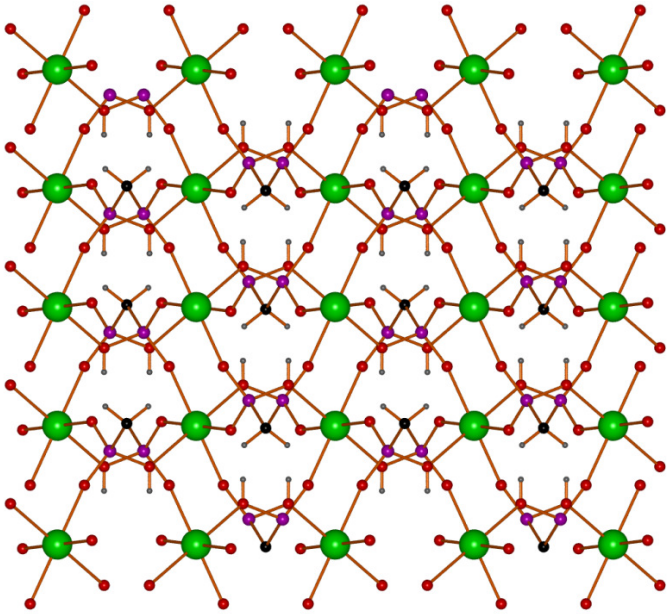

**Figure 7.4.** Extended structure of compound **10** viewed along the a-axis, showing the propagation of the structure in two dimensions. The green spheres represent the calcium ions coordinated by six phosphonate oxygen atoms shown in red. The phosphorus atom is represented by the purple, carbon black and hydrogen as grey spheres.

The coordinating P-OH (H3) species is also involved in hydrogen bonding with O2 at a O3···O2 distance of 2.605(1) Å, and a DHA angle of 155.5 ° (Figure 7.5).

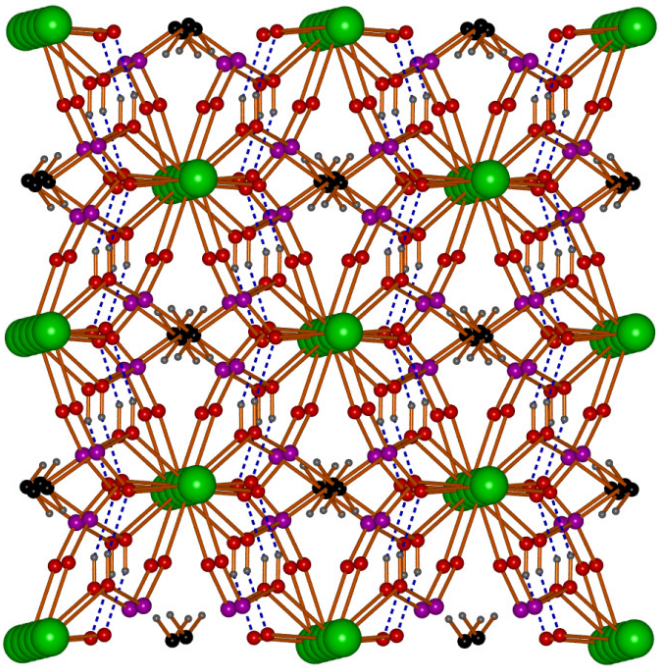

**Figure 7.5.** Three dimensional structure of **10,** showing hydrogen bonds in blue dotted lines.

There are several examples of bisphosphonates, some of which are calcium based,[15,29-31,33] indicating the ligand's affinity for $Ca^{2+}$ ions.[4] Compound **10** however represents a novel 3D species based on a non-substituted methylenebisphosphonic acid ($H_4MDPA$). The only other alkaline earth based $H_4MDPA$ compound is the one-dimensional $Na_3Mg(O_3PCH_2PO_3)(\mu\text{-}F)\cdot H_2O$. [32]

In most bisphosphonate based compounds, the methylene hydrogen atoms in $H_4MDPA$ are substituted by OH, $CH_3$, Cl or $NH_2$.[29,31,33-41] Notably, among these are dichloro methylenephosphonates, as reported in $[Ca(CCl_2(PO_3H)_2(H_2O)_5]_n$.[29] The dichloro species contains a doubly deprotonated ligand, hepta-coordinated calcium, surrounded by phosphonate oxygen atoms and five water molecules; the chlorine atoms are not involved in the metal coordination. In analogy to the dichloro species

$[Ca(CCl_2(PO_3H)_2(H_2O)_5]_n$, the ligand in 10 is doubly deprotonated and coordinates the metal centers in a bidentate chelate fashion, a feature which is not observed in compound **10**.

Another example of a calcium compound based on substituted $H_4$MDPA is $CaC(CH_3)(OH)(PO_3H)_2(H_2O)_2$ [31] in which the coordination number of the calcium is eight. The predominant structural feature is a six membered chelate ring involving the P-OH group as well as a five membered chelate ring involving the methylene hydroxyl groups.

The mean Ca-O and P-O bond distance in the dichloro species are 2.390(1) Å and 1.530(9) Å respectively, the methyl/hydroxyl species values differ slightly ((2.457(2) Å and1.5174(2) Å) but compare favorably with the respective Ca-O (2.353(3) Å) and P-O (1.535(3) Å) average distances in **10**. Indicating the effect of ligand substitution, the Ca-O bond lengths resulting from the methyl/hydroxyl substituted ligand is significantly longer (2.608(3).

### 7.3.2 Heterobimetallic sodium calcium ethylenediphosphonate, $NaCa[HO_3P(CH_2)_2PO_3H_2][HO_3P(CH_2)_2PO_3H]\}_n$ (11):

The unique three dimensional heterobimetallic **11** was synthesized by sealing an aqueous solution of ethylenediphosphonic acid, $Ca(NO_3)_2{\cdot}4H_2O$, NaOH and concentrated HCl in a Carius tube at about 40 mTorr and keeping it at 170 $^oC$ for three days. Crystals of **11** grew from slow evaporation of solvent at room temperature. Compound **11** crystallizes in the triclinic *P*-1 space group, crystal data, details of data collection and refinement of compounds **11** are provided in Table 7.1 in the experimental section of this chapter.

The asymmetric unit of **11** (shown in Figure 7.6) is comprised of one calcium and one sodium ion and two ethylenediphosphonate ligands with both metals in an inversion center. To achieve charge neutrality, one of the two ligands is singly deprotonated ($H_3EDP^-$), leaving three free OH groups on the two P-O while the other is doubly deprotonated ($H_2EDP^{2-}$). The compound has no water of crystallization.

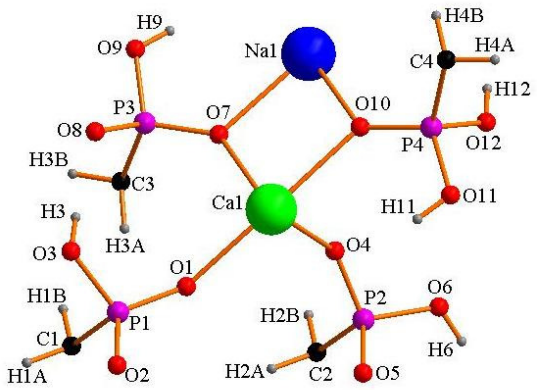


**Figure 7.6.** Labeling scheme in asymmetric unit structure of compound **11.**

The coordination sphere of $Ca^{2+}$ is saturated by six phosphonate oxygen atoms to achieve a distorted octahedral environment, as represented by a wide variation of bond distances (Ca – O 2.267(3) – 2.385(3) Å) and angles (O-Ca-O 81.86(6)° - 101.78(9)°). Of the two diphosphonate ligands, the doubly deprotonated one is coordinating to calcium, while the other coordinates to sodium. The P=O, P-O$^-$ and P-OH moieties are distinguished by their difference in P-O bond lengths, with P=O the shortest (1.493(3), 1.512(2), 1.506(2), and 1.488(2) Å), P=O$^-$ intermediate 1.514(2), 1.513(2) and 1.515(3) Å and P-OH the longest 1.591(3), 1.584(3), 1.581(3) and 1.561(3) Å.

All the metal centers are bridged by the O-P-O units, while the third P=O links alternating chains of calcium and sodium to form a sheet as shown in Figure 7.7. These sheets are joined by the organic linkers to form a pillared three dimensional structure.

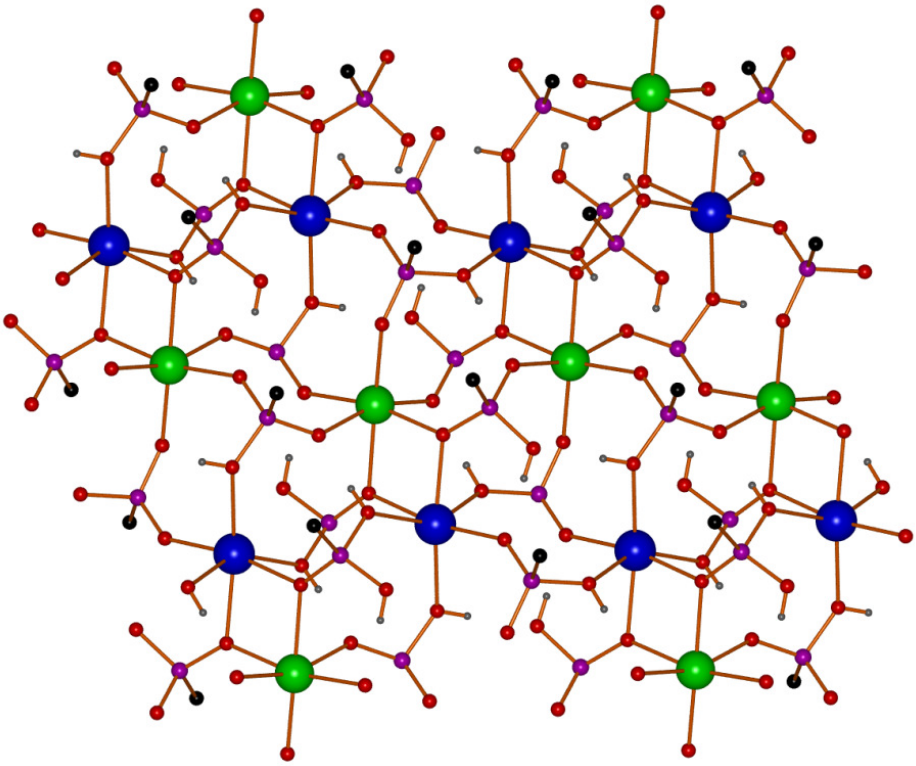

**Figure 7.7**. Structure of compound **11** showing the coordination environments of sodium (blue) and calcium (green) and bridging oxygen atoms (red) between the two metals. One of the carbon atoms (black) have been eliminated for clarity.

Figure 7.8 displays the polyhedral form of the three dimensional structures of compound **11** dipicting the pillared layered structure, typical of metal diphosphonates.[16,42-52]

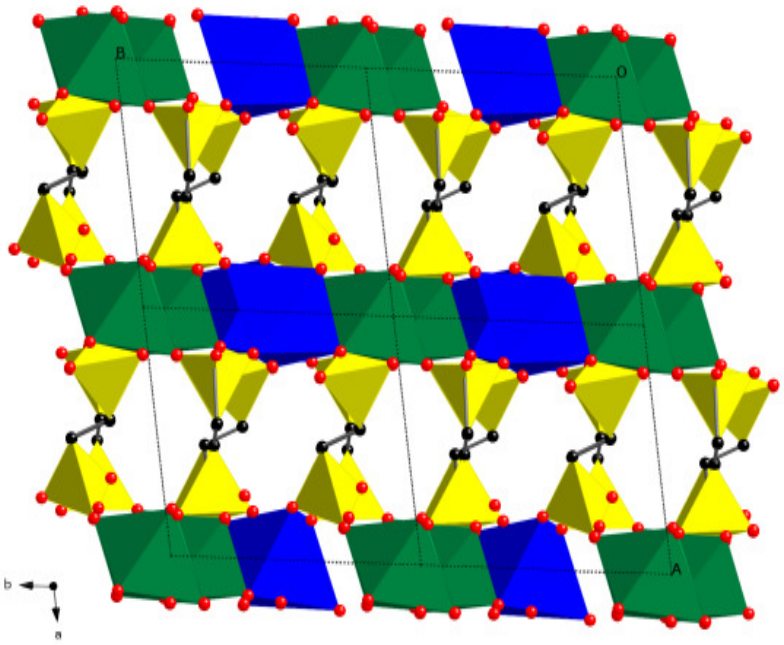


**Figure 7.8**. Polyhedral form of compound **11**, displaying the pillar layered structure. The phosphonate is represented by yellow tetrahedron, $NaO_6$ by blue octahedron, $CaO_6$ by green octahedron, oxygen red spheres and carbon black spheres.

Considering the similar size of $Ca^{2+}$ (114pm) and $Na^{+}$ (116pm),[11] the coordination environment of sodium is also distorted octahedral with Na-O bond distances ranging from 2.283(3) - 2.539(3) Å and O-Na-O bond angles from 76.61(9) – 170.01(1)º. However, the coordination environment of $Na^{+}$ is distinctively different from the coordination sphere of the $Ca^{2+}$. While six oxygen atoms (O2, O3, O6, O7, O10, O12) from the two separate ligands coordinate, these six oxygen atoms form three donor sets comprising three P-OH (O3, O6, O12) groups, two P=O groups (O7, O10) and one deprotonated $P\text{-}O^{-}$ group (O2). Again, the distinction between the protonated and deprotonated oxygen sites can be made based on P-O distances, with P-OH the longest distances (1.591(2), 1.584(3), 1.561(3) Å), $P\text{-}O^{-}$ an intermediate distance (1.514(2) Å and

P=O groups have the shortest P-O bond (1.506(2), 1.488(2) Å)). There are two free pendant P-OH groups (O9 and O11) with long P-O bonds (1.581(3), 1.558(3) Å), however, these are shorter than the corresponding bridging P-OH distance (P-O3 1.591(3) Å). Selected bond distances and angles of compound **11** are provided in Table 7.3.

**Table 7.3.** Selected bond lengths [Å] and angles [°] for sodium calcium ethylenediphosphonate **11**

| Bond lengths | | Bond lengths | | Bond angles | |
|---|---|---|---|---|---|
| Na(1)-O(2)#3 | 2.283(3) | P(1)-O(1) | 1.495(3) | O(2)#3-Na(1)-O(10) | 170.01(1) |
| Na(1)-O(10) | 2.357(3) | P(1)-O(2) | 1.514(2) | O(7)-Na(1)-O(3)#1 | 76.73(9) |
| Na(1)-O(7) | 2.383(3) | P(1)-O(3) | 1.591(3) | O(2)#3-Na(1)-O(3) #1 | 98.53(9) |
| Na(1)-O(3)#1 | 2.462(3) | P(1)-C(1) | 1.796(3) | O(2)#3-Na(1)-O(6) #1 | 94.02(1) |
| Na(1)-O(6)#4 | 2.476(3) | P(2)-O(4) | 1.512(2) | O(7)#1-Na(1)-O(6) | 165.49(9) |
| Na(1)-O(12)#4 | 2.539(3) | P(2)-O(5) | 1.513(2) | O(4)-Na(1)-O(10) | 78.70(9) |
| Ca(1)-O(1) | 2.267(3) | P(2)-O(6) | 1.584(3) | O(10)-Na(1)-O(3) #1 | 76.61(9) |
| Ca(1)-O(8)#1 | 2.350(3) | P(2)-C(2) | 1.793(3) | Na(1)-O(10)-Ca(1) | 97.88(9) |
| Ca(1)-O(4) | 2.366(3) | P(3)-O(7) | 1.506(2) | Ca(1)-O(7)-Na(1) | 99.15(9) |
| Ca(1)-O(7) | 2.313(2) | P(3)-O(8) | 1.515(3) | O(7)-Ca(1)-O(5)#2 | 167.54(9) |
| Ca(1)-O(5)#2 | 2.347(3) | P(3)-O(9) | 1.581(3) | O(1)-Ca(1)-O(8)#1 | 101.79(9) |
| Ca(1)-O(10) | 2.385(2) | P(3)-C(3) | 1.804(4) | O(1)-Ca(1)-O(4) | 95.16(9) |
| Ca(1)-O(10) | 2.385(2) | P(4)-O(10) | 1.488(2) | O(8)#1-Ca(1)-O(7) | 87.08(9) |
| | | P(4)-O(11) | 1.558(3) | O(8)#1-Ca(1)-O(10) | 84.03(9) |
| | | P(4)-O(12) | 1.561(3) | O(4)-Ca(1)-O(10) | 78.70(9) |
| | | P(4)-C(4) | 1.791(3) | | |

Symmetry transformations used to generate equivalent atoms:

#1 -x,-y,-z+1 #2 -x,-y,-z #3 x,y+1,z #4 -x,-y+1,-z+1

#5 x,y-1,z #6 -x+1,-y,-z+1 #7 x+1,y,z #8 x-1,y,z

The comparison of 11 with the barium analog $Ba[HO_3P(CH_2)_2PO_3H]$ reveals the influence of metal centers, with an increased coordination number, as shown in Figure 7.9, with each oxygen atom originating from a different phosphonate group.

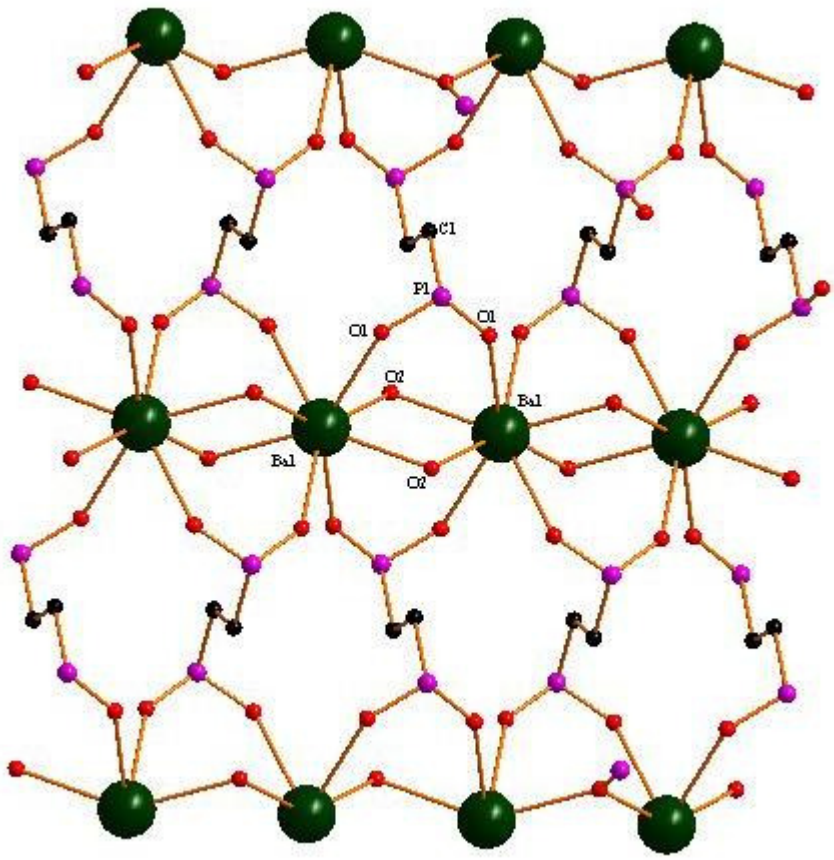


**Figure 7.9** Structure of barium ethylenediphosphonate, displaying the eight coordinate environment of $Ba^{2+}$. All hydrogen atoms are eliminated for clarity.[28]

Each ligand is doubly deprotonated and there are two types of bridging modes involving Ba-O-Ba and Ba-O-P-O-Ba fragments. Again this is an example of a pillared structure, with organic linkers extending the metal oxide sheets in a third dimension. The

Ba-Ba distance within each layer is 4.238 (1) Å but the interlayer distance based on the Ba-Ba centers are 6.498 (1) Å. The barium compound therefore has a more open structure than **11** whose interlayer distance is 5.4457(1) Å based on the calcium centers.

Heterobimetallic ethylenediphosphonates involving transition and alkali metal are quite common, with combinations such as V/K, Co/Cs, Ga/K, Mo/K and Zn/Na.[53] There is also an example of heterotrimetallic species containing Cu/K/V. [54]

Other related compounds include $[NaZn(O_3P(CH_2)_2PO_3H]$, involving a triply deprotonated HEDP,$^{3-}$ in contrast to two differently deprotonated ligands in **11**. The Zn center in the three-dimensional framework of $[NaZn(O_3P(CH_2)_2PO_3H]$ has a tetrahedral geometry while Na has a distorted octahedral environment with an average Na-O bond distances of 2.463(1) Å; not surprisingly, similar to those in **11** (2.417(2)Å.

### 7.3.3 Calcium nitrate ethylenediphosphonate, $[Ca_2(NO_3)_2(HO_3P(CH_2)_2PO_3H)(H_2O)]$ (12):

Large sword-like crystals of compound **12** grew in a sodium silicate nanohydrate gel prepared with ethylenediphosphonic acid ($H_4EDPA$). The compound crystallizes in the monoclinic C2/c space group. Crystal data, details of data collection and refinement of compound **12** are provided in Table 7.1 in the experimental section of this chapter.

The asymmetric unit of **12** contains one $Ca^{2+}$, a nitrate, one water molecule, and half of a ligand as indicated in Figure 7.10. The calcium center in **12** is coordinated by eight oxygen atoms; one from water (O1W), four from the diphosphonate ligand (2 O1 and 2 O2), and three from the nitrate (O4, O5, O6).

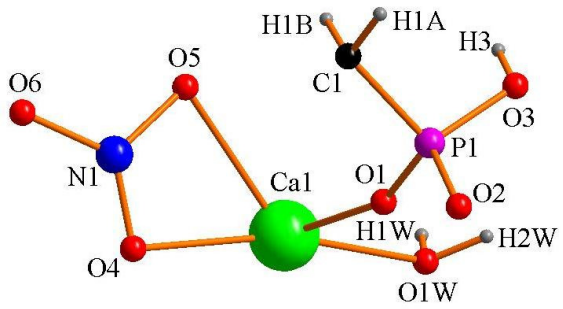


**Figure 7.10.** Asymmetric unit of compound **12**. Calcium is represented by green sphere, oxygen by red, phosphorus by purple and nitrogen by blue spheres. All hydrogen atoms have been removed for clarity.

Each $H_4$EDPA ligand is doubly deprotonated and bridges the calcium centers *via* O1 and O2. In addition O1 and O2, as well as two nitrate oxygen atoms (O4 and O5) bind to the $Ca^{2+}$ ion, resulting in a sheet structure as shown in Figure 7.11.

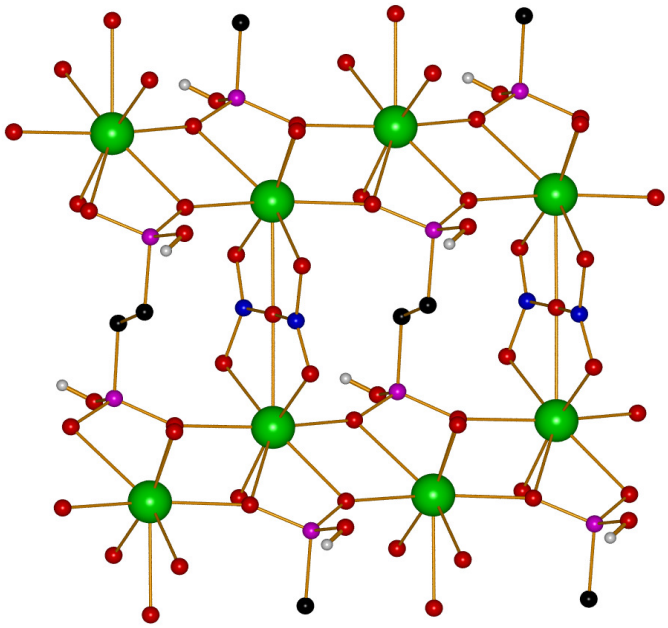

**Figure 7.11.** 2D sheet of compound **12.** Calcium is represented by green sphere, oxygen by red, phosphorus by purple and nitrogen by blue spheres. All hydrogen atoms have been removed for clarity.

In the sheet structure one oxygen atom is shared beteween two nitrogen atoms, indicating a 50 : 50 disorder of the O5 which has a 50% occupancy.

The sheets are extended into a three-dimensional structure through interlayer hydrogen bonding involving the pendant OH groups on the diphosphonates and the metal-bound water molecule, with a O···O distance is of 2.726 Å and a DHA angle of 146.2 $^{o}$, indicating weak hydrogen bonding, as shown in Figure 7.12. Bond lengths and angles of **12** are provided in Table 7.5.

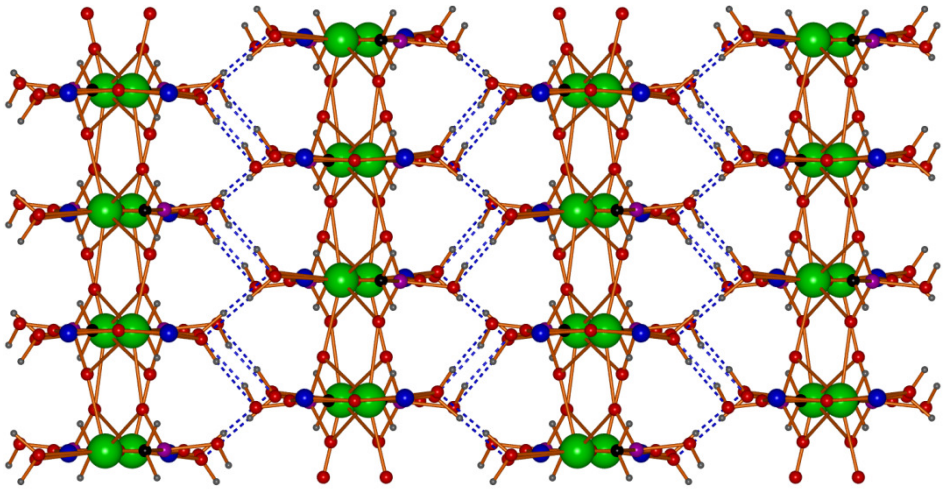

**Figure 7.12.** Structure showing hydrogen bonds in blue dotted lines linking sheets of Ca in **12**.

**Table 7.4.** Selected Bond lengths [Å] and angles [°] for calcium ethylene nitrate diphosphonate **3**

| Bond length | | Bond angles | |
|---|---|---|---|
| Ca(1A)-O(2A)#1 | 2.295(3) | O(2A)#1-Ca(1A)-O(1A) | 158.23(10) |
| Ca(1A)-O(1A) | 2.304(2) | O(2A)#1-Ca(1A)-O(6A) | 85.09(10) |
| Ca(1A)-O(6A) | 2.408(3) | O(1A)-Ca(1A)-O(6A) | 83.07(9) |
| Ca(1A)-O(1A)#2 | 2.476(3) | O(2A)#1-Ca(1A)-O(1A)# | 271.59(9) |
| Ca(1A)-O(5A) | 2.493(3) | O(1A)-Ca(1A)-O(1A)#2 | 125.34(7) |
| Ca(1A)-O(4A) | 2.6368(8) | O(6A)-Ca(1A)-O(1A)# | 285.52(9) |
| Ca(1A)-O(2A)#2 | 2.641(3) | O(2A)#1-Ca(1A)-O(5A) | 99.68(11) |
| Ca(1A)-O(7A) | 2.651(3) | O(1A)-Ca(1A)-O(5A) | 95.93(10) |
| Ca(1A)-Ca(1A)#4 | 3.9775(8) | O(6A)-Ca(1A)-O(5A) | 166.78(12) |
| P(1A)-O(2A) | 1.513(2) | O(1A)#2-Ca(1A)-O(5A) | 84.34(10) |
| P(1A)-O(1A) | 1.518(2) | O(2A)#1-Ca(1A)-O(4A) | 87.31(11) |
| P(1A)-O(3A) | 1.557(3) | O(1A)-Ca(1A)-O(4A) | 88.39(11) |
| P(1A)-C(1A) | 1.792(4) | O(6A)-Ca(1A)-O(4A) | 135.43(8) |
| O(4A)-N(1A) | 1.488(6) | O(1A)#2-Ca(1A)-O(4A) | 132.76(8) |
| O(4A)-Ca(1A)#3 | 2.6368( | O(1A)-Ca(1A)-O(7A) | 77.13(10) |
| O(5A)-N(1A) | 1.371) | O(2A)#1-Ca(1A)-O(2A)#2 | 128.93(7) |
| N(1A)-O(7A)#3 | 1.5(8) | O(4A)-Ca(1A)-O(2A)#2 | 130.43(8) |

Symmetry transformations used to generate equivalent atoms:

#1 x,y+1,z #2 -x+3/2,y+1/2,-z+1/2 #3 -x+1,y,-z+1/2

#4 -x+3/2,y-1/2,-z+1/2 #5 x,y-1,z

Compound **12** is the only known phosphonate with nitrate embedded in its structure. More commonly, fluoride containing diphosphonates have been reported as a result of NaF addition to improve the crystallinity of products.[55-59]

### 7.3.4 Calcium propylenediphosphonate, $[Ca(HO_3P(CH_2)_3PO_3H)]_n$ (13):

Calcium propylenediphosphonate **13** crystallizes from a solution containing calcium nitrate and propylenediphosphonic acid at room temperature. Compound **13** crystallizes in the orthorhombic Pbcm space group. Crystal data, details of data collection and refinement of compound **13** are provided in Table 7.1 in the experimental section of this chapter.

Compound **13** is three-dimensional; the asymmetric unit is comprised of a half occupied calcium ion and one half of a dianionic ligand (Figure 7.13). Ca, $C_2$, $H_3$ and $H_4$ are all located on special positions (two fold) with occupancies of 0.5.

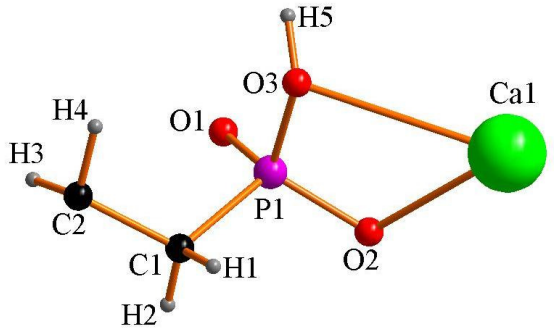


**Figure 7.13**. Asymmetrical graphical representation of **13:** indicating full atom labelling.

The coordination number of calcium in **13** is eight. All six diphosphonate oxygen atoms ligand are coordinated to a Ca center, with O2 bridging two calcium centers. In addition, two chelate rings involving the $Ca^{2+}$, O2 and O3 are observed as shown in Figure 7.14.

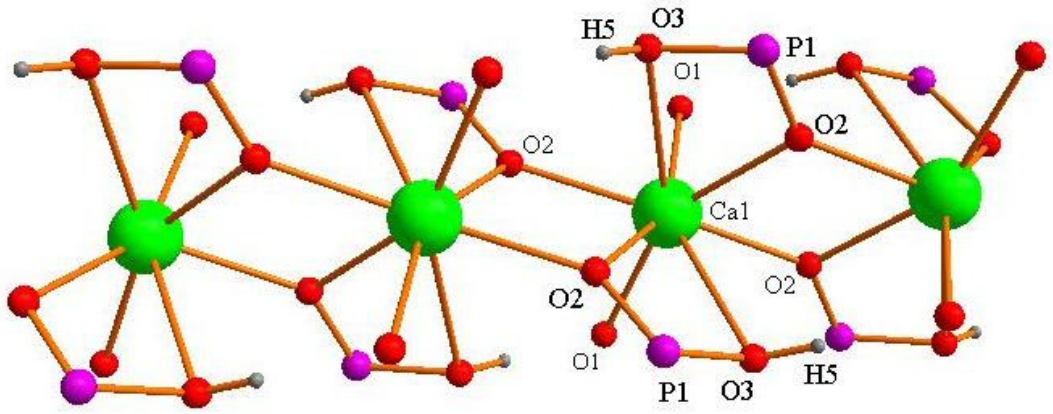


**Figure 7.14.** Structure showing the eight coordinate $Ca^{2+}$ centers, two chelates and O2 bridging in **13**.

The structure is therefore propagated by Ca-O-Ca chains and linked by the O-P-O units into a sheet. Sheets of CaO polyhedral (Figures 7.15) are linked by carbon chains to form a three dimensional compound with a pillared layered structure, as displayed in Figure 7.16.

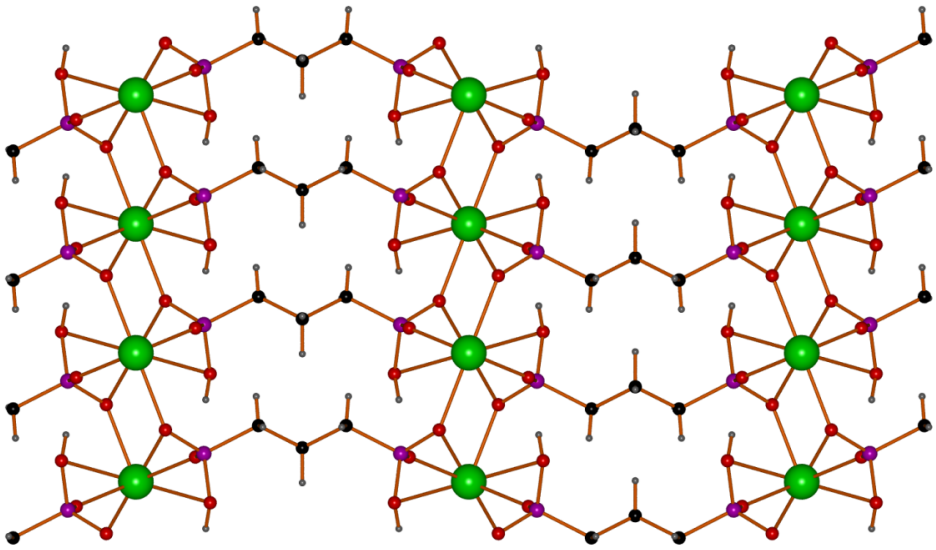

**Figure 7.15** Sheet structure of compound **13**. Calcium is represented by green spheres, oxygen in red, phosphorus in purple, carbon in black and hydrogen in grey spheres.

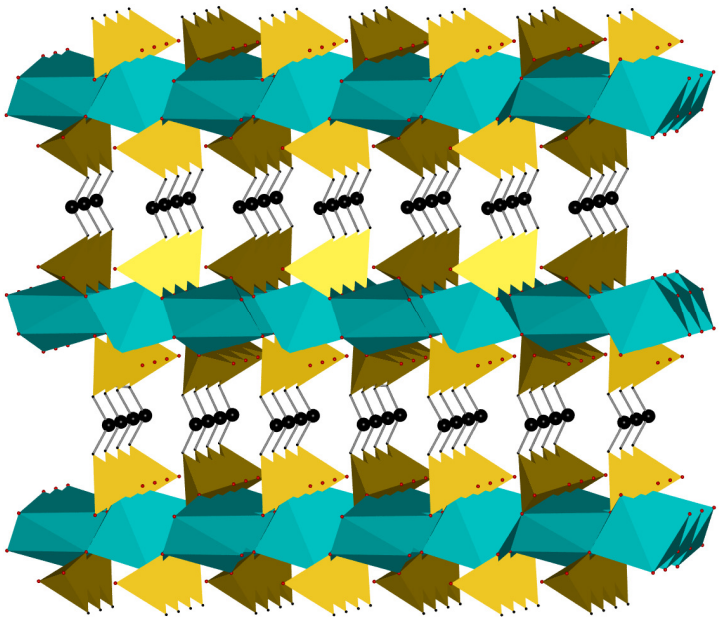

**Figure 7.16.** Polyhedral representation of calcium propylenediphosphonate **13**, showing the pillar layered structure carbons atoms are shown in black, phosphonate group as gold tetrahedron and CaO polyhedra represented in turquoise.

By virtue of the long P-O3 distance (1.570(2) Å), compared with other P-O distances ranging from 1.505(2)-1.512(2) Å, it is the O3 that remains protonated. Selected bond distances and angles of **13** are provided in Table 7.5.

**Table 7.5** Selected Bond lengths [Å] and angles [°] for calcium propylene diphosphonates, **13**.

| | | | |
|---|---|---|---|
| Ca(1)-O(2)#1 | 2.385(2) | O(2)#1-Ca(1)-O(2)#2 | 163.58(11) |
| Ca(1)-O(2)#2 | 2.385(2) | O(2)#1-Ca(1)-O(1)#3 | 83.64(8) |
| Ca(1)-O(1)#3 | 2.395(2) | O(2)#2-Ca(1)-O(1)#3 | 85.91(8) |
| Ca(1)-O(1)#4 | 2.395(2) | O(1)#3-Ca(1)-O(1)#4 | 100.78(11) |
| Ca(1)-O(2) | 2.426(2) | O(2)#1-Ca(1)-O(2) | 122.86(8) |
| Ca(1)-O(2)#5 | 2.426(2) | O(2)#2-Ca(1)-O(2) | 70.15(9) |
| Ca(1)-O(3)#5 | 2.864(3) | O(1)#3-Ca(1)-O(2) | 151.79(8) |
| Ca(1)-O(3) | 2.864(3) | O(1)#4-Ca(1)-O(2) | 91.44(8) |
| P(1)-O(1) | 1.511(2) | O(2)#1-Ca(1)-O(3)#5 | 123.20(7) |
| P(1)-O(3) | 1.566(2) | O(2)#2-Ca(1)-O(3)#5 | 68.54(7) |
| P(1)-C(1) | 1.793(4) | O(1)#3-Ca(1)-O(3)#5 | 86.49(7) |
| | | O(2)-Ca(1)-O(3)#5 | 71.25(8) |
| | | O(1)#3-Ca(1)-O(3) | 150.76(7) |
| | | O(3)#5-Ca(1)-O(3) | 100.98(10) |

Symmetry transformations used to generate equivalent atoms:
#1 -x,y+1/2,z #2 -x,-y,-z+1 #3 x-1,-y+1/2,-z+1
#4 x-1,y,z #5 x,-y+1/2,-z+1 #6 -x,-y+1,-z+1
#7 x+1,y,z #8 x,y,-z+1/2

Compound **13** represents the first propylenediphosphonate, prior alkaline earth examples are limited to a barium species, {$Ba_2[O_3P(CH_2)_3PO_3 \cdot 3H_2O_n$, with a pillared layered three-dimensional compound comprised of $BaO_8$ sheets connected by three-carbon chains (Figure 7.17). The $PDPA^{4-}$ ligand is fully deprotonated, all the oxygen

atoms are involved in metal coordination.

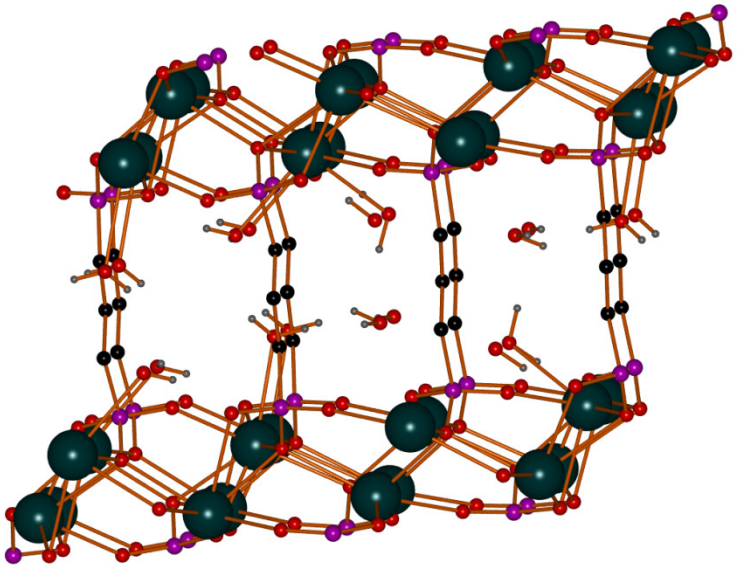

**Figure 7.17.** Pillared layered structure of $Ba_2[O_3P(CH_2)_3PO_3 3H_2O]$. Barium is represented by dark green spheres, phsophrus purple, oxygen red, carbon black and hydrogen by gray spheres.

Compounds **10, 11, 12** and **13** are all based on alkyl diphosphonates with varying carbon chain lengths, with a methylene unit in **10**, ethylene in **11** and **12**, and propylene in **13**. There are major differences in their synthesis and crystallization as well as overall structural features, with metal coordination number of six (**11**) to eight (**13**).

## 7.4 Conclusions

Three-dimensional compounds of methylene, ethylene and propylenediphosphonate compounds have been prepared. By increasing the lengths of the alkyl linker in the diphosphonates and thereby increasing the interlayer distance, it is possible to achieve pillared layered compounds with a less dense framework.

## 7.5 Experimental

### 7.5.1 Synthesis of calcium methylenediphosphonate, (10):

Methylenediphosphonic acid (0.1g, 0.056 mmol), phenylphosphinic acid (0.08g, 0.056 mmol) and $Ca(NO_3)_2{\cdot}4H_2O$ (0.15g, 0.056 mmol) were dissolved in 5 mL distilled water. The resulting clear colorless solution was sealed in a Carius tube at 40mTorr and kept at 150 $^oC$ for one week. Colorless crystals formed in the Carius tube from a yellowish green solution. Crystals were isolated by filtration, washed with water and air dried. Yield: 0.009 g, 0.042 mmol 81 %; m.p.: 450 $^oC$ (decomposition); IR (Nujol): 2728.6(s), 1465.4(s), O-H 1378.6, 1304.6(m), 1154.4(m) 965.8(m), 722.3.

### 7.5.2 Synthesis of sodium calcium ethylenediphosphonate (11):

Ethylenediphosphonic acid, $H_4EDA$, (1 mL, 1.05 mmol, 1.05 M) and NaOH (1.05 mL, 2.10 mmol, l2 M) were mixed in a 25 mL beaker and stirred for one minute, attaining a clear solution. To this, 1 mL of 1.05 M $CaCl_2$ (1.05mmol) solution was added, upon which the solution turned cloudy under formation of a white precipitate. 100 µL of concentrated HCl were added, upon which the precipitate dissolved, resulting in a clear, colorless solution. 3 mL of distilled $H_2O$ were then added while stirring. The clear solution was transferred into a Carius tube and sealed under 40 mTorr of pressure. The tube was heated at 170 ºC for three days. The resulting clear solution was filtered. Colorless blocks of crystals formed within two weeks at room temperature. Yield 0.11 g 0.25 mmol, 21.6 %. Yield: 0.07g, 0.30 mmol, 58.9%. IR (Nujol): 2724.1 (w), C-H 1489.9(s), O-H 1376.2 (s), 1004.0(w), 722.5(m).

### 7.5.3 Synthesis of calcium nitrate ethylenediphosphonate (12):

Sodium metasilicate nano hydrate (12.20 g, 0.043 mol) was dissolved in 25 mL distilled water and warmed gently to dissolve the sodium metasilicate. In a separate beaker, ethylenediphosphonic acid (7.80 g, 0.041 mol) was dissolved in 25ml distilled water and warmed to 40 $^{o}$C. The silicate was then added dropwise while stirring. The resulting clear colorless mixture was quickly transferred into 15cm x 2cm test tubes and left to stand for two days allowing the gel to set. To the surface of the set gel, about 1mL of calcium nitrate solution was added slowly. After about 5 weeks, large sword-like crystals grew in the tubes. Yield: 0.73 g, 0.003 mol 76 %. m.p.: 491 $^{o}$C (decomposes); IR (Nujol): 3486.1(m), 2669.7(w) 1665.5(m), 1467.1(s), 1303.7(m), 1152.0(m), 1035.3(m), 936.1(m), P-C 720.1(s), 609.3(w), 550.9(w).

### 7.5.4 Synthesis of calcium propylenediphosphonate (13):

Compound **13** was prepared by dissolving propylene diphosphonic (0.050g, 0.250 mmol) of acid and $Ca(NO_3)_2 \cdot 4H_2O$ (0.058 g, 0.250 mmol) in 4 mL of distilled water. The colorless clear solution was kept in a small vial at 85$^{o}$C for three days. The clear solution was then left at room temperature until colorless crystals appeared after three weeks. Yield: 0.022 g, 0.045 mmol, 18.3 %; m.p.: 360 $^{o}$C (decomposes); IR (Nujol): 2728.9(m), 1488.3(s), 1389.5(s), 1304.4(m), 1154.6(w), 722.4(s).

## 7.6 Experimental Details

Triethylphosphite ($P(OEt)_3$), phenylphosphinic acid, $Mg(NO_3)_2.6H_2O$, $Ca(NO_3)_2.4H_2O$, $CaCl_2$, NaOH, $H_3PO_3$, DMF, $NH_4Cl$, $CH_2O$, acetone, acetonitrile, 1, 3-dibromopropane and 1, 2-dibromoethane were obtained commercially. $P(OEt)_3$ was distilled prior to use, while the other reagents were used as purchased. $^1H$ NMR spectra were recorded using a Bruker DPX 300 spectrometer. A Perkin-Elmer PE 1600–FT-IR spectrometer was used to collect IR spectra as Nujol mulls between KBr plates.

## 7.7 X-ray crystallography

X-ray quality crystals of compounds **10** - **13**, were grown as described above. Crystals were taken out of the solutions and covered with viscous hydrocarbon oil (Infineum). Using a microscope, suitable crystals were selected and attached to a glass fiber. The crystals were mounted onto a 3-circle goniometer under the nitrogen stream of the low temperature device. Crystallographic data of **10** - **13** were collected using a Bruker diffractometer equipped with a SMART CCD system, and using MoKα-radiation ($\lambda$ = 0.71073 Å) at 96(2) K (**10**), 99(2) K(**11**), 100(2) K, (**12**) and 97(2) K (**13**). Crystal data, details of data collection and refinement of compounds **10** – **13** are provided in Table 7.1. The structures of **10** – **13** were solved by direct methods with the aid of SHELXS-97 and the structures were refined withSHELXL-97.[60]

Positions of hydrogen atoms of the hydroxyl groups on the phosphonate ligands were calculated; those on the on water molecules in **13**, were however located from the Fourier difference map and refined freely.

**Table 7.1**. Crystal data and structure refinement for compounds **10- 13**

| | **10** | **11** | **12** | **13** |
|---|---|---|---|---|
| **Empirical formula** | $CH_4CaO_6P_2$ | $C_4H_{13}CaNaO_{12}P_4$ | $C_4H_8CaNO_{26}P_4$ | $C_6H_{16}Ca_2O_{12}P_4$ |
| **Formula weight** | 214.05 | 440.09 | 812.34 | 484.23 |
| **Temperature (K)** | 96(2) | 99(2) | 100(2) | 97(2) |
| **Wavelength** (Å) | 0.71073 | 0.71073 | 0.71073 | 0.71073 |
| **Crystal system** | Monoclinic | Triclinic | Monoclinic | Orthorhombic |
| **Space group** | C2/c | P-1 | C2/c | Pbcm |
| **a (Å)** | 7.80(2) | 8.38(1) | 13.92(2) | 5.50(1) |
| **b (Å)** | 8.03(2) | 8.91(1) | 6.97(1) | 7.37(2) |
| **c (Å)** | 9.63(2) | 10.46(1) | 14.11(2) | 19.05(3) |
| **α** (°) | 90 | 109.69(2) | 90 | 90 |
| **β** (°) | 102.68(2) | 103.4 2(2) | 103.95(2) | 90 |
| **γ** (°) | 90 | 93.28(2) | 90 | 90 |
| **Volume (Å$^3$)** | 588.9(2) | 706.93(2) | 1329.2(3) | 773.0(2) |
| **Z** | 4 | 2 | 2 | 2 |
| **Dcalc(mg/mm$^3$)** | 2.392 | 2.068 | 2.030 | 2.080 |
| **μ (mm$^{-1}$)** | 1.57 | 0.99 | 1.20 | 1.21 |
| **Crystal size( mm$^3$)** | 0.30 | 0.25 | 0.60 | 0.30 |
| | 0.15 | 0.18 | 0.35 | 0.20 |
| | 0.10 | 0.06 | 0.15 | 0.10 |
| **2θ range** (°) | 3.69-28.47 | 2.15-28.29 | 2.97-28.29 | 3.70-23.46 |
| **Reflections collected** | 2516 | 7504 | 6452 | 4668 |
| **Independent reflections** | 692 | 3482 | 1657 | 588 |
| **R1 [I>2sigma(I)]** | 0.0311 | 0.0520 | 0.0525 | 0.0255 |
| **wR2 [I>2sigma(I)]** | 0.1089 | 0.1242 | 0.1713 | 0.0626 |
| **R1 (all data)** | 0.0316 | 0.0573 | 0.0549 | 0.0348 |
| **wR2 (all data)** | 0.1105 | 0.1270 | 0.1733 | 0.0648 |

## 7.8 References:


(1) Mathew, M.; Fowler, B. O.; Breuer, E.; Golomb, G.; Alferiev, I. S.; Eidelman, N. *Inorg. Chem.* **1998**, *37*, 6485.
(2) Räsänen, J. P.; Pohjala, E.; Nikander, H.; Pakkanen, T. A. *J. Phys. Chem. A* **1997**, *101*, 5196.
(3) Zhang, Y.; Leon, A.; Song, Y.; Studer, D.; Haase, C.; Koscielski, L. A.; Oldfield, E. *J. Med. Chem.* **2006**, *49*, 5804.
(4) Rogers, M. J.; Crockett, J. C.; Coxon, F. P.; Mönkkönen, J. *Bone* **2011**, *49*, 34.
(5) Ebetino, F. H.; Hogan, A.-M. L.; Sun, S.; Tsoumpra, M. K.; Duan, X.; Triffitt, J. T.; Kwaasi, A. A.; Dunford, J. E.; Barnett, B. L.; Oppermann, U.; Lundy, M. W.; Boyde, A.; Kashemirov, B. A.; McKenna, C. E.; Russell, R. G. G. *Bone* **2011**, *49*, 20.
(6) Demoro, B.; Caruso, F.; Rossi, M.; Benítez, D.; Gonzalez, M.; Cerecetto, H.; Parajón-Costa, B.; Castiglioni, J.; Galizzi, M.; Docampo, R.; Otero, L.; Gambino, D. *J. Inorg. Biochem.* **2010**, *104*, 1252.
(7) R. Graham G, R. *Bone* **2007**, *40*, S21.
(8) Coleman, R. E.; McCloskey, E. V. *Bone* **2011**, *49*, 71.
(9) Jeong, J. M.; Chung, J.-K. *Cancer Biother. Radiopharm.* **2003**, *18*, 707.
(10) Tanwar, J.; Datta, A.; Tiwari, A. K.; Thirumal, M.; Chuttani, K.; Mishra, A. K. *Bioconjugate Chem.* **2011**, *22*, 244.
(11) Fernandez, D.; Vega, D.; Goeta, A. *Acta Crystallographica Section C* **2003**, *59*, m543.
(12) Kontturi, M.; Peräniemi, S.; Vepsäläinen, Jouko J.; Ahlgrén, M. *Eur. J. Inorg. Chem.* **2004**, *2004*, 2627.
(13) Rogers, M. J. *Curr Pharm Des* **2003**, *9*, 2643.
(14) Kramer, J. M.; Fantasia, J. E. *Clin. Rev. Bone Miner. Metab.* **2011**, *9*, 38.
(15) Jokiniemi, J.; Peraniemi, S.; Vepsalainen, J.; Ahlgren, M. *Acta Crystallogr. Sect. E* **2009**, *65*, m436.
(16) Merrill, C. A.; Cheetham, A. K. *Inorg Chem* **2005**, *44*, 5273.
(17) Serre, C.; Férey, G. *Inorg. Chem.* **2001**, *40*, 5350.
(18) Riou, D.; Serre, C.; Férey, G. *J. Solid State Chem.* **1998**, *141*, 89.
(19) Riou, D.; Baltazar, P.; Férey, G. *Solid State Sciences* **1998**, *2*, 127.
(20) Bonavia, G. H.; Haushalter, R. C.; Lu, S.; O'Conner, C. J.; Zubieta, J. *J. Solid State Chem.* **1997**, *132*, 144.
(21) Kongshaug, K. O.; Riou, D. *J. Chem. Soc., Dalton Trans.* **2002**.
(22) Fu, R.; Xia, S.; Xiang, S.; Hu, S.; Wu, X. *J. Solid State Chem.* **2004**, *177*, 4626.
(23) Cheng, C.-Y.; Lin, K.-J. *Acta Crystallographica Section C* **2006**, *62*, m363.
(24) Rao, K. P.; Vidyasagar, K. *Eur. J. Inorg. Chem.* **2006**, *2006*, 813.
(25) Attfield, M. P.; Harvey, H. G.; Teat, S. J. *J. Solid State Chem.* **2004**, *177*, 2951.
(26) Serpaggi, F.; Ferey, G. *J. Mater. Chem.* **1998**, *8*.
(27) Haupt, E. T. K.; Kopf, J.; Petrova, J.; Arabadzhiev, V.; Momchilova, S. *Heteroat. Chem* **2006**, *17*, 36.
(28) Tuikka, M.; Haukka, M.; Ahlgrén, M. *Solid State Sci.* **2007**, *9*, 535.
(29) Nardelli, M.; Pelizzi, G.; Staibano, G.; Zucchi, E. *Inorg. Chim. Acta* **1983**, *80*, 259.

(30) Freire, E.; Vega, D. R.; Baggio, R. *Acta Crystallographica Section C* **2010**, *66*, m166.
(31) Uchtman, V. A. *J.Phys. Chem.* **1972**, *76*, 1304.
(32) Distler, A.; L. Lohse, D.; C. Sevov, S. *J. Chem. Soc., Dalton Trans.* **1999**, 1805.
(33) Lin, L.; Zhang, T.-J.; Fan, Y.-T.; Ding, D.-G.; Hou, H.-W. *J. Mol. Struct.* **2007**, *837*, 107.
(34) Rochdaoui, R.; Silvestre, J.-P.; Quy Dao, N.; Lee, M.-R.; Neuman, A. *Acta Crystallogr. Sect. C* **1992**, *48*, 2132.
(35) Tong, F.; Zhu, Y.; Sun, Z.; Wang, W.; Zhao, Y.; Xu, L.; Gong, J. *Inorg. Chim. Acta* **2011**, *368*, 200.
(36) Kunnas-Hiltunen, S.; Haukka, M.; Vepsalainen, J.; Ahlgren, M. *Dalton Trans.* **2010**, *39*, 5310.
(37) Philippot, E.; Jumas, J. C.; Brun, G.; Maurin, M. *Cryst. Struct. Commun.* **1972**, *1*, 103.
(38) Uchtman, V. A.; Gloss, R. A. *J. Phys. Chem.* **1972**, *76*, 1298.
(39) Kontturi, M.; Peraniemi, S.; Vepsalainen, J. J.; Ahlgren, M. *Acta Crystallographica Section E* **2004**, *60*, m1060.
(40) Kontturi, M.; Vuokila-Laine, E.; Peraniemi, S.; Pakkanen, T. T.; Vepsalainen, J. J.; Ahlgren, M. *J. Chem. Soc., Dalton Trans.* **2002**, 1969.
(41) Lin, L.; Zhang, T.-J.; Fan, Y.-T.; Ding, D.-G.; Hou, H.-W. *J. Mol. Struct.* **2007**, *837*, 107.
(42) Alberti, G.; Elsevier: 1996; Vol. 7, p 151.
(43) Alberti, G.; Costantino, U.; Vivani, R.; Zappelli, P.; Rossodivita, A.; Eniricerche S.p.a, Italy . 1992, p 28 pp.
(44) Attfield, M. P.; Yuan, Z.; Harvey, H. G.; Clegg, W. *Inorg. Chem. (Washington, DC, U. S.)* **2010**, *49*, 2656.
(45) Cao, D.-K.; Gao, S.; Zheng, L.-M. *J. Solid State Chem.* **2004**, *177*, 2311.
(46) De, B. P.; Liu, H.; Ouellette, W.; O'Connor, C. J.; Zubieta, J. *Inorg. Chim. Acta* **2010**, *363*, 4065.
(47) Ouellette, W.; Yu, M. H.; O'Connor, C. J.; Zubieta, J. *Inorg. Chem.* **2006**, *45*, 7628.
(48) Su, Y.-H.; Cao, D.-K.; Duan, Y.; Li, Y.-Z.; Zheng, L.-M. *J. Solid State Chem.* **2010**, *183*, 1588.
(49) Wang, Y.; Bao, S.-S.; Xu, W.; Chen, J.; Gao, S.; Zheng, L.-M. *J. Solid State Chem.* **2004**, *177*, 1297.
(50) Zhang, N.; Huang, C.-Y.; Sun, Z.-G.; Zhang, J.; Liu, L.; Lu, X.; Wang, W.-N.; Tong, F. *Z. Anorg. Allg. Chem.* **2010**, *636*, 1405.
(51) Ouellette, W.; Yu, M. H.; O'Connor, C. J.; Zubieta, J. *Inorg Chem* **2006**, *45*, 7628.
(52) Conary, G. S.; McCabe, D. J.; Meline, R. L.; Duesler, E. N.; Paine, R. T. *Inorg. Chim. Acta* **1993**, *203*, 11.
(53) Fu, R.; Hu, S.; Wu, X. *Crystal Growth & Design* **2007**, *7*, 1134.
(54) Cheng, C.-Y.; Fu, S.-J.; Yang, C.-J.; Chen, W.-H.; Lin, K.-J.; Lee, G.-H.; Wang, Y. *Angew. Chem. Int. Ed.* **2003**, *42*, 1937.
(55) Ouellette, W.; Yu, M. H.; O'Connor, C. J.; Zubieta, J. *Inorg. Chem.* **2006**, *45*, 7628.
(56) Yuan, Z.; Clegg, W.; Attfield, M. P. *J. Solid State Chem.* **2006**, *179*, 1739.

(57) Harvey, H. G.; Teat, S. J.; Tang, C. C.; Cranswick, L. M.; Attfield, M. P. *Inorg. Chem.* **2003**, *42*, 2428.
(58) Harvey, H. G.; Herve, A. C.; Hailes, H. C.; Attfield, M. P. *Chem. Mater.* **2004**, *16*, 3756.
(59) Meng, L.; Li, J.; Sun, Z.-G.; Zheng, X.-f.; Dong, D.-P.; Chen, H.; Zhu, Y.-Y.; Zhao, Y.; Zhang, J. *Z. Anorg. Allg. Chem.* **2008**, *634*, 571.
(60) Chadwick, S.; Englich, U.; Ruhlandt-Senge, K. *Chem. Commun.* **1998**, 2149.

# CHAPTER 8

## Synthesis and Characterization of Calcium amino trimethylenephosphonate

### 8.1 Introduction

Recent research on metal organic frameworks (MOFs) has focused on predicting the dimension of the solids by careful choice of ligands.[1-3] While the predictable preparation of design solids has not been achieved, may fascinating hybrid materials of different dimensions and with unique characteristic and functions have been prepared.[4-6] In the preceding chapters, the chemistry of the mono- and diphosphonate alkaline earth metal based materials was discussed. The focus of discussion in this chapter is on the effect of the geometry of a triphosphonic acid ligand on the dimensionality of alkaline earth MOF structures.

Phosphonates are good chelating agents, however the introduction of an amine group to form aminophosphonic acid has been shown to increase their metal binding abilities.[7] Like the phosphonic acids, the aminophosphonic acids also form important medicinal compounds.[8-10] Hence, ever since the first naturally occurring 2-aminoethylphosphonic acid was discovered in living systems, the synthesis of the amino bis- and triphosphonic acids have been explored for their medicinal applications.[11]

We herein present structural studies of alkaline earth metal compounds involving amino tris(methylenephosphonic) acid ($H_6$ATMP), also called nitrilotrismethylene triphosphonic acid, other abbreviations used include ATMP,[12] AMP,[13] or $H_6$ntmp.[14] The structure of the $H_6$ATMP ligand is shown in Figure 8.1, it's synthesis and properties have been discussed in Chapter 3.

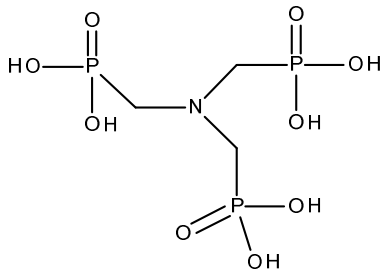


($pKa_1 < 2$, $pKa_2 < 2$, $pKa_3$ 4.30, $pKa_4$ 5.46, $pKa_5$ 6.66, $pKa_6$ 12.34)[15]

**Figure 8.1.** Amino tris(methylenephosphonic) acid ($H_6ATMP$)

The chelating property of the $H_6ATMP$ makes it useful as scale inhibitor,[16] corrosion inhibitor,[17-19] and as cement retarder to delay the setting time of cements.[14] The polyphosphonic acids are also used in supramolecular chemistry and crystal engineering. In industry, triphosphonates have applications in oilfield drilling, mineral processing, corrosion control, metal complexation and sequestration.[20]

Despite these special properties, the $H_6ATMP$ ligand has not been used extensively in coordination chemistry. Hence, studies on the synthesis and structural characterization of calcium amino triphosphonate (**14**) $\{Ca[HN(CH_2PO_3H)_3]\}_n$ were conducted. These will expand insight into alkaline earth metal triphosphonate chemistry and promote the understanding of how an additional phosphonate moiety will affect the structural characteristics of the resulting MOFs.

In analogy with diphosphonates, a variety of metal-ligand binding modes, as illustrated in Figure 8.2, are possible.

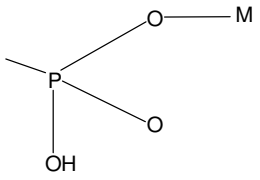


$\mu\eta^1$

**(a)**

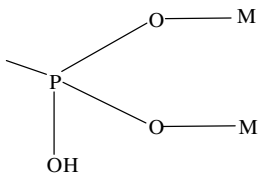


$\mu^2\eta^1\eta^1$

**(b)**

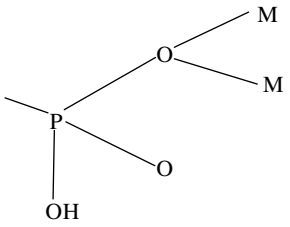


$\mu^2\eta^2$

**(c)**

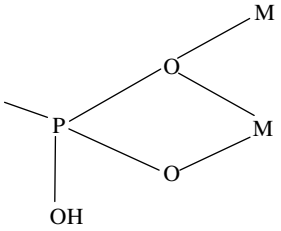


$\mu^3\eta^2\eta^1$

**(d)**

**Figure 8.2.** Different binding modes of phosphonates in the alkaline earth amino trimethylene phosphonates compounds.

Of these possibilities,. Table 8.1 gives a summary of alkaline earth AMTPA compounds and their respective binding modes.the compounds and their binding modes.

**Table 8.1.** Binding modes of the alkaline earth metal amino trimethylenephosphonate compounds.

| Compound | P1 | P2 | P3 |
|---|---|---|---|
| $\{Ca[HN(CH_2PO_3H)_3]\}_n$ (**14**) | $\mu^2\eta^1\eta^1$ | $\mu^2\eta^2$ | $\mu^2\eta^1\eta^1$ |
| $[Ca(HN(CH_2PO_3H)_3)(H_2O)]_\infty \cdot 3.5H_2O$ [13,20] | $\mu\eta^1$ | $\mu^2\eta^1\eta^1$ | $\mu^2\eta^1\eta^1$ |
| $\{Mg[HN(CH_2PO_3H)_3(H_2O)_3]\}_n$ [20] | $\mu^0$ | $\mu^2\eta^1\eta^1$ | $\mu\eta^1$ |
| $\{Sr[HN(CH_2PO_3H)_3]\}_n$ [20] | $\mu^2\eta^1\eta^1$ | $\mu^3\eta^2\eta^1$ | $\mu^2\eta^1\eta^1$ |
| $\{Ba[HN(CH_2PO_3H)_3(H_2O)]\}_n$ [20] | $\mu^2\eta^1\eta^1$ | $\mu^2\eta^1\eta^1$ | $\mu\eta^1$ |

## 8.2 Synthetic Considerations

Advantages of using the amino trimethylenephosphonic acid as a ligand include solubility in water and increased denticity due to the larger number of phosphonate sites for metal-ligand interaction, as compared to the more common diphosphonates. Furthermore, the $H_6$AMTP ligand has six acidic protons that may deprotonate to form anions with a range of charges. In addition, the ligand shows zwitterionic characteristics, as shown in Figure 8.3.[21]

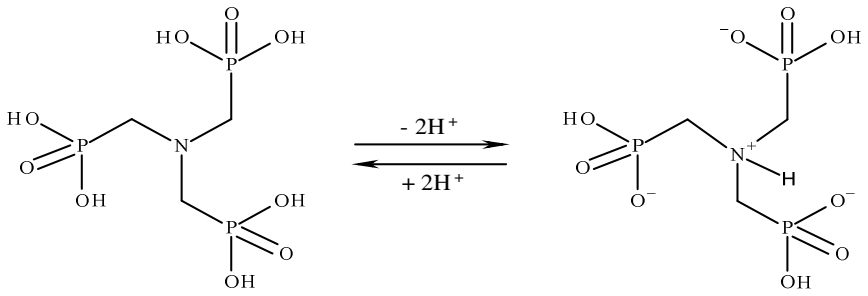


**Figure 8.3.** Amino trimethylenephosphonic acid ($H_6$AMTP) in equilibrium with its zwitterions.

A closely related ligand demonstrating zwitterion behavior is 2-amino ethylphosphonic acid (Figure 8.4), with pKa values of 6.21 and 10.92[22] for the acid dissociation.

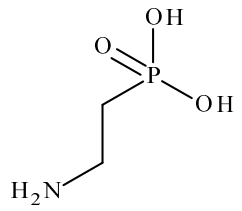


**Figure 8.4.** 2-aminophosphonic acid

Calcium amino trimethylenephosphonate (**14**) $\{Ca[HN(CH_2PO_3H)_3]\}_n$ is prepared by dissolving calcium nitrate and amino trimethylenephosphonic acid in water. Colorless crystals appear overnight at room temperature. Crystal formation can be accelerated in the presence of phosphonic acid, as shown in Scheme 8.1.

$$Ca(NO_3)_2{\cdot}4H_2O + N(CH_2PO_3H_2)_3 \xrightarrow{H_3PO_3/H_2O} Ca[HN(CH_2PO_3H)_3]_n$$

**Scheme 8.1.** Synthesis of calcium amino trimethylenephosphonate (**14**)

The ease of coordinating amino trimethylenephosphonic acid ligand to metals is a result of its good solubility due to its zwitterionic form.[20,21] By carefully selecting soluble metal salts, quality single crystals may be obtained even at room temperature. Crystals of

compound **14** were obtained at ambient and hydrothermal conditions; however those obtained hydrothermally at 200°C were of higher quality. Furthermore, initial crystallization attempts included the introduction of phosphonic acid, and it is believed that this promotes rapid crystallization.

Previous alkaline earth metal amino trimethylenephosphonate compounds include $[Ca(HN(CH_2PO_3H)_3)(H_2O)]_n \cdot 3.5H_2O$,[13,14,20] $\{Mg[HN(CH_2PO_3H)_3(H_2O)_3]\}_n$, $\{Sr[HN(CH_2PO_3H)_3]\}_n$ and $\{Ba[HN(CH_2PO_3H)_3(H_2O)]\}_n$,[20] prepared under similar reactions conditions. Details of the synthesis of the novel anhydrous $\{Ca[HN(CH_2PO_3H)_3]$ **14** and it's structural parameters are herein discussed.

### 8.3 Structural Aspects of Calcium amino trimethylenephosphonate, (14):

Compound **14** crystallizes in the monoclinic space group $P2_1/c$. The compound displays a three dimensional network with an octahedral calcium geometry. Crystal data, details of data collection and refinement of compounds **14** are provided in Table 8.2 in the experimental section of this chapter.

The asymmetric unit of **14** consists of one calcium and a triply deprotonated ligand and a protonated N, the result of the zwitterionic form of the ligand. (Figure 8.5). The coordination environment of calcium in **14** (Figure 8.5) is completed by six phosphonate oxygen atoms from two symmetrically identical ligands. Each dianionic $H_4ATMP^{2-}$ pairs with one the $Ca^{2+}$ ion to maintain charge neutrality.

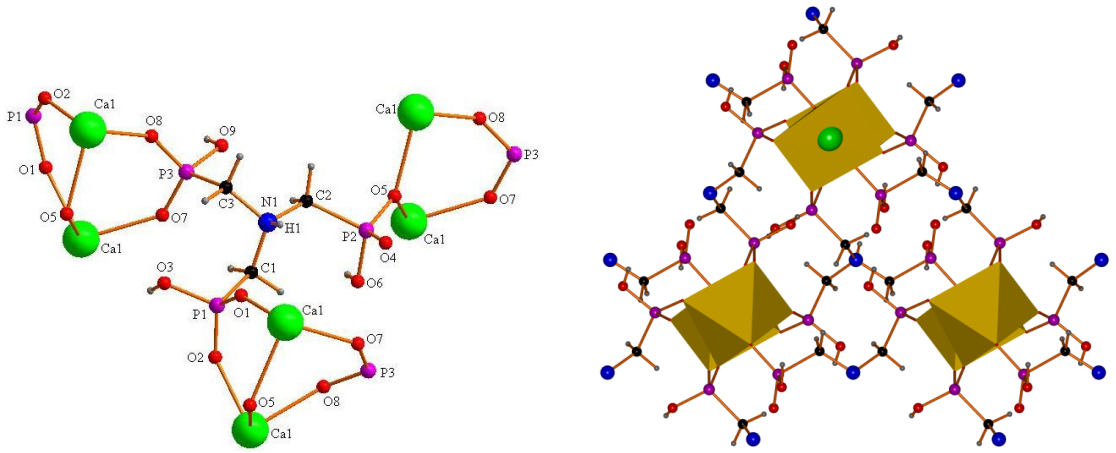


**Figure 8.5. Figure a.** The environment of one doubly deprotonated ligand in $[Ca(H_4ATMP]_n$. The zwitter ion is indicated with the protonation of N. **b.** Structure of **14** showing zwitterionic effects in the amino trimethylenephosphonate. The gold polyhedral represent the octahedral calcium (green sphere) environment while the blue, puple, black and grey spheres represent nitrogen, phosphorus, carbon and hydrogen atoms respectively.

A calcium derivative involving the $H_6ATMP$ ligand has been reported previously in the form of the hydrated species $[Ca(HN(CH_2PO_3H)_3)(H_2O)]_n \cdot 3.5H_2O$. [13,14,20] This compound displays a sheet structure comprising of a central calcium coordinated by six oxygen atoms, five of which originate from the doubly deprotonated phosphonate ligand and one from a coordinated water molecule (Figure 8.6). In addition, the nitrogen center in the amino triphosphonate ligand is protonated. The protonation of the nitrogen is evident from the tetrahedral structure of the N with C-N-C bond angles of 110.96 - 112.88 (1) ° (Table 8.3). However N-H IR stretches for **14** were not observed.

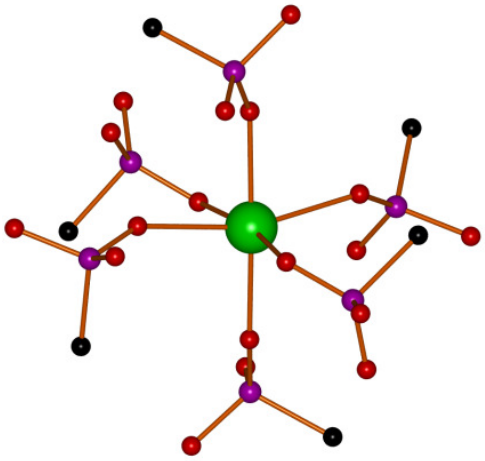

**Figure 8.6.** The coordination environments of calcium in $[Ca(H_4ATMP]_n$ (**14** ). The octahedral geometry of calcium in **14** is comprised of six phosphonate oxygen atoms. All hydrogen atoms except those on the coordinating water molecule have been removed for clarity.

**Table 8.3.** Selected bond [Å] lengths and angles [°] for anhydrous calcium amino trimethylenephosphonate (**14**)

| Bond length | | | | Bond angle | |
|---|---|---|---|---|---|
| Ca(1)-O(1)#1 | 2.2592(1) | N(1)-C(2) | 1.510(2) | O(1)#1-Ca(1)-O(2) | 176.81(5) |
| Ca(1)-O(2) | 2.3121(1) | N(1)-C(3)#5 | 1.506(2) | O(2)-Ca(1)-O(7)#1 | 79.86(5) |
| Ca(1)-O(7)#1 | 2.3284(1) | N(1)-C(1)#3 | 1.508(2) | O(1)#1-Ca(1)-O(8) | 95.31(5) |
| Ca(1)-O(8) | 2.3371(1) | P(3)-C(3) | 1.8322(2) | O(2)-Ca(1)-O(8) | 84.03(5) |
| Ca(1)-O(5)#2 | 2.4428(1) | P(3)-O(9) | 1.5714(2) | O(7)#1-Ca(1)-O(8) | 163.25(5) |
| Ca(1)-O(5) | 2.5257(1) | | | O(1)#1-Ca(1)-O(5)#2 | 90.50(5) |
| P(1)-O(1) | 1.4922(2) | | | O(7)#1-Ca(1)-O(5)#2 | 98.11(5) |
| P(1)-O(2) | 1.5091(1) | | | O(8)-Ca(1)-O(5)#2 | 87.13(5) |
| P(1)-O(3) | 1.5733(1) | | | O(1)#1-Ca(1)-O(5) | 85.59(5) |
| P(1)-C(1) | 1.8209(2) | | | O(2)-Ca(1)-O(5) | 91.25(5) |
| P(2)-O(4) | 1.4970(2) | | | O(7)#1-Ca(1)-O(5) | 90.34(5) |
| P(2)-O(5) | 1.5214(1) | | | O(8)-Ca(1)-O(5) | 85.41(5) |
| P(2)-O(6) | 1.5784(2) | | | O(5)#2-Ca(1)-O(5) | 171.22(2) |
| P(2)-C(2) | 1.829(2) | | | N(1)#3-C(1)-P(1) | 113.50(1) |
| P(3)-O(7) | 1.4950(1) | | | N(1)-C(2)-P(2) | 118.00(1) |
| P(3)-O(8) | 1.5105(1) | | | N(1)#4-C(3)-P(3) | 120.48(1) |

Symmetry transformations used to generate equivalent atoms:

#1 -x+1/2,y+1/2,-z+1/2 #2 -x+1/2,y-1/2,-z+1/2
#3 -x,-y+2,-z+1 #4 -x-1/2,y-1/2,-z+1/2 #5 -x-1/2,y+1/2,-z+1/2

In **14**, the calcium centers are linked by O-P-O units involving O1,O2 or O7,O8 and by O5 as shown in Figure 8.7, resulting in two six-membered rings (Ca-O2-P1-O1-Ca-O5) and (Ca-O2-P1-O1-Ca-O5), and an eight-membered ring (Ca-O2-P1-O1-Ca-O7-

P3-O8). A three dimensional structure is achieved by extending above and below the six and eight membered ring systems (Figure 8.8). Ca –O bond distances (2.259(1) - 2.443(1) Å) as well as the P-O bond distances 1.492(2) - 1.578(2) Å of **14** compare favorably with those of $[Ca(HN(CH_2PO_3H)_3)(H_2O)]_n \cdot 3.5H_2O$ (Ca-O 2.305-2.511 Å and P-O1.483-1.569 Å), slight variation are based on the different metal-ligand binding modes.

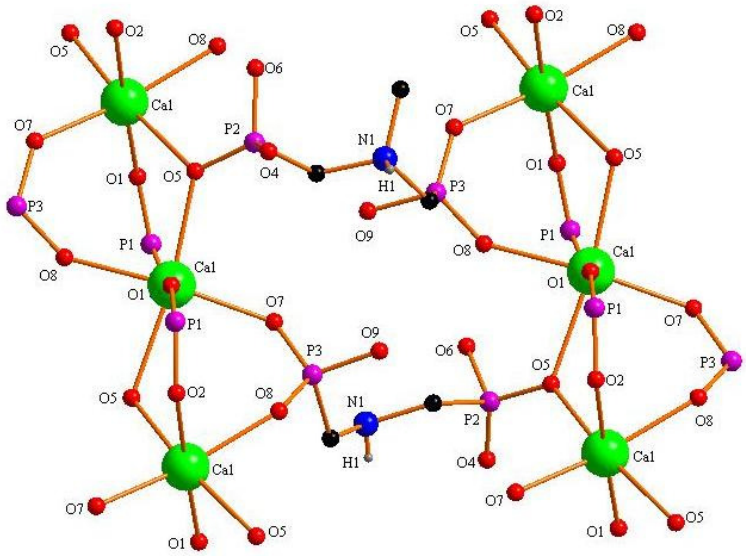


**Figure 8.7.** Labeling scheme of $[Ca(H_4AMTP]_n$ showing chelating and bridging modes of the ligand in the extended sheet. All hydrogen atoms have been removed for clarity, except the ammonium hydrogen.

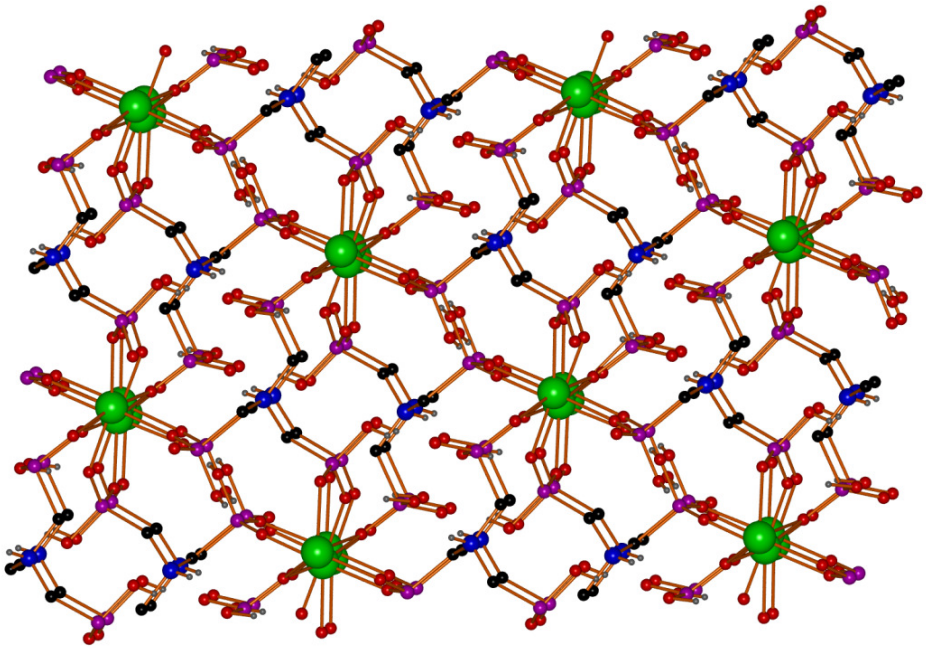

**Figure 8.8.** Extended three dimensional view of **14**, all methylene and hydroxyl hydrogen atoms have been removed for clarity.

Remarkably, the three-dimensional array in **14** is achieved without hydrogen bond interactions considering that **14** was prepared in water. Previous examples of hydrated ATMP species include $M[NH(CH_2PO_3H)_3(H_2O)_3]$ (M = Co, Mn, Ni, Cu Zn, Cd),[23] in addition to $[Ca(HN(CH_2PO_3H)_3)(H_2O)]_\infty \cdot 3.5H_2O$[20] where the three-dimensional structures were obtained by extensive hydrogen bonding (H···O distance of 1.70-1.96 Å). For manganese hydrated and anhydrous phases exist $Mn[NH(CH_2PO_3H)_3(H_2O)_3]$ and $[NH(CH_2PO_3H)_3]$ has three dimensional structure.[24]

As shown in Figure 8.9, pendant P-OH groups in **14** (O3, O6 and O9) generate a number of hydrogen bonds to the phosphonate oxygen atoms (O2, O4, O6 and O8) with average H···A distances of 2.11 Å and D-H···A angles that range from 126.6-177.0 $^{o}$ as

indicated in Table 8.4. In addition, there are hydrogen bonds from the N-H group to O1 and O4.

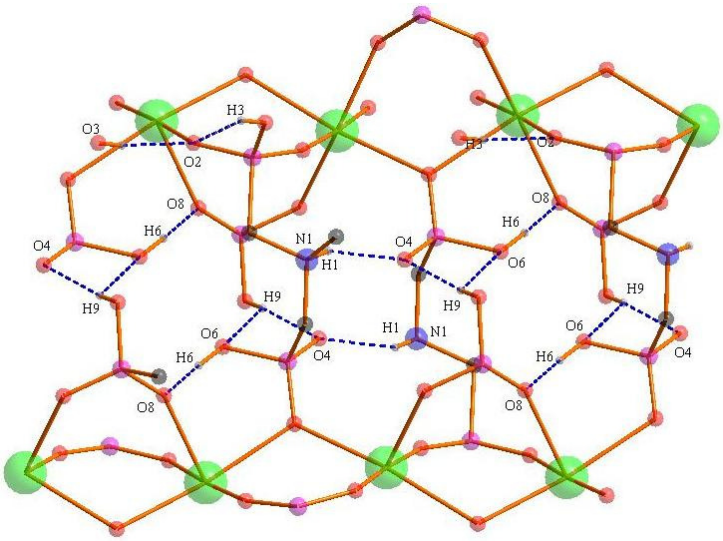


**Figure 8.9.** Hydrogen bonding shown between phosphonate oxygen atoms (O2, O4 and O8) the pendant O-H groups (H, H6 and H9) and N-H in compound **14**.

**Table 8.4.** Hydrogen bond distances and angles of **14**

| D- H ···A | d(D-H) | d(H···A) | <DHA | d(D···A) |
|---|---|---|---|---|
| N1-H1···O4 | 0.801 | 2.000 | 147.83 | 2.711 |
| N1-H1···O1 | 0.801 | 2.621 | 112.10 | 3.015 |
| O3-H3···O2 | 0.684 | 2.004 | 174.42 | 2.685 |
| O6-H6···O8 | 1.029 | 1.496 | 177.03 | 2.524 |
| O9-H9···O4 | 0.770 | 1.991 | 164.81 | 2.741 |
| O9-H9···O6 | 0.770 | 2.554 | 126.60 | 3.075 |

The overall structural parameters of **14** and the hydrated form $[Ca(H_4AMTP)(H_2O)]_n \cdot 3.5H_2O$ compare well, as shown in Figure 8.10. The main difference is that the three-dimensional hydrated phase is achieved *via* hydrogen bonding.

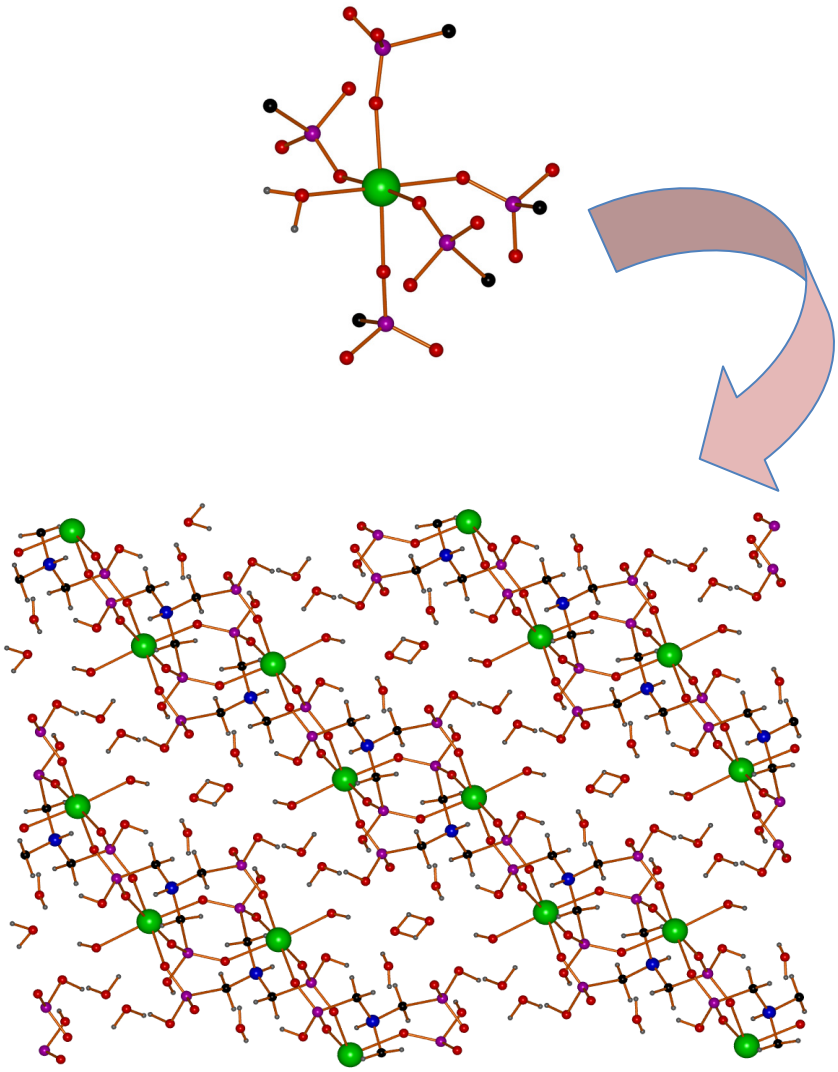

**Figure 8.10.** Structure of the hydrated $[Ca(HN(CH_2PO_3H)_3)(H_2O)]_n \cdot 3.5H_2O$[20] showing the coordination environments of calcium its extended structure. The octahedral geometry of calcium is comprised of five phosphonate oxygen atoms and one water molecule. All hydrogen atoms except those on the coordinating water molecule have been removed for clarity.

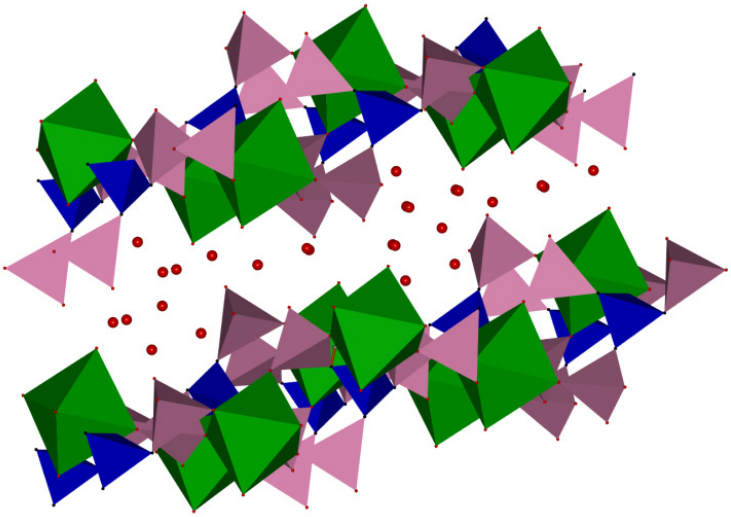

**Figure 8.11.** .Polyhedral structure of the hydrated compound,[20] showing the phosphonates as pink tetrahedrons, calcium as green octahedrons, while the ammonium ion is represented by blue tetrahedrons. The water molecules are red spheres, lying in the space between parallel sheets of calcium trimethylenephosphonate. Hydrogen atoms have been removed for clarity.

## 8.4 Powder Diffraction Pattern Studies

The bulk purity of compound **14** was verified by X-ray powder diffraction. Figure 8.12 shows an overlay of the powder patterns of **14** (red) and the hydrated form (black),[20] (calculated from single crystal data). The difference in the diffraction patterns indicates different structural composition between **14** and its hydrated form.

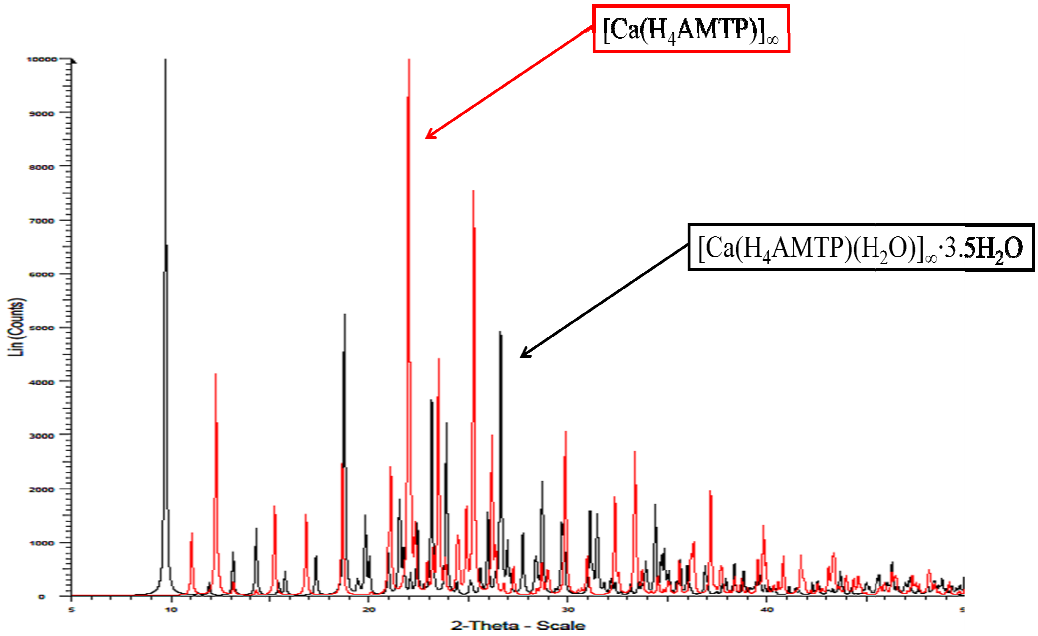


**Figure 8.12.** Powder diffraction pattern for **14** in red. The black trace shows a calculated powder pattern for the hydrated form (calculated from single crystal data).

## 8.5 Thermogravimetric Studies

The thermogravimetric analysis of **14** (Figure 8.13) indicated decomposition around 350 $^{o}$C, with gradual weight loss to about 650 $^{o}$C, consistent with the loss of one phosphonate group, leaving about 76.25 % (wt) residue corresponding to $Ca_3(PO_4)_2$.

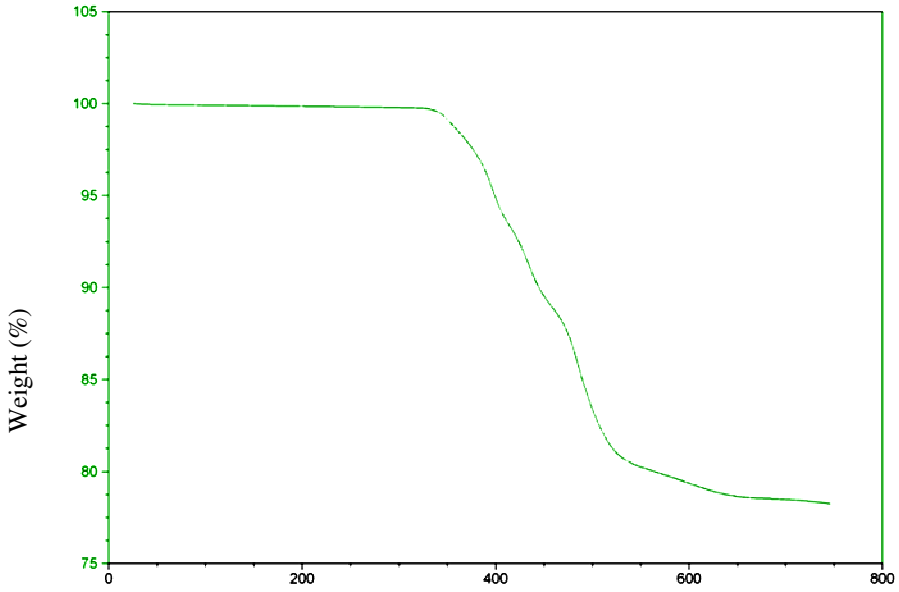


**Figure 8.13.** Thermogravimetric analysis of $[Ca(H_2AMTP)]_\infty$, **14**.

Compound **14** is a novel anhydrous calcium triphosphonate. Most other trimethylenephosphonates contain at least one $H_2O$ donor.The presence of water frequently results in hydrogen bonding.[23,25,26] In compound **14**, a three-dimensional structure is achieved without hydrogen bonding, making the compound thermally quite robust.

Amino trimethylenephosphonates compounds involving Mg, Sr and Ba have been prepared under similar conditions of low pH and ambient temperatures,[20] by dissolving equimolar amounts of the ligand and alkaline earth metal chlorides in water. With the exception of strontium, all the compounds contain at least one coordinating water molecule. Figure 8.14 shows the coordination sphere of magnesium in $\{Mg[HN(CH_2PO_3H)_3(H_2O)_3]\}_n$,[20] comprised of three phosphonate oxygen atoms and

three water molecules. A zigzag chain is formed by the use of two ligand phosphonates to bridge the magnesium centers, leaving one phosphonate group uncoordinated (denoted by $\mu^0$ in Table 8.1). The three coordinating water molecules are involved in hydrogen bonding between the zigzag chains (Figure 8.15), resulting in a two-dimensional structure.

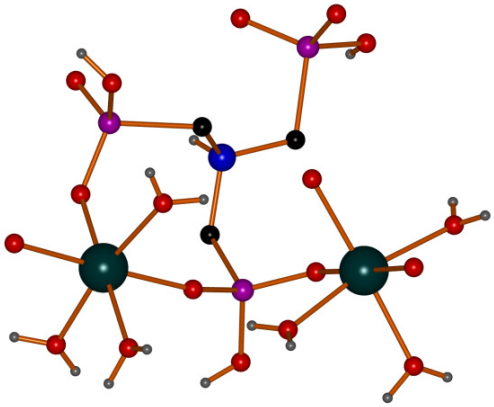

**Figure 8.14.** Stucture of magnesium amino trimethylenephosphonate, showing the bridging between two $Mg^{2+}$ centers by two phosphonate and the unbound phosphonate group. Dark green spheres represent magnesium ion, purple phosphorus, blue nitrogen, red oxygen, black carbon and grey hydrogen atoms.

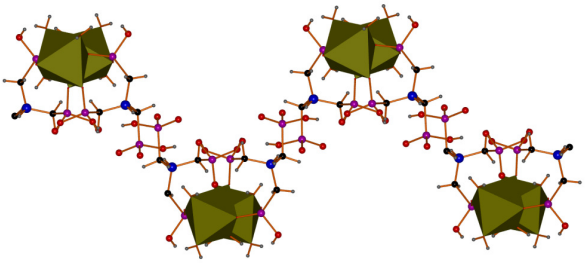

**Figure 8.15.** The octahedral geometry of magnesium in $\{Mg[HN(CH_2PO_3H)_3(H_2O)_3]\}_n$, ( dark yellow polyhedron), propagated in a zigzag chain fashion is shown. The phosphonate oxygen atoms are represented by red spheres, phosphorus as purple spheres, nitrogen (blue), carbon (black) and hydrogen black.

Showcasing the role of metal diameter, the three dimensional anhydrous strontium compound $\{Sr[HN(CH_2PO_3H)_3]\}_n$, is hepta-coordinated, whereas the barium species $\{Ba[HN(CH_2PO_3H)_3(H_2O)]\}_n$, displays a three-dimensional structure with two crystallographically independent $Ba^{2+}$ centers. One $Ba^{2+}$ is nine-coordinate while the other is ten-coordinate. As expected, M-O bond lengths increase with increasing metal size.

Other structurally characterized examples involving amino trimethlenephosphonates of divalent metals include several Zn species such as $Zn_2[HO_3PCH_2NH(CH_2PO_3H)_2]$, $Zn[NH(CH_2PO_3H)(H_2O)_3]$, $Zn[NH(CH_2PO_3H)_3]$,[18,24] and Al,[24] Cu,[27] Cd,[25,28] Ti,[12,29] Mn,[23] Pb[30] and Pr.[31]

As mentioned above, the $H_6ATMP$ ligand can deprotonate to various degrees, a rare example involving $H_5ATMP^-$ exist,[32] the most common anionic species is $H_4ATMP^{2-}$, also observed in **14** but $H_2ATMP^{4-}$ and the fully deprotonated form have also been reported.[33]

## 8.6 Conclusions

Simple synthetic methods have been used to prepare a novel, anhydrous form of calcium amino trimethylenephosphonate. Synthetic studies of **14** have shown that the presence of phosphonic acid in the synthesis of compound **14** greatly improved crystal quality and isolated yield. This may be extended to other synthetic routes towards the preparation of phosphonate compounds.

## 8.7 Experimental

Compound **14** was prepared by dissolving aminotrimethylenephosphonic acid, $H_6$ATMPA, (0.1g, 0.334 mmol) in 5mL of water to afford a colorless clear solution. To this, $Ca(NO_3)_2{\cdot}4H_2O$ (0.0789 g, 0.334 mmol) and $H_3PO_3$ (0.088g, 0.107mmol) were added and stirred. The clear solution was left in a test tube at room temperature. Colorless blocks of single crystals were obtained overnight. Yield: 0.05g , 0.15 mmol, 50%. IR (Nujol): 3358.4(w), 2716.3(m), 1374.4(s), 12985(m), 937.6(m). Due to low solubility, NMR spectra could not be obtained.

## 8.8 Experimental Details

Amino trimethylenephosphonic acid was synthesized by the Mannich reaction[34] involving an amine, formaldehyde and phosphorous acid, as described in detail in chapter 3. $Ca(NO_3)_2{\cdot}4H_2O$ and $H_3PO_3$ were obtained commercially and used as received. A Perkin-Elmer PE 1600–FT-IR spectrometer was used to collect IR spectra as Nujol mulls between KBr plates.

## 8.9 X-ray Crystallography

X-ray quality crystals of **14** were grown as described above. Crystals were taken out of the solution and covered with viscous hydrocarbon oil (Infineum). Using a microscope, suitable crystals were selected and attached to a glass fiber. The crystal was mounted onto a 3-circle goniometer under a low temperature nitrogen stream of the low temperature device. Crystallographic data of **14** was collected using Bruker diffractometer equipped with a SMART CCD system, and MoKα-radiation ($\lambda$ = 0.71073

Å) at 86(2) K. The structure of **14** was solved by the Direct Method with the aid of SHELXS-97; and the structures were refined with SHELXL-97.[35] Positions of hydrogen atoms of the hydroxyl groups on the phosphonate ligands were placed on calculated positions and refined isotropically. The hydrogen atom on nitrogen in **14** was located from the Fourier difference map and refined freely. All other hydrogens of the ligand in **14** were placed in calculated positions based on geometric considerations. Crystal data and structure refinement information is presented in Table 8.2.

.

**Table 8.2.** Crystal data and structure refinement for compound **14**

| | |
|---|---|
| Empirical formula | $C_3H_{10}O_9CaNP_3$ |
| Formula weight | 337.11 |
| Temperature (K) | 86(2) |
| Wavelength (Å) | 0.71073 |
| Crystal system | Monoclinic |
| Space group | P2(1)/n |
| a (Å) | 9.28(7) |
| b (Å) | 8.43(6) |
| c (Å) | 13.61(1) |
| α (°) | 90 |
| β (°) | 96.44(1) |
| γ (°) | 90 |
| Volume ($Å^3$) | 1057.6(1) |
| Z | 4 |
| dcal($mg/m^3$) | 2.117 |
| μ ($mm^{-1}$) | 1.087 |
| Crystal size( $mm^3$) | 0.40 x 0.20 x 0.15 |
| 2θ range (°) | 2.53-28.27 |
| Reflections collected | 10267 |
| Independent reflections | 2620 |
| R1 [I>2sigma(I)] | 0.0275 |
| wR2 [I>2sigma(I)] | 0.0766 |
| R1 (all data) | 0.0300 |
| wR2 (all data) | 0.0786 |

## 8.10 Thermogravimetric Studies

Thermogravimetric analysis was performed using a Q-500 Quantachrome Analyzer (TA-Instruments). Compound **14** was loaded on a platinum pan. Purified nitrogen gas was used with a balance purge rate of 40 mL/min and a sample purge rate of 60 mL/min. The temperature was ramped at 10 °C per minute until a final temperature of 800° C was reached. At about 650 $^{o}$C, about 23.75% of weight loss was recorded and a black residue remained in the pan.

## 8.11 References:


(1) James, S. L. *Chem. Soc. Rev.* **2003**, *32*, 276.
(2) Evans, O. R.; Lin, W. *Acc. Chem. Res.* **2002**, *35*, 511.
(3) Rowsell, J. L. C.; Yaghi, O. M. *Microporous Mesoporous Mater.* **2004**, *73*, 3.
(4) Collins, D. J.; Zhou, H.-C. *J. Mater. Chem.* **2007**, *17*.
(5) Janiak, C. *Angew. Chem., Int. Ed.* **1997**, *36*, 1431.
(6) Li, J.-R.; Kuppler, R. J.; Zhou, H.-C. *Chem. Soc. Rev.* **2009**, *38*.
(7) Naydenova, E. D.; Todorov, P. T.; Troev, K. D. *Amino Acids* **2010**, *38*, 23.
(8) Naydenova, E. D.; Todorov, P. T.; Troev, K. D. *Phosphorus, Sulfur Silicon Relat. Elem.* **2010**, *185*, 1315.
(9) Naydenova, E.; Topashka-Ancheva, M.; Todorov, P.; Yordanova, T.; Troev, K. *Bioorg. Med. Chem.* **2006**, *14*, 2190.
(10) Kafarski, P.; Lejczak, B.; John Wiley & Sons Ltd.: 2000, p 407.
(11) Palacios, F.; Alonso, C.; de los Santos, J. M. *Chem. Rev.* **2005**, *105*, 899.
(12) Ma, T.-Y.; Yuan, Z.-Y. *Eur. J. Inorg. Chem.* **2010**, *2010*, 2941.
(13) Demadis, K. D.; Katarachia, S. D. *Phosphorus, Sulfur Silicon Relat. Elem.* **2004**, *179*, 627.
(14) Bishop, M.; Bott, S. G.; Barron, A. R. *Chem. Mater.* **2003**, *15*, 3074.
(15) Carter, R. P., Jr.; Carroll, R. L.; Irani, R. R. *Inorg. Chem.* **1967**, *6*, 939.
(16) Jansen, D. R.; Rijn, Z. J.; Denkova, A.; Kolar, Z. I.; Krijger, G. C. *Langmuir* **2009**, *25*, 2790.
(17) Demadis, K. D.; Nova Science Publishers, Inc.: 2007, p 109.
(18) Demadis, K. D.; Mantzaridis, C.; Lykoudis, P. *Ind. Eng. Chem. Res.* **2006**, *45*, 7795.
(19) Papadaki, M.; Demadis, K. D. *Comments Inorg. Chem.* **2009**, *30*, 89.
(20) Demadis, K. D.; Katarachia, S. D.; Raptis, R. G.; Zhao, H.; Baran, P. *Crystal Growth Des.* **2006**, *6*, 836.
(21) Clearfield, A. *J. Alloys Compd.* **2006**, *418*, 128.
(22) Schier, A.; Gamper, S.; Müller, G. *Inorg. Chim. Acta* **1990**, *177*, 179.
(23) Cabeza, A.; Ouyang, X.; Sharma, C. V. K.; Aranda, M. A. G.; Bruque, S.; Clearfield, A. *Inorg. Chem.* **2002**, *41*, 2325.
(24) Mao, J.-G.; Wang, Z.; Clearfield, A. *New J. Chem.* **2002**, *26*, 1010.
(25) Li, H.; Zhang, L.; Li, G.; Yu, Y.; Huo, Q.; Liu, Y. *Microporous Mesoporous Mater.* **2010**, *131*, 186.
(26) Fu, R.; Hu, S.; Wu, X. *J. Solid State Chem.* **2011**, *184*, 159.
(27) Cabeza, A.; Bruque, S.; Guagliardi, A.; Aranda, M. A. G. *J. Solid State Chem.* **2001**, *160*, 278.
(28) Sharma, C. V. K.; Clearfield, A.; Cabeza, A.; Aranda, M. A. G.; Bruque, S. *J. Am. Chem. Soc.* **2001**, *123*, 2885.
(29) Gholivand, K.; Farrokhi, A. R. *Acta Crystallogr. Sect. E* **2010**, *66*, m873.
(30) Cabeza, A.; Aranda, M. A. G.; Bruque, S. *J. Mater. Chem.* **1999**, *9*, 571.
(31) Cunha-Silva, L.; Mafra, L.; Ananias, D.; Carlos, L. D.; Rocha, J.; Almeida Paz, F. A. *Chem. Mater.* **2007**, *19*, 3527.
(32) Demadis, K. D.; Mantzaridis, C.; Lykoudis, P. *Industrial & Engineering Chemistry Research* **2006**, *45*, 7795.

(33) Georgantas, V.; Kotsakis, N.; Raptopoulou, C. P.; Terzis, A.; Iordanidis, L.; Zervou, M.; Jakusch, T.; Kiss, T.; Salifoglou, A. *J. Inorg. Biochem.* **2009**, *103*, 1530.
(34) Moedritzer, K.; Irani, R. R. *J. Org. Chem.* **1966**, *31*, 1603.
(35) Chadwick, S.; Englich, U.; Ruhlandt-Senge, K. *Chem. Commun.* **1998**, 2149.

# CHAPTER 9

## Conclusions

The purpose of this project is to design magnesium and calcium based frameworks suitable as scaffolds for bone ingrowths or as potential biocompatible and bioactive additives to bone cement. In contrast to extensive work on transition metal bisphosphonates, very limited information is available on the main group counterparts, specifically alkaline earth metal based compounds. This thesis is exploring multiple synthetic avenues as well as crystallization methodologies to obtain samples suitable for structural analysis. Illustrating the synthetic challenges involved in the preparation of the target compounds, a range of synthetic methodologies was employed. Likewise, X-ray quality single crystals were grown using hydrothermal/solvothermal approaches, gel crystallization and slow evaporation, but at this time, no uniform methodology is emerging. However, one-dimensional calcium phosphinate, sheets of magnesium phosphonates, and finally three dimensional pillar layered calcium phosphonates, were synthesized by careful choice of ligand and reaction conditions.

The outcome of this research has provided a library of calcium and magnesium based compounds with interesting structural features. Novel compounds obtained include a 1D calcium phenylphosphinate (**1**), 2D anhydrous calcium hydrogen phosphite (**3**), 2D magnesium ethylenediphosphonate (**8**), 2D magnesium propylenediphosphonate (**9**), 3D calcium methylenediphosphonate (**10**), 3D calcium sodium ethylenediphosphonate (**11**), 3D calcium nitrate ethylenediphosphonate (**12**), 3D calcium propylenediphosphate (**13**) and 3D calcium amino trimethylenephosphonate (**14**). All novel compounds have been

successfully characterized by single crystal X-ray diffraction. Structural studies of the novel compounds and closely related alkaline earth metal phosphonates indicate there is a correlation between ligand type and compound dimensionality.

Each of these compounds however required a different synthetic approach and even for closely related ligands that differ only by a single linker carbon atom such as ethylenediphosphonate $(HO_3P(CH_2)_2PO_3H)^{2-}$ and propylenediphosphonate $(HO_3P(CH_2)_3PO_3H)^{2-}$, remarkable structural differences are observed. Crystalline products of compounds **3**, **8**, **10**, **11** and **12** were all obtained by hydrothermal synthesis at temperatures ranging between 150 - 170 $^{o}$C while crystals of **1**, **9** and **13** were formed from solutions heated to 80 $^{o}$C followed by slow evaporation at room temperature. In contrast, crystals of **12** were obtained only by gel crystallization while crystals of **14** formed at room temperature. Synthetic studies of **14** have shown that, the presence of phosphonic acid in the synthesis of **14** greatly improved crystal quality and yields.

The dimensions of the resulting compounds rely on the number of deprotonated oxygen atoms in the sample. These results outline the challenge to predict solid state structures as small changes in parameters often result in drastic structural effects.

Another important structural feature observed among the three-dimensional methylene, ethylene and propylenediphosphonates is length of organic linker and their role in the interlayer distance of the resulting compounds. Mostly, with a linker length of two or more carbon atoms, it is possible to achieve pillared layered three-dimensional compounds, as in **11** and **13.** The longer the length of the linker, the less dense the framework.

**Victoria Naa Kwale Bampoh**

Department of Chemistry, Syracuse University
111 College Place, Syracuse, NY, 13244
Tell: (315) 373 3939
vnbampoh@syr.edu

## Education

Doctoral Candidate, Chemistry, Syracuse University, Syracuse NY
Thesis: Calcium and Magnesium Phosphinate and Phosphonate Compounds
Advisor: Dr. Karin Ruhlandt
December 2010 - Present

MS. Chemistry, Syracuse University, Syracuse NY
Thesis: *S*-block metal phosphonates by hydrothermal and solvothermal synthesis
Advisor: Dr. Karin Ruhlandt
August 2006 - December 2010

M.Ph. Chemistry, University of Cape Coast, Cape Coast, Ghana
Thesis: The State of some Coastal Environments in Ghana: Rainwater as Substrate for Analysis
Advisor: Dr. David Dodoo
September 2001- March 2006

B.Sc. Chemistry, University of Cape Coast, Cape Coast, Ghana
Thesis: Optimization of pH for the Elution of Citric Acid by Column Chromatography
Advisor: Dr. David Doku
September 1991 - June1996

## Professional Experience

Five years research experience in the field of inorganic material synthesis with proficient skills in:

Designing Metal Organic Framework (MOFs) materials with applications as bone substitute material.

Crystallizing compounds by hydro/solvothermal synthesis, gel and slow evaporation of solvent.

Handling air-sensitive ligands by use of dry-box and Schlenk-line techniques.

Using analytical instruments such as single crystal X-Ray diffractometer, FT-NMR and FT-IR instruments to characterize new compounds.

## Research Experience

**2006-present**
Graduate student, Department of Chemistry, Syracuse University, Syracuse, NY:

Design and synthesis of phosphinic/phosphonic acid ligands and the preparation of three-dimensional with potential applications as scaffold material for bone cell growth and additives to bioactive cements. Novel compounds are characterized using single crystal X-Ray diffractometer, FT-IR and FT-NMR instruments.

**2001-2006**
Graduate student, Department of Chemistry, University of Cape Coast, Ghana:

Water quality analysis; Determination of pH, conductivity, alkalinity, turbidity, total hardness and ion content of rain water samples. Designed novel equipment for rain water sampling as part of this project.

## Teaching Experience

**2012-present**
Chemistry Laboratory Coordinator, Syracuse University:

Purchasing basic laboratory supplies, (consumables, glassware, small equipment, and chemicals).

Preparation of reagents and laboratory set-up for teaching undergraduate General Chemistry

**2006-2011**
Graduate Teaching Assistant, Syracuse University:

Organizing recitation for undergraduate General Chemistry.

Teaching undergraduate Honors General Chemistry laboratory course.

Teaching undergraduate General Chemistry Laboratory.

Mentoring international undergraduate students during summer 2008 as part of the International Research Experience for Students (iRES).

Assisting with teaching General Chemistry as a Guest lecturer.

Proctoring undergraduate examination.

**2001-2006**
Graduate Teaching Assistant, University of Cape Coast, Ghana:

Teaching undergraduate laboratory courses.

**2003-2006**
Professional teacher, University Practice and Armed Forces Secondary School, Ghana:

Teaching high school general chemistry

Writing, grading and administering quizzes.

Evaluating tests for West Africa Examination Council as an examiner.

Developing learning tools such as 'Snake and Ladder' games to generate interest in and facilitate the learning of the periodic table for high school students during my teaching practice.

## Competencies

Expert on Carius tube hydrothermal and solvothermal chemistry.

Expert on single crystal X-ray diffractometer, FT-IR and FT-NMR analysis.

Proficient in using CHEM DRAW and Scifinder.

Proficient in using MS Word, MS Excel and MS Power Point.

## Awards and Affiliations

Recipient of Syracuse University Scholarship for Graduate Studies.

First Placement Achievement, 2$^{nd}$ Syracuse Biomaterials Institute Research Poster Session, August 28, 2009.

Member of American Chemical Society since January 2010.

Member of Women in Science and Engineering, Syracuse University, 2007-2008

Participant of Future Professoriate Program, Syracuse University, 2007-2008

**Presentations**

Victoria N.K. Bampoh and Karin Ruhlandt, "Calcium and Magnesium based Metal Organic Frameworks as Bioactive Bone Scaffolding Materials and Additives to Bone Cements". Poster presentation: 3rd CNY Biotechnology Symposium, June 2, 2011.

Victoria N.K. Bampoh and Karin Ruhlandt, "Exploring Calcium Triphosphonate compounds for bone substitute materials. Presentation: Stevenson Biomaterials Lecture Poster Session", February 23, 2011.

Victoria N.K. Bampoh and Karin Ruhlandt. "Preparation and characterization of calcium and magnesium phosphonates." Abstracts: 37th Northeastern Regional Meeting of the American Chemical Society, Potsdam, NY, June 2-5, 2010.

Yuriko Takahashi, Victoria N.K Bampoh, Karin Ruhlandt, "Three-dimensional Magnesium and Calcium Phosphonates and Carboxylates-new avenues towards bioactive materials." Poster presentation: 37th Northeastern Regional Meeting of the American Chemical Society, Potsdam, NY, June 2-5, 2010.

Victoria N.K. Bampoh, William Maudez, Sarina Clancy, and Karin Ruhlandt, Preparation of Calcium and Magnesium Phosphonates by Hydrothermal and Solvothermal Methods. Poster presentation: 2nd Annual Stevenson Biomaterials Lecture offsite Meeting, August 28, 2009, Syracuse NY.

Victoria N.K. Bampoh, "Graduate School Experience."April 2009, Morrisville State College, Morrisville.

**Publication**

Kin S. Yang, Venkata S. Kandula, Zachary D. Miller, Kevin C. Pels, Joshua A. Long, Victoria N.K. Bampoh, Ana Torvisco, Karin Ruhlandt, Donald C. Dittmer, "Telluride-triggered Enolate Formation Involving Evans' Chiral Oxazolidinone Auxiliaries." Journal: *J.Org.Chem*, *in press*.